ENHANCEMENT OF MECHANICAL PROPERTIES OF A POTTING COMPOUND BY ADDITION OF FUNCTIONALIZED SINGLE-WALLED AND MULTI-WALLED CARBON NANOTUBES

A Thesis by

Mauricio E. Guzman

Bachelor of Science, Universidad Tecnológica del Centro, 2002

Submitted to the Department of Mechanical Engineering
and the faculty of Graduate School of
Wichita State University
in partial fulfillment of
the requirements for the degree of
Master of Science

May 2010

ENHANCEMENT OF MECHANICAL PROPERTIES OF A POTTING COMPOUND BY ADDITION OF FUNCTIONALIZED SINGLE-WALLED AND MULTI-WALLED CARBON NANOTUBES

The following faculty members have examined the final copy of this thesis for form and content, and recommend that it be accepted in partial fulfillment of the requirement for the degree of Master of Science with a major in Mechanical Engineering.

_____
Bob Minaie, Committee Chair

_____
Ramazan Asmatulu, Committee Member

_____
William Stevenson, Committee Member

ACKNOWLEDGEMENTS

I would like to express my gratitude to my advisor, Professor Bob Minaie, for giving me the opportunity to perform this work. His support, guidance, and encouragement as well as his scientific advice helped me accomplish this work successfully. I would like to express my gratitude to Dr. Ramazan Asmatulu and Dr. William Stevenson for serving on my thesis committee. I also want to thank Dr. Melanie Violette for her helpful comments and suggestions during this investigation.

I would like to thank my colleagues Alejandro Rodriguez and Chee Sern Lim in Professor Minaie's group for their unconditional friendship and academic support. Their consistent encouragement made this work more interesting and enjoyable.

Financial support by the Office of Naval Research, National Aeronautics and Space Administration, Kansas Technology Enterprise Corporation, and Wichita State University is gratefully acknowledged.

ABSTRACT

Potting compounds are composite materials made up of a mixture of a polymer matrix and hollow particles called microballoons. They are used for reinforcing the core section of honeycomb laminates around fastener locations in aerospace applications. Commercially, different compounds of various densities as well as compressive and shear strengths are available; nevertheless, their selection as reinforcement material depends on the type of load to be supported. Normally, the higher the strength, the heavier the compound used in the reinforcement of the core. Another important characteristic to take into account is moisture absorption. Potting compounds are known for absorbing moisture, which represents a disadvantage in sandwich laminates since the integrity of the structure could be compromised due to decrease in mechanical properties of the potting compound.

In this research, a potting compound was developed in such a way that high strength could be obtained under dry and hygrothermal conditions without having a substantial increase in density. The compound was made by incorporating different types of microballoons and either single-walled or multi-walled carbon nanotubes as reinforcing particles. In order to obtain high strength and low density compounds, two studies were conducted to understand the effect of glass microballoons and carbon nanotubes on the mechanical properties of the potting compound. In the first study, four different types of glass microballoons were used to manufacture one-part compounds with physical and mechanical properties similar to those of a two-part compound (EC-3500). Results suggested that several compounds could be attained with properties similar to those of EC-3500 with minimum increase in density. In the second study, carbon nanotubes were incorporated into both a low and a high density potting compound with the purpose of studying the effect of the nanotubes on their mechanical properties. Three

different mixing methods (ultrasound, calendering, and centrifugal) were employed to disperse the functionalized single-walled and multi-walled carbon nanotubes in the resin of the potting compound. Through various processing parameters, several nano-enhanced potting compound samples were made and tested for mechanical properties under dry and hot/wet conditions. Results showed a significant increase in compressive and lap shear strength with a minimum increase in density for the nano-enhanced specimens prepared with vacuum compared to the properties of EC-3500.

TABLE OF CONTENTS

Chapter Page

INTRODUCTION 1

1.1 Motivation and Scope 1
1.2 Research Objectives 4

LITERATURE REVIEW 5

2.1 Potting Compounds 5
2.2 Carbon Nanotube Atomic Structure 8
2.3 Carbon Nanotube Morphology 11
2.4 Synthesis of Carbon Nanotubes 12
2.5 Mechanical Properties of Carbon Nanotubes 13
2.6 Nanotube/Polymer Composites 14
2.7 Nanomaterial/Potting Compounds 17

TECHNICAL APPROACH 19

3.1 Materials 19
3.2 Experimental Studies 21
3.2.1 Effect of Microballoon Type and Concentration on the Physical and Mechanical Properties of Potting Compounds 21
3.2.2 Effect of Carbon Nanotubes on the Physical and Mechanical Properties of Potting Compounds 22
3.3 Mechanical and Physical Characterization Methods 26

RESULTS AND DISCUSSION 28

4.1 Characterization of Functionalized SWNTs and MWNTs 28
4.1.1 FTIR Spectroscopy of SWNTs and MWNTs 28
4.1.2 TGA of SWNTs and MWNTs 30
4.2 Effect of Microballoon Type and Concentration on the Physical and Mechanical Properties of Potting Compounds 32
4.3 Effect of Microballoon Type and Concentration on the Physical and Mechanical Properties of Potting Compounds Subjected to Hot/Wet Conditions 35
4.4 Effect of Carbon Nanotube Addition on the Physical and Mechanical Properties of Potting Compounds 37
4.4.1 Properties of Nano-enhanced Potting Compounds Prepared with Vacuum 37
4.4.2 Properties of Nano-enhanced Potting Compounds Prepared without Vacuum 44
4.4.3 Effect of F-SWNTs and F-MWNTs on the Mechanical Properties of Selected Microballoon Compounds 48

TABLE OF CONTENTS (continued)

Chapter Page

4.5 Effect of Carbon Nanotube Addition on the Physical and Mechanical Properties of Potting Compounds Subjected to Hot/Wet Conditions 53
4.5.1 Properties of Nano-enhanced Potting Compounds Prepared with Vacuum and Subjected to Hot/Wet Conditions..... 53
4.5.2 Properties of Nano-enhanced Potting Compounds Prepared without Vacuum and Subjected to Hot/Wet Conditions 57
4.5.3 Effect of F-SWNTs and F-MWNTs on Specimens Prepared with the Selected Microballoons and Subjected to Hot/Wet Conditions..... 60

CONCLUSIONS..... 66

REFERENCES 70

APPENDICES 77

A. Design of Experiment I - Glass Microballoons 78

B. Design of Experiments II - Carbon Nanotubes..... 79

LIST OF TABLES

Table		Page
1.	Properties of Corfil 625-1 and EC-3500	19
2.	Properties of Glass Microballons	21
3.	Factors for the DOE-II	23
4.	Refluxing Time and Temperature for Functionalization of Single-walled and Multi-walled Carbon Nanotubes	25
5.	Three Roll Mill Set Up	26
6.	Mechanical and Physical Properties of compounds A, B, Corfil 625-1, and EC-3500	35

LIST OF FIGURES

Figure Page

1. Assembly of honeycomb laminated structures and potting compound reinforcement [1]. 1

2. (a) Schematic diagram showing the chiral vector and the chiral angle in the honeycomb lattice of ghaphene [21], and (b) molecular models of the different conformations of carbon nanotubes: armchair, chiral, and zigzag. 9

3. Stone-Wale diatomic interchange in a nanotube hexagonal wall. 10

4. Structure of single-walled carbon nanotubes (SWNTs) and multi-walled carbon nanotubes (MWNTs). 11

5. Polymerization of Corfil 625-1. 20

6. Traditional configurations of (a) the three roll mill from EXAKT [76], and (b) the vacuum centrifugal mixer from THINKY [77]. 24

7. (a) Compression and (b) lap shear specimens. 27

8. IR spectra of as-received SWNTs (AR-SWNTs) and functionalized SWNTs (F-SWNTs) at different times and temperatures. 29

9. IR spectra of as-received MNWTs (AR-MWNTs) and functionalized MWNTs (F-MWNTs) at different times and temperatures. 29

10. TGA plots of as-received SWNTs (AR-SWNTs) and functionalized SWNTs (F-SWNTs) at different times and temperatures. 31

11. TGA plots of as-received MWNTs (AR-MWNTs) and functionalized MWNTs (F-MWNTs) at different times and temperatures. 31

12. Density results for the glass microballoon specimens tested at RT. 33

13. Compressive strength results for the glass microballoon specimens tested at RT. 34

14. Lap shear strength results for the glass microballoon specimens tested at RT. 34

15. Compressive strength results for the glass microballoon specimens conditioned at 71^{o}C and 85% RH, and tested at 82^{o}C. 36

16. Lap shear strength results for the glass microballoon specimens conditioned at 71^{o}C and 85% RH, and tested at 82^{o}C 36

17. Density results for microballoon specimens (S38HS & S60HS and H50 & S60HS) mixed with vacuum and without vacuum. 39

LIST OF FIGURES (continued)

Figure Page

18. Density results for specimens containing F-SWNTs and S38HS & S60HS glass microballoons. 39

19. Density results for specimens containing F-MWNTs and S38HS & S60HS glass microballoons. 40

20. Density results for specimens containing F-SWNTs and H50 & S60HS glass microballoons. 40

21. Density results for specimens containing F-MWNTs and H50 & S60HS glass microballoons. 41

22. Compressive strength results for microballoon specimens (S38HS & S60HS and H50 & S60HS) mixed with vacuum and without vacuum. 41

23. Compressive strength results for specimens containing F-SWNTs and mixed using vacuum. 42

24. Compressive strength results for specimens containing F-MWNTs and mixed using vacuum. 42

25. Lap shear strength results for microballoon specimens (S38HS & S60HS and H50 & S60HS) mixed with vacuum and without vacuum. 43

26. Lap shear strength results for specimens containing F-SWNTs and mixed using vacuum. 43

27. Lap shear strength results for specimens containing F-MWNTs and mixed using vacuum. 44

28. Microscopy images of carbon nanotube potting compounds mixed at (A) full vacuum (specimen #9), and (B) zero vacuum (specimen #14). Magnifications correspond to 50x and 200x for left and right columns, respectively. 45

29. Compressive strength results for specimens containing F-SWNTs and mixed without vacuum. 46

30. Compressive strength results for specimens containing F-MWNTs and mixed without vacuum. 47

31. Lap shear strength results for specimens containing F-SWNTs and mixed without vacuum. 47

LIST OF FIGURES (continued)

Figure Page

32. Lap shear strength results for specimens containing F-MWNTs and mixed without vacuum. 48

33. Compressive strength results for specimens prepared with F-SWNTs and S38HS & S60HS glass microballoons. 49

34. Compressive strength results for specimens prepared with F-MWNTs and S38HS & S60HS glass microballoons. 50

35. Compressive strength results for specimens prepared with F-SWNTs and H50 & S60HS glass microballoons. 50

36. Compressive strength results for specimens prepared with F-MWNTs and H50 & S60HS glass microballoons. 51

37. Lap shear strength results for specimens prepared with F-SWNTs and S38HS & S60HS glass microballoons. 51

38. Lap shear strength results for specimens prepared with F-MWNTs and S38HS & S60HS glass microballoons. 52

39. Lap shear strength results for specimens prepared with F-SWNTs and H50 & S60HS glass microballoons. 52

40. Lap shear strength results for specimens prepared with F-MWNTs and H50 & S60HS glass microballoons. 53

41. Compressive strength results for F-SWNT-resin-glass microballoon specimens mixed using vacuum and subjected to hot/wet conditioning. 55

42. Compressive strength results for F-MWNT-resin-glass microballoon specimens mixed using vacuum and subjected to hot/wet conditioning. 55

43. Lap shear strength results for F-SWNT-resin-glass microballoon specimens mixed using vacuum and subjected to hot/wet conditioning. 56

44. Lap shear strength results for F-MWNT-resin-glass microballoon specimens mixed using vacuum and subjected to hot/wet conditioning. 56

45. Compressive strength results for F-SWNT-resin-glass microballoon specimens mixed without vacuum and subjected to hot/wet conditioning. 58

LIST OF FIGURES (continued)

Figure Page

46. Compressive strength results for F-MWNT-resin-glass microballoon specimens mixed without vacuum and subjected to hot/wet conditioning. 59

47. Lap shear strength results for F-SWNT-resin-glass microballoon specimens mixed without vacuum and subjected to hot/wet conditioning. 59

48. Lap shear strength results for F-MWNT-resin-glass microballoon specimens mixed without vacuum and subjected to hot/wet conditioning. 60

49. Compressive strength results for specimens prepared with F-SWNTs and S38HS & S60HS glass microballoons and subjected to hot/wet conditioning 61

50. Compressive strength results for specimens prepared with F-MWNTs and S38HS & S60HS glass microballoons and subjected to hot/wet conditioning. 62

51. Compressive strength results for specimens prepared with F-SWNTs and H50 & S60HS glass microballoons and subjected to hot/wet conditioning. 62

52. Compressive strength results for specimens prepared with F-MWNTs and H50 & S60HS glass microballoons and subjected to hot/wet conditioning. 63

53. Lap shear strength results for specimens prepared with F-SWNTs and S38HS & S60HS glass microballoons and subjected to hot/wet conditioning. 63

54. Lap shear strength results for specimens prepared with F-MWNTs and S38HS & S60HS glass microballoons and subjected to hot/wet conditioning. 64

55. Lap shear strength results for specimens prepared with F-SWNTs and H50 & S60HS glass microballoons and subjected to hot/wet conditioning. 64

56. Lap shear strength results for specimens prepared with F-MWNTs and H50 & S60HS glass microballoons and subjected to hot/wet conditioning. 65

LIST OF ABBREVIATIONS / NOMENCLATURE

CNT(s)	Carbon Nanotube(s)
FTIR	Fourier Transform Infrared Spectroscopy
HW	Hot/Wet
IR	Infrared
MWNTs	Multi-walled Carbon Nanotubes
RH	Relative Humidity
RT	Room Temperature
SWNTs	Single-walled Carbon Nanotubes
TGA	Thermal-gravimetric Analysis

LIST OF SYMBOLS

^{o}	Degree
m	Meter
μ	Micron
n	Nano
Δ	Heat

CHAPTER 1

INTRODUCTION

1.1 Motivation and Scope

Parts made of sandwich structures comprising honeycomb core and skin layers bonded together are of extensive use in the aircraft industry due to their high stiffness and low weight. These structures, often referred to as honeycomb laminates, are particularly effective at carrying distributed loads along the normal direction of the core cell. However, the weakness of the core along the transverse direction makes sandwich structures not suitable for point loads. Therefore, to maintain the integrity of the structure, a local reinforcement of the core is usually required when mechanical fasteners (bolts and rivets) are to be utilized to join laminated composites. This reinforcement is normally accomplished through the addition of potting compounds. The structure of honeycomb laminates is described in Figure 1.

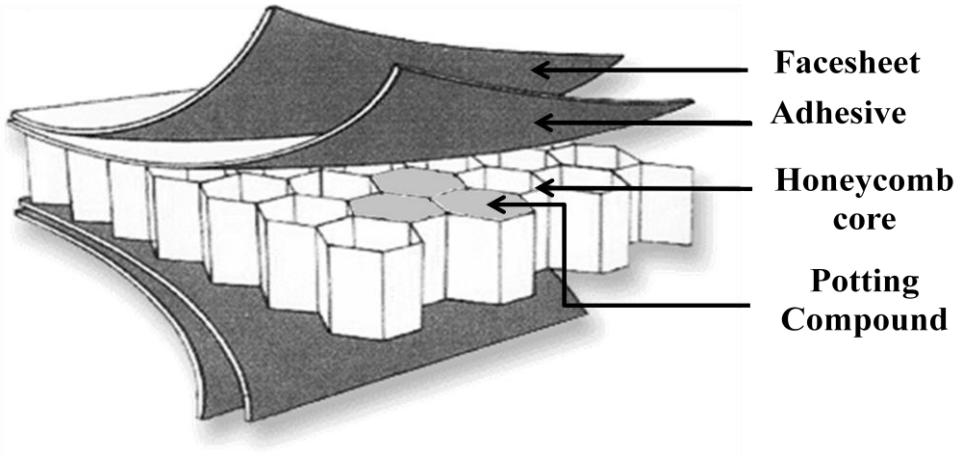

Figure 1. Assembly of honeycomb laminated structures and potting compound reinforcement [1].

Potting compounds are lightweight composite materials synthesized by dispersing silica-glass microsphere particles (microballoons) in a polymer matrix (phenolic or epoxy resin). They are normally used as strength/density modifiers since they can be tailored with different

microballoons of different strengths and densities to achieve properties (mechanical, thermal, and physical) not possible with other materials. Potting compounds are commercially found as either a one-part or a two-part compound formulated for use in insert and edge filling of cellular cores of honeycomb laminates, as shown in Figure 1. They are characterized for having low density, low coefficient of thermal expansion, high strength, and excellent compatibility with the cure cycle used for sandwich laminated structures.

Multiple compounds of various strength and density (EC-3500, Corfil 623-1, Corfil 625-1) are used in reinforcing the core of sandwich laminates; however, their utilization is limited by their density and strength. Typically the higher the strength, the heavier the potting compound, causing considerable weight gains in honeycomb laminates. Normally, denser and stronger materials consisting of a two-part compound require an additional mixing process compare to less dense and lower strength materials, one-part compounds. Therefore, there is a need to design one-part potting compounds that can support high compressive and lap shear strength with minimum change in density.

It is believed that because of their resilience, large surface area, and excellent mechanical and physical properties, carbon nanotubes can be an ideal reinforcement material to be added to potting compounds in order to improve their mechanical properties without affecting their density significantly.

In this investigation, the enhancement of compressive and lap shear strength of a one-part potting compound is achieved by adding microballoons as well as either single-walled or multi-walled carbon nanotubes. In order to evaluate and understand the effect of microballoon and carbon nanotube reinforcement on the physical and mechanical properties of a potting compound, two studies are carried out. In the first study, four different types of glass

microballoons are used to form one-part potting compounds with mechanical properties similar to that of a two-part compound (EC-3500). Based on the results obtained from this study, two standard compounds are selected, one containing medium-high density microballoons and the other containing high-high density microballoons. These compounds represent the building block upon which the effect of carbon nanotube addition will be investigated in a further study. In the second study, carbon nanotubes are added to the resin of the compounds selected previously to form nano-enhanced potting compounds. The objective is to improve the compressive and lap shear strength of the base composites without affecting their density considerably. Before integrating the nano-scale materials into the polymer resin, single-walled and multi-walled carbon nanotubes are functionalized to introduce carboxylic acid moieties on their surface(s). For the dispersion of functionalized carbon nanotubes in the resin, a combine dispersion approach including ultrasonic, calendering, and centrifugal mixing is performed. Through various processing parameters, several nano-enhanced potting compounds are made and tested for mechanical properties under dry and hot/wet conditions.

This work is organized in the following manner. A review of the research done in the area of potting compounds and carbon nanotube/polymer composites is provided in the second chapter. The third chapter describes materials and methodologies used to fabricate both potting compounds with different morphologies and nano-enhanced potting compounds. The fourth chapter provides the results achieved through these methods, and the final chapter concludes and summaries the work performed in this investigation.

1.2 Research Objectives

The general objective of this research is to develop a one-part potting compound with high strength under dry and hygrothermal conditions by addition of microballoons and carbon nanotubes.

Specific objectives of this research are:

1. Enhance the mechanical properties of a low-density one-part potting compound by addition of microballoons.
2. Obtain potting compounds with properties similar to that of 3M's EC-3500 and with a density between 608.7 and 688.7 kg/m^3.
3. Investigate the effect of carbon nanotube addition on the density, compressive and lap shear strength of potting compounds.
4. Study the effect of environmental conditioning (elevated temperature and moisture) on the mechanical properties of neat and nano-enhanced potting compounds.

CHAPTER 2

LITERATURE REVIEW

2.1 Potting Compounds

Syntactic foams or potting compounds are lightweight composites made of two constituent materials: polymer based matrix (binder) and microballoons (filler). Such polymeric compounds are characterized by having large quantities of hollow microspheres dispersed in a resinous matrix. Thermosetting polymers such as epoxy and phenolic resins, polyimide, and silicone are the preferred systems used in the fabrication of potting compounds due to ease of processing. On the other hand, hollow microballoons of different diameters, wall thickness, and strength are commonly made of glass, ceramic, aluminum, and steel. However, their utilization depends mostly on strength and density requirements, which can vary according to the desired resin/microballoon composition. Puterman et al. [2] showed that the compressive strength of syntactic foams was a function of the proportion of resin-microballoon-void as well as identified that the void content of syntactic foam was primarily a function of the resin volume fraction. Later, Narkis et al. [3] evaluated the effect of resin volume fraction on the compressive properties of syntactic foams and confirmed that the compressive strength and modulus could be increased by more than an order of magnitude by increasing the resin content and maintaining the microballoon volume fraction constant. Gupta et al. [4] observed that the tensile strength of epoxy-resin syntactic foams containing low density microballoons increased with decreasing their volume fraction and emphasized the load bearing role of the matrix during tensile loads. In different publications, Gupta et al. [5, 6] investigated the effect of microballoon wall thickness on the mechanical properties of potting compounds and concluded that the compressive strength, modulus, and fracture characteristics of syntactic foams were strongly related to a parameter

called Radius Ratio (η), which is defined as the ratio of inner to outer radius of microballoons. Hence, the lower η, the higher density and strength of the potting. Woldesenbet et al. [7] studied the effect of microballoon reinforcement at different volume fractions on the compressive properties of syntactic foam composites. Results obtained for high strain and quasi-static strain rates suggested that a decrease in both modulus and compressive strength was attributed to an increase in microballoon volume fraction. They also pointed out that during failure the propagation of the crack came from either the matrix material or the matrix-microballoon interface. Tagliavia et al. [8] employed vibration techniques to assess the dynamic mechanical properties of syntactic foams as a function of both microballoon wall thickness and volume fraction. Their findings showed the dependence of loss tangent and storage modulus on the viscoelastic properties of the constituents (resin and microballoons) and on the wall thickness and volume fraction of microballoons.

Potting compounds are also known for exhibiting low moisture absorption capabilities in relation to other polymeric foams. The degree of water absorption depends on the chemical and physical properties of the matrix and the microballoons as well as their volume fraction [9]. Hobaica et al. [10] investigated the absorption properties of syntactic foams used for buoyancy applications. Their observations indicated that the resin-microballoon interface as well as the microballoon volume concentration played a remarkable effect on the water uptake of composite foams. In addition, they highlighted that water could diffuse more readily around the microballoons than through the matrix, originating possible failure areas at the interface. Earl et al. [11] studied the moisture uptake mechanism in closed cell polyvinyl chloride (PVC) foams and concluded that the progressive diffusion of water into polymeric cell wall structures and cavities might be attributed to a multi-stage absorption process defined by a linear mass increase

relative to the square root of time. Gupta et al. [12] evaluated the hygrothermal properties of potting compounds under different media and found that a considerable decrease in compressive modulus was attained due to an increase in moisture content. Moreover, they highlighted that the peak strength for both the low temperature and high temperature hygrothermal specimens (25^{o}C and 70^{o}C, respectively) did not show a significant difference relative to the dry specimens.

The mechanical properties of potting compounds can be tailored by varying the ratio of resin-to-microballoon volume fraction. For such compounds, the density is a function of the wall thickness of the microballoons. Okuno et al. [13] compared experimental results with theoretical calculations and found a good relation between the mechanical properties of potting compounds and the type of glass microballoon used. Gupta et al. [14] investigated the compressive strength of potting compounds fabricated with cenospheres of various wall thickness in different volume fractions and found a linear relation between the compressive strength and the compound density. Bardella et al. [15] developed a model to evaluate the elastic behavior of potting compounds as a function of both the presence of unwanted voids and the distribution of wall thickness of the filler particles. They concluded that the presence of voids had the most significant effect on the elastic modulus of such composites.

Deformation and fracture mechanisms of potting compounds have also been studied for several loading conditions. Such studies have been oriented towards understanding the role of matrix materials and microballoon characteristics (size, wall thickness) on the properties of potting compounds. Kim et al. [16] investigated the impact behavior of potting compounds and found similarity in compressive failure mode between pseudo-static and impact loadings, demonstrating that the inclusion of glass microballoons in resin reduced the impact failure. Gupta et al. [17] carried out investigations to identify the deformation and fracture characteristics

of potting compounds under compression loading conditions and found considerable differences in the macroscopic fracture behavior with the variation of specimen aspect ratio. Shearing and wedge shaped cracks were the primary failure mode for both high and low aspect ratio specimens tested under compression loadings. On the other hand, in the microscopy fracture behavior, they found a substantial amount of crushed microballoons on the fracture surfaces, revealing that failure under compression was the dominant mode of failure [18]. Kim et al. [19] also conducted compressive tests on potting compounds of various densities and concluded that two different modes of failure under compression loading could be observed: (1) longitudinal splitting attributed to a low density foam and (2) layered crushing attributed to a high density foam. Their findings agreed well with investigations made by Gupta et al. [5]. Rizzi et al. [9] modeled the elastic behavior of potting compounds and defined a cohesive law to capture the fracture process of three-point bending tests of composite foams. Their bi-modulus modified model was found to be in good agreement with the experimental data.

2.2 Carbon Nanotube Atomic Structure

Carbon nanotubes are tubular structures typically of more than a few nanometers in diameter and hundreds of microns in length. They can be described as a graphene sheet rolled about a cylindrical axis, forming a tube-like structure. Unlike diamond, an allotrope of carbon with atoms arranged in a tetrahedral lattice (Sp^3 hybridized), carbon nanotubes are Sp^2 hybridized molecules arranged in a helical fashion (the Sp^2 forms a hexagonal lattice which is typical of graphene). The helicity and diameter of carbon nanotubes can be characterized in terms of the chiral vector and the chiral angle. The chiral vector (C_n) is defined by two integers (n, m) along the hexagonal lattice and two unit vectors (a_1, a_2) of the graphene sheet cylinder,

as shown in equation (2.1). The chiral angle (θ) is defined by the angle between the chiral vector and the zigzag direction of the graphene sheet [20].

$$\boldsymbol{Cn = na_1 + ma_2} \tag{2.1}$$

In terms of the chiral vector, nanotubes made from lattice of the form (*n*, 0) are referred to as zigzag nanotubes, in which some of the carbon-carbon (C-C) bond lie parallel to the tube axis, whereas those made from the lattice of the form (*n*, *n*) are referred to as armchair nanotubes, in which some of the C-C bonds lie crosswise to the tube axis. Nanotubes with lattice of the form (*n*, *m*, where $m \neq 0$ and *n*) are identified as chiral nanotubes. A schematic representation of a graphene sheet showing different ways to roll and form different tubule structures is shown in Figure 2a. In terms of the chiral angle, nanotubes having an angle equal to 0^o are referred to as zigzag nanotubes, while those having an angle equal to 30^o are referred to as armchair nanotubes. Those in-between such angles are described as chiral nanotubes. The difference conformations of armchair, chiral, and zigzag nanotube is shown in Figure 2b.

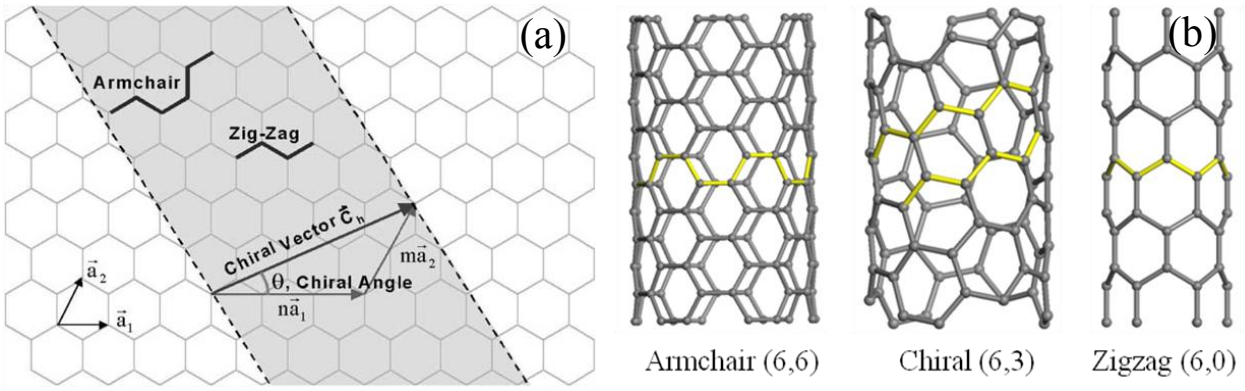

Figure 2. (a) Schematic diagram showing the chiral vector and the chiral angle in the honeycomb lattice of ghaphene [21], and (b) molecular models of the different conformations of carbon nanotubes: armchair, chiral, and zigzag.

Some authors have investigated the influence of chirality on the mechanical properties of carbon nanotubes. Yakobson et al. [22] employed molecular dynamic simulations to model the

morphological behavior of nanotube under compression, tension, and bending. Their simulations showed that carbon nanotubes were significantly resilient, sustaining high strain without brittleness or plasticity. Even though chirality had relatively minor influences on the elastic properties of nanotubes, the authors identified that the plastic deformation of nanotubes was ascribed to abrupt changes in morphological pattern. Such changes were described in terms of the Stone-Wales transformation, a reversible dislocation dipole in the honeycomb lattice that changes the structure to two pentagon-heptagon pairs, as shown in Figure 3. Troya et al. [23] performed quantum mechanical studies to simulate the fracture mechanism of carbon nanotubes. Their studies showed that the failing bonds lied within the pentagon rings. They also highlighted that tube chirality governed the effect of defect formation on the nanotube failure mechanisms and mechanical properties.

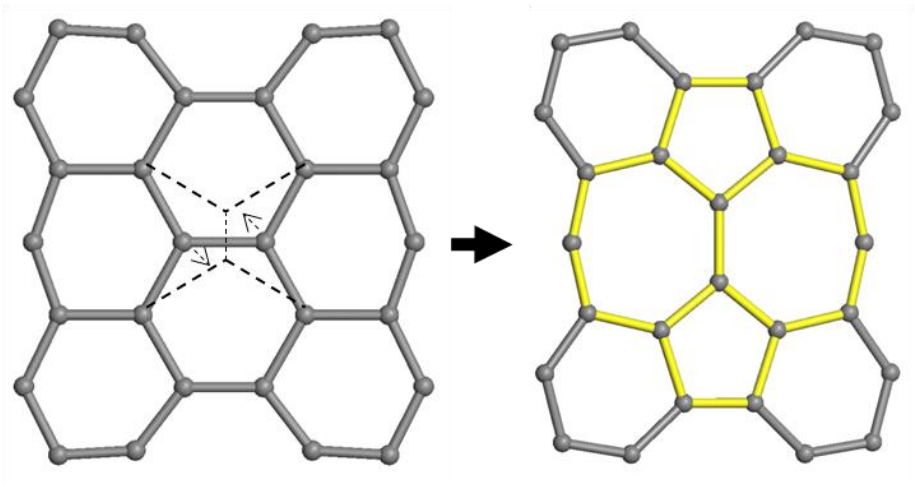

Figure 3. Stone-Wale diatomic interchange in a nanotube hexagonal wall.

As shown in Figure 3, the Stone-Wales transformation creates new defects in the nanotube structure. Such defects can considerably affect the properties of individual nanotubes. Hao et al. [24] investigated the influence of defects on the buckling properties of nanotubes by molecular dynamic simulation. Their findings showed that the carrying capability of nanotubes

depended on both the density of defects and the relative position of defects along the hexagonal lattice. They also concluded that defects were more significant in small tubes than in large ones. Lu et al. [25] used atomistic simulations to predict the elastic modulus, ultimate strength, and ultimate strain of a carbon nanotube with a pre-existing Stone-Wales defect and study the dependence of these properties on the loading rates. Their results indicated that the defected carbon nanotube broke at a much smaller elongation than the defect-free tube as well as that at small loading speed the effect of defect did not affect the Young's modulus considerably.

2.3 Carbon Nanotube Morphology

Besides the various tube morphologies resulting from defects, carbon nanotubes are classified in two categories, single-walled and multi-walled. Their atomic structures are shown in Figure 4.

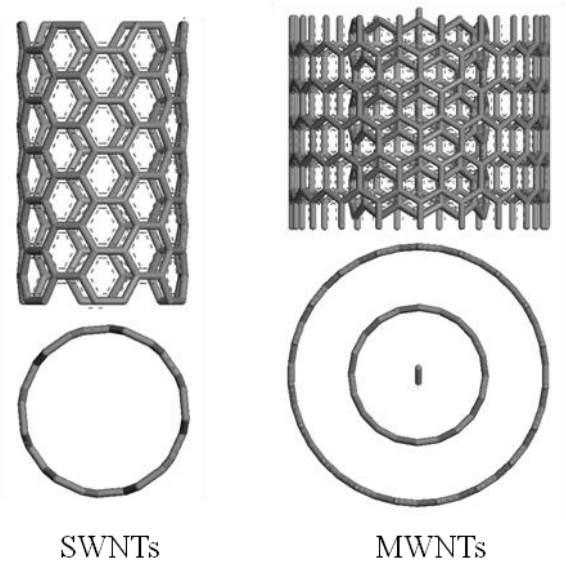

Figure 4. Structure of single-walled carbon nanotubes (SWNTs) and multi-walled carbon nanotubes (MWNTs).

Single-walled carbon nanotubes (SWNTs) are described as narrow seamless cylinders of nanoscale graphene with carbon atoms 1.42 Å apart, diameters between 1 and 2 nm [26], and lengths of up to several hundreds of microns. For defect-free single-walled carbon nanotubes the

Young's moludus is estimated to be between 990 and 1,105 GPa [27], the strength between 97 and 110 GPa [27] with a the density ranging from 1.33 to 1.4 g/cm^3 [28].

Multi-walled carbon nanotubes (MWNTs), on the other hand, can be envisioned as multishell structures of concentric tubes with intershell spacing similar to that of graphite interlayer spacing of 3.4 Å [29], outer shell diameter of more than 10 nm, and length up to several mm [30, 31]. The Young's modulus has been experimentally tested to be between 590 and 932 GPa [27], the strength between 35 and 82 GPa [27], and the density variety from 1.3 to 2.25 g/cm^3 [28].

2.4 Synthesis of Carbon Nanotubes

Since carbon nanotubes were recognized as a new and important form of carbon nearly two decades ago, different techniques have been developed to produce nanotubes. Such techniques include: electric arc-discharge [32-34], laser ablation [35, 36], gas-phase catalytic growth from carbon monoxide [37], and chemical vapor deposition (CVD) from hydrocarbons [31, 38, 39]. Arc-discharge and laser ablation methodologies entail condensation of carbon atoms that are produced from evaporation of solid carbon sources. The temperatures employed in these methods are near the melting point of graphite (3000-4000^{o}C). However, both methods present some processing limitations. The use of a finite source of carbon limits the volume of nanotubes produced. Hence, the costs associated with large-scale synthesis of nanotubes through these methods will make the cost of nanotubes prohibitive. Another issue with these methods is the high production of by-products such as catalyst particles, amorphous carbon, and non-tubular fullerenes. Therefore, additional purification processes are needed to remove the impurities and separate the nanotubes, increasing the production costs. The gas-phase techniques (catalytic growth and CVD), on the other hand, are highly promising for scale-up production of nearly-

defect free carbon nanotubes. They use a continuous source of carbon (gas) to produce large quantities of nanotubes at relatively low costs. The gas-phase catalytic growth from carbon monoxide is a refine process to grow bulk quantities of highly pure and randomly oriented single-walled carbon nanotubes [37]. Similarly, CVD is a mass production method that uses hydrocarbon gases as a continuous carbon source to produce both single-walled and multi-walled carbon nanotubes. This technique involves the dissociation of a high-carbon-content hydrocarbon gas (Methane, Ethylene, etc) in the presence of an active catalyst (transition-metal nanoparticles formed on a support material such as alumina) at elevated temperatures (from 700^{o}C to 1000^{o}C) [40]. The dissociated carbon atoms are catalyzed and dissolved by the transition-metal and precipitated to form carbon nanotubes. One unique feature of this method is the ability to grow aligned arrays of carbon nanotubes with control diameter and length [38, 41].

2.5 Mechanical Properties of Carbon Nanotubes

The mechanical properties of carbon molecules are mainly related to the nature of their bond structures, C-C single bond, C-C double bond, and C-C triple bond. When carbon atoms are arranged to form a graphene-like structure, sp^2 hybridization occurs. Such orbital hybridization provides the strength of carbon molecules and in particular carbon nanotubes. As such, since the structure of defect-free carbon nanotubes is composed primarily of sp^2 bonds (C-C double bond), they are expected to be strong along their axes direction. In fact, several simulations have been carried out to predict the strength of individual nanotubes. Meo et al. [42] investigated the influence of tube diameter and chirality on the Young's modulus of single-walled carbon nanotubes of different sizes using a finite element model. Their results showed an average Young's modulus of 915 GPa, which was in agreement with numerical and experimental values reported in the literature. Later, the same group [43] reported the failure evolution of both

zigzag and armchair carbon nanotubes under uniaxial tensile loading, showing the complete load-displacement relationship curve of both nanotubes up to failure. Their results showed tensile strength of 94 GPa and 123 GPa for zigzag and armchair nanotubes, respectively. In addition, the authors reaffirmed the strong dependence of the ultimate stress on the chirality of nanotubes. Bending dominated failure in the case of zigzag, while shear dominated in the case of armchair nanotubes. Ragab et al. [44] also computed the stresses in an armchair single-walled carbon nanotube under uniaxial tension by molecular dynamics and concluded that the length of carbon nanotubes could affect the value of maximum stress by about 10%.

Besides simulation studies, some experimental investigations have been performed to measure the strength of carbon nanotubes. Peng et al. [27] reported the first direct measurements of single shell failure for multi-walled carbon nanotubes using an *in situ* transmission electron microscopy (TEM) method and a microelectromechanical tensile testing systems. Their results showed the failure cross-section of multi-walled carbon nanotubes as well as the effect of cross-linking between shells in the maximum sustainable load. Recently, Locascio et al. [45] employed the same techniques used by Peng to tailor the load carrying capability of multi-walled carbon nanotubes through inter-shell bringing. They proved that irradiation-induced cross-linking was indeed a tunable mechanism by which load could be transferred to various shells of multi-walled carbon nanotubes. Moreover, their computational studies showed that in highly cross-linked tubes the maximum stress occurred at the outermost shell, suggesting that failure would occur from the outside in.

2.6 Nanotube/Polymer Composites

Since the first publication of carbon nanotubes (CNTs) in 1991 [32], numerous research has been oriented toward developing hybrid (carbon nanotube/polymer) materials with superior

mechanical and functional properties [46, 47]. Enhancement of the mechanical properties (tensile, compressive and shear strength) of polymeric compounds by the addition of carbon nanotubes can be achieved when a good interaction between the nanoscale material and the polymer matrix takes place [48]. However, due to the exceptional structure of CNTs, particular processing challenges arise when embedding nanoscale materials into a polymer matrix. Thostenson et al. addressed some of the critical issues in the processing of CNT polymer composites in their review [21]. These are mainly attributed to dispersion of CNTs in the matrix and load transfer between the CNTs and the matrix by molecular bonding [49].

One of the most significant challenges associated with CNTs is their dispersion and exfoliation into polymeric materials. At the nanometer scale, interatomic forces (Van der Waal forces) are intensified due to the large specific surface area of CNTs. Such forces make the nanotubes pull towards each other, forming agglomerates that both reduce the reinforcement aspect ratio and create weak interfacial interaction with the matrix system. Therefore, different techniques are needed in order to effectively disperse nanotubes within the polymer matrix and obtain interfacial interaction that can lead to considerable load transfer from the matrix to the particles.

The dispersion of single-walled carbon nanotubes (SWNTs) or multi-walled carbon nanotubes (MWNTs) into a polymer matrix has been found to be challenging due to agglomeration of nanotubes as a result of Van der Waal interactions. Several techniques have been reported in the literature to disperse the nanotubes and improve the interfacial interaction between the CNTs and the polymer resin. These include: solution chemistry to functionalize the CNT surface [50-52], the use of polymers like surfactants to coat the CNT surface [53, 54], *in situ* polymerization [55, 56], ultrasonic dispersion [48, 57], and mechanical mixing [58, 59].

Gojny et al. [60] used a calendering approach to untangle and disperse double-walled carbon nanotubes (DWNTs) in a polymer matrix, obtaining a moderate increase in mechanical properties. Zaragoza et al. [61] carried out an *in-situ* suspension polymerization along with sonication to synthesize multi-walled carbon nanotubes/polystyrene composites. Their findings highlighted the effect of strong cavitation forces induced by sonication during the CNT dispersion and suggested that possible decrease of storage modulus in the reinforced nanocomposite could occur as a result of CNT fragmentation. Lijie et al. [62] employed solution dispersion, sonication, and mechanical stirring to evaluate the reinforcement role of carbon nanotubes in different matrix stiffness. Results showed contributions to the mechanical properties of composites even though poor interface interaction between the carbon nanotubes and the matrix was observed. Chow et al. [63] correlated the flexural strength and fracture toughness of epoxy/CNT nanocomposites with the loading of nanotubes and the mixing method. They emphasized that sonication could be a good approach to disperse CNTs and obtain enhanced mechanical properties. Thostenson et al. [64] studied the mechanical properties of highly aligned and randomly oriented polystyrene nanocomposite films fabricated using a twin-screw extruder. Their results showed an increase in Young's modulus of about 45% for the aligned composites with respect to the randomly oriented composites with the addition of CNTs. Park et al. [65] established a correlation between the dispersibility of MWNTs in composites by chemical and calendering routes. They concluded that the presence of carboxylic acid groups on the MWNT surface contributed to the separation and stabilization of nanotubes in the composite matrix. Yang et al. [66] investigated the functionalization effects on the structure and morphology of MWNTs and epoxy composites. Their results showed a significant increase in impact and bending strength (89% and 29%, respectively) compared to the pure epoxy matrix.

Frankland et al. [67] proved by molecular dynamic simulation that the shear strength of a polymer-nanotube interface with low interaction could be increased by more than an order of magnitude when chemical bonds between the nanotube and the matrix exit, highlighting the significance of functionalization in the achievement of strong CNT-matrix interface. Shiren et al. [68] investigated the characteristics of interface and load transfer between the functionalized SWNTs and the polymer matrix throughout dynamic Raman spectroscopy. They indicated that large slope values in the G band described strong interfacial bonding between the CNTs and the matrix that could lead to efficient mechanical load transfer.

Although improvements in mechanical properties have been reported throughout various nanotubes/polymer composites, there is still a lot of discrepancy between the results reported and the results predicted. Rio et al. [69] applied the Cox-Krenchel, Halpin-Tsai and Mori-Tanaka micromechanical models to their SWNT nanocomposites and found that the models overestimated the effect of reinforcement. They attributed the large difference mainly to waviness as well as curvature of embedded nanotubes and concluded that such nanotube geometries could decrease the effect of stiffness of the nanotubes relative to straight nanotube models.

2.7 Nanomaterial/Potting Compounds

Some efforts have been made toward enhancing the mechanical properties of potting compounds by the incorporation of nano-scale materials such as nanoclay, carbon nanofibers, and carbon nanotubes. Woldensenbet et al. [70] studied the effects of nanoclay reinforcement and microballoon radius ratio on the flexural properties of potting compounds. Their findings showed an increase in shear and bending stress with respect to the plain structures. Baalman et al. [71, 72] investigated the compressive properties of a potting compound by the incorporation

of carbon nanofibers, multi-walled carbon nanotubes, and fullereness and found considerable increase in compressive properties with respect to the neat compound. Li et al. [73] dispersed multi-walled carbon nanotubes and glass microballoons into shape memory polystyrene to fabricate self-healing smart syntactic foams. Their results showed that the impact tolerance and load carrying capability of the material could be healed after multiple impact tests. Dimchev et al. [74] observed an increase in tensile strength and modulus of hollow particle filled composites with the addition of 0.25 wt% carbon nanofibers. However, the compressive strength results obtained in their study decreased significantly due to microballoon crushing. Gupta et al. [75] observed a decrease in compressive strength of hollow particles filled composites with the addition of 2% nanoclay and attributed such decrement to the presence of nanoclay clusters in the specimens. However, they obtained an increase in toughness between 80% and 200% with the addition of nanoclay in the same compounds.

CHAPTER 3

TECHNICAL APPROACH

3.1 Materials

In this investigation, two commercially available potting compounds were used. The first potting compound used was Cytec's Corfil 625-1, which is a lightweight one-part composite made from a mixture of a polymer matrix (resin) and hollow particles of silica (microballoons). The second potting compound used was 3M's EC-3500, which is a high performance two-part epoxy system designed for reinforcing honeycomb core. The epoxy is mixed with the hardener at a mixing ratio of 2:3 by weight. The physical and mechanical properties of Corfil 625-1 and EC-3500 are shown in Table 1, as provided by their manufactures. The resin of Corfil 625-1 without microballoons and accelerator was obtained separately and used as the base polymer in which the CNTs would be exfoliated and dispersed. According to the manufacture's specifications, this resin contains prepolymers with phenyl glycidyl ether end groups as well as anhydride molecules. As such, the polymerization is believed to proceed in the following manner. The catalyst joins the epoxide group present in the chain to give an active hydroxyl group. Then, the anhydride molecule reacts with the hydroxyl group to form cross-linking. A schematic of the polymerization reaction is depicted in Figure 5.

TABLE 1

PROPERTIES OF CORFIL 625-1 AND EC-3500

Material	Density (kg/m^3)	Compressive strength (MPa)	Lap shear strength (MPa)
Corfil 625	400 - 496.6	20.7	-
EC-3500	640.7	41.36 - 62.05	~ 6.5

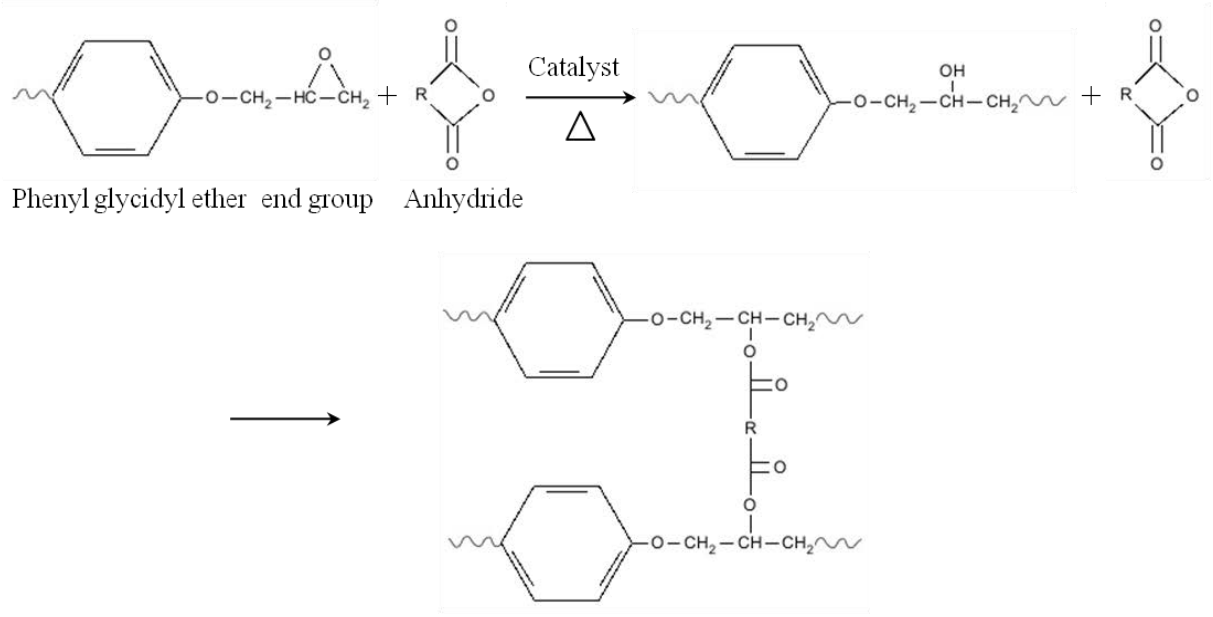

Figure 5. Polymerization of Corfil 625-1.

For the manufacturing of nanocomposites, four different types of Scotchlite^{TM} hollow glass microballoons manufactured and supplied by 3M were employed. Their mechanical properties are provided in Table 2.

Single-walled and multi-walled carbon nanotubes produced by chemical vapor deposition (CVD) were obtained from SES research and Cheap Tubes Inc., respectively. The single-walled carbon nanotubes (SWNTs) used in this investigation have an outer diameter of less than 2 nm, a length range of 5-15 μm, purity of more than 90 wt% carbon nanotubes and more than 50 wt% SWNTs, ash content of less than 2 wt%, and amorphous carbon of less than 5 wt%, as provided by the vendor. The multi-walled carbon nanotubes (MWNTs) used have an outer diameter of 20-30 nm, an inside diameter of 5-10 nm, a length range of 10-30 μm, purity of more than 95 wt%, ash content of less than 1.5 wt%, and specific surface area of 100 m^2/g, as provided by the vendor.

All the chemicals used in this investigation were obtained from Fisher Scientific and used as-received.

TABLE 2

PROPERTIES OF GLASS MICROBALLONS

Microballoon	Density (kg/m^3)	Compressive strength (MPa)
S15	149.93	2.07
S38HS	379.96	37.92
S60HS	600.05	124.11
H50	499.94	68.95

3.2 Experimental Studies

In order to investigate the effect of microballoons and nanotubes on the physical and mechanical properties of a potting compound, two studies were carried out. In the first study, four different types of glass microballoons were combined with the resin to obtain potting compounds with various densities and strengths. In the second study, carbon nanotubes (CNTs) were incorporated into two potting compounds selected from the previous study with the aim at investigating their effect on density and strength.

3.2.1 Effect of Microballoon Type and Concentration on the Physical and Mechanical Properties of Potting Compounds

To evaluate the effect of microballoons on the physical and mechanical properties of the potting compound (Corfil 625-1), several specimens were prepared by mixing the base resin with silica glass microballoons of different strength and density. The aim was to attain one-part potting compounds with properties equivalent to those of EC-3500. The configuration of each specimen depended on variables (factors) defined using a design of experiments approach (DOE-I) with resolution 1 (Appendix A). The objective of this DOE-I was to define the minimum number of experiments needed to identify major cause-effect relationships between a given set of factors that could affect the performance of potting compounds. The factors were defined as

following: (1) type of glass microballoons, and (2) concentration of microballoons (percentages by weight -wt%-).

From this study, two different combinations of potting compounds were chosen to further investigate the effect of nanotube reinforcement on their properties. The compounds were selected based on the values of density and strength obtained after mechanical testing.

3.2.1.1 Microballoon Sample Preparation

For the manufacturing of potting compounds, 30g of resin were added to a 250 ml beaker and mixed by mechanical stirring with the accelerator at a mixing ratio of 74:7 by weight, according to the instructions provided by the vendor. The silica glass microballoons were subsequently added to the mixture resin-accelerator following the parameters defined in the DOE-I. The resulting mixture was hand-mixed for about 15 minutes to obtain a uniform dispersion.

3.2.2 Effect of Carbon Nanotubes on the Physical and Mechanical Properties of Potting Compounds

To evaluate and understand the effect of CNT addition on the density, compressive and lap shear strength of potting compounds, a second design of experiments (DOE-II) with resolution 4 was developed. Details are provided in Appendix B. Eight critical factors were studied in a series of 35 tests. The factors are described in Table 3.

In order to address the surface modification of nanotubes (factors E and F in Table 3), SWNTs and MWNTs were functionalized with the purpose of creating active sites (organic moieties) on their surface(s) that could interact with the epoxide groups of the resin, creating inter-molecular linkages. The methodology of functionalization is described in the following subsection.

TABLE 3

FACTORS FOR THE DOE-II

	Variables	-1	1	0
A	Nanotubes (wt%)	0.5	1.5	1.0
B	Mixing time (min)	20	30	25
C	Vacuum (kPa)	0.2	97.5	48.8
D	Sonication power (W)	5	10	8
E	Acid time (min)	60	240	120
F	Acid temp (^{o}C)	60	90	75
G	Nanotube type	SWNTs	MWNTs	MWNTs
H	Bead type	A	B	B

To disperse SWNTs and MWNTs within the polymer matrix, three techniques were employed: ultrasonic, calendering, and centrifugal mixing. The parameters upon which carbon nanotubes were dispersed and exfoliated in the polymer matrix are detailed in Appendix B. The ultrasound mixing was performed using a sonicator equipped with a cup-horn. The calendering mixing was carried out using a commercially available laboratory scale three roll mill, consisting of three stainless steel rolls of about 80 mm in diameter. The small gaps (5-100 μm) as well as mismatch angular velocity (9:3:1) between the rollers result in high shear forces that enable CNTs to be unraveled and dispersed in polymeric materials. The traditional configuration of the three roll mill is shown in Figure 6a. The centrifugal mixing, a non-contact mixing technique, was performed using a vacuum centrifugal mixer, as shown in Figure 6b. This technique combines vacuum along with acceleration forces (centrifugal and revolving forces) to disperse nanoscale particles in polymeric compounds. During this process, a mixture CNT-resin revolves and rotates at a 2:1 fixed ratio and at speeds up to 2000 RPM while it is contained in a vacuum chamber that can apply pressures from 0.2 kPa to 97.5 kPa. Putting it differently, the container is spun around the center of the chamber while it is rotating around its central axis. These effects

generate forces of more than 400 times the force of gravity, causing kneading effects that expulse air out of the compound and create uniform dispersion.

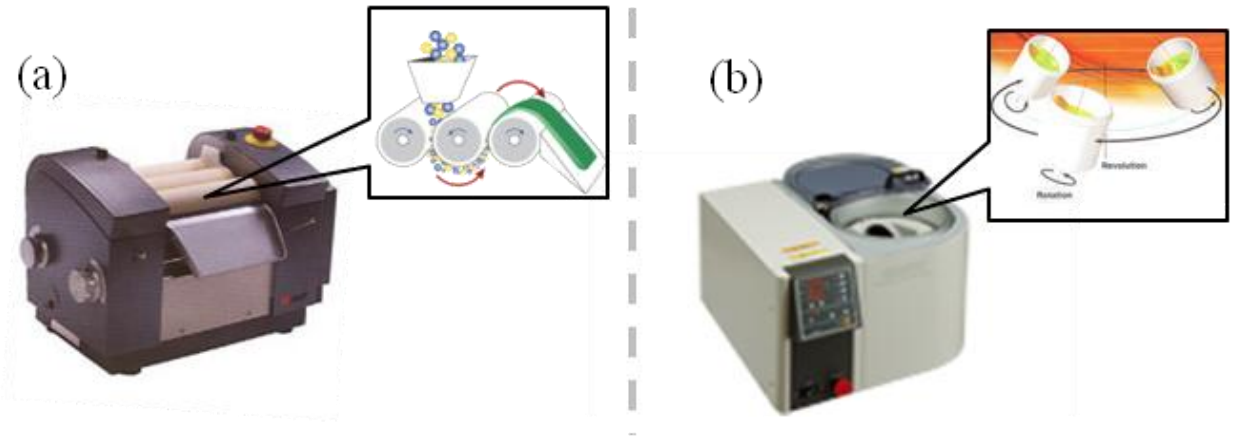

Figure 6. Traditional configurations of (a) the three roll mill from EXAKT [76], and (b) the vacuum centrifugal mixer from THINKY [77].

3.2.2.1 Functionalization Scheme

The functionalization of SWNTs and MWNTs was performed through a three-step process: purification, thermal oxidation, and carboxylation. The purification of SWNTs and MWNTs involved the oxidation with nitric acid (HNO_3) at 126^{o}C for 120 minutes. For this step, 2.0 grams of either as-received SWNTs (AR-SWNTs) or as-received MWNTs (AR-MWNTs) were mixed with HNO_3 and sonicated at maximum power (156 W) for 30 minutes. The solution (CNT-HNO_3) was refluxed, diluted in deionized water, and filtered via membrane microfiltration until the excess acid was completed removed (pH of filtrate ~7). After drying in vacuum for 10 h, the purified nanotubes (P-SWNTs or P-MWNTs) were air oxidized at 550^{o}C for 30 minutes to remove residual amorphous carbons. The oxidized carbon nanotubes (O-SWNTs or O-MWNTs) were subsequently functionalized using a 3:1 v/v mixture of 98% sulfuric acid (H_2SO_4) and 68% nitric acid (HNO_3) under vigorous stirring at the temperatures and times showed in Table 4. The resulting carboxylic acid nanoparticles (F-SWNTs or F-MWNTs) were filtered and washed

following the aforementioned procedures and dried overnight in a vacuum oven at 75°C. After the period elapsed, the functionalized CNTs (F-CNTs) were stored inside a desiccant box until further use.

TABLE 4

REFLUXING TIME AND TEMPERATURE FOR FUNCTIONALIZATION OF SINGLE-WALLED AND MULTI-WALLED CARBON NANOTUBES

Functionalized Nanotubes	**Refluxing Time (min)**	**Temperature (°C)**
F-SWNTs	60	60
F-SWNTs	60	90
F-SWNTs	240	60
F-SWNTs	240	90
F-MWNTs	60	60
F-MWNTs	60	90
F-MWNTs	150	75
F-MWNTs	240	60
F-MWNTs	240	90

3.2.2.2 Nanocomposite Sample Preparation

For the sample preparation, the F-CNTs were initially mixed with 40 ml of acetone and dispersed in 30g of resin using ultrasound. The acetone was removed by heating the CNT-resin mixture for 60 minutes to just above the boiling point of acetone (56.53°C). This preserved the initial dispersion of CNTs in the polymer matrix and removed at least 97% of the acetone added. Subsequently, the mixture was allowed to cool to room temperature before degassing it for 5 minutes at full vacuum (0.2 kPa) at speed of 2000 RPM using the centrifugal mixer. This step removed the residual solvent present in the matrix yielding a compound free of acetone. High shear mixing was then used to disperse and break the remaining CNT aggregates present in the resin after the sonication process. For this step, the nanocomposite mixture was run through the three roll mill 2 times. The gaps and number of times were varied in a ratio 2:1 (Table 5). Once

the final product from the mill was collected, it was mixed with the accelerator and with one of the two combinations of glass microballoons chosen from the DOE-I (either A or B) using the centrifugal mixer according to the factors set in the DOE-II.

TABLE 5

THREE ROLL MILL SET UP

Times through the Mill	Feed Roller (μm)	Center Roller (μm)	Speed (RPM)
1	20	10	150
2	10	5	300

3.3 Mechanical and Physical Characterization Methods

Prepared mixtures of resin-glass microballoons, CNT-resin-glass microballoons, Corfil 625-1, and EC-3500 were cast to produce both compression and lap shear test specimens. Compression specimens were potted in cylindrical molds (12.7 mm diameter, 50.8 mm length) and cured at 177ºC for 60 min in a hot press. After removing the specimens from the mold, they were ground down to a length of 25.4 mm, as shown in Figure 7a. The specimens were then tested according to ASTM D 695-02a [78]. Lap shear specimens were prepared according to ASTM D 1002-05 [79] using aluminum coupons and cured following the same cure cycle for the compression samples. A diagram of a lap shear specimen is depicted in Figure 7b.

For each test method, a total of 8 compression and 10 lap shear specimens were prepared and separated into two halves. The first half of specimens (4 compression and 5 lap shears) was tested under dry conditions at room temperature, and the average strength along with its standard deviation was calculated and reported. The compression specimens were also used for density measurements before mechanical testing. The other half was subjected to hygrothermal conditioning for 30 days at 71^{o}C and 85% relative humidity (RH). The moisture content of the specimens was measured based on weight changes. For weight measurement, the specimens

were taken out of the hot/wet chamber, rapidly weighed and quickly returned to the chamber so that desorption of moisture was kept to a minimum. The maximum length of time during which each specimen was out of the environmental chamber was 2 min. Specimens were always measured in the same manner using a Mettler Toledo analytical balance with an accuracy of 0.1 mg. After the conditioning period elapsed, the hot/wet specimens were removed from the hygrothermal atmosphere and quickly placed into an environmental test box already heated to 82^{o}C. Before testing, the specimens were heated inside the test chamber for 5 minutes to reach thermal equilibrium and to retain enough moisture at the time of failure. The specimens were tested inside the environmental test chamber, and the average strength together with its standard deviation was calculated and reported.

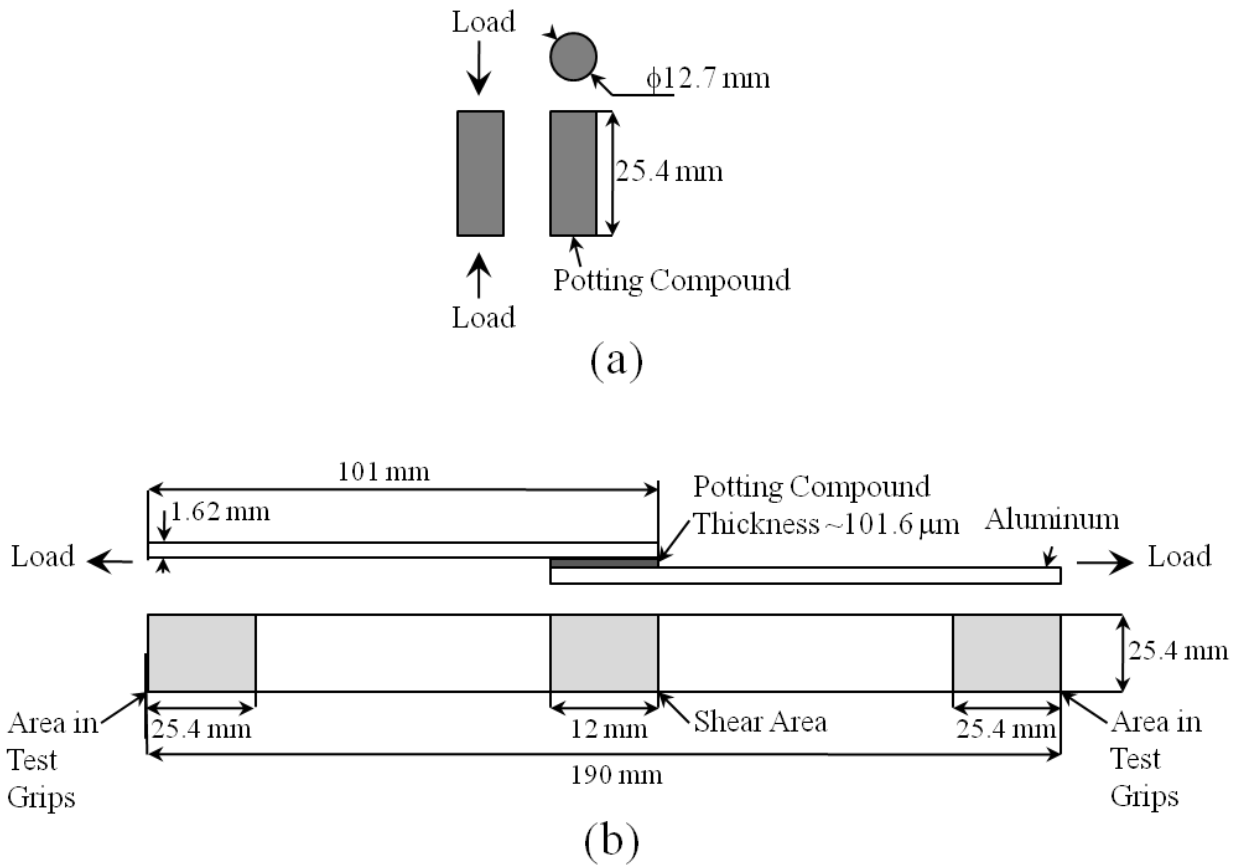

Figure 7. (a) Compression and (b) lap shear specimens.

CHAPTER 4

RESULTS AND DISCUSSION

4.1 Characterization of Functionalized SWNTs and MWNTs

The presence of functional groups on the surface(s) of SWNTs and MWNTs was confirmed by fourier transform infrared (FTIR) spectroscopy and thermo-gravimetric analysis (TGA). Their analysis is detailed herein.

4.1.1 FTIR Spectroscopy of SWNTs and MWNTs

The existence of different functional groups on the surface(s) of SWNTs and MWNTs was initially investigated by FTIR spectroscopy. Spectra of the different functionalization methods performed for both CNTs are shown in Figure 8 and Figure 9, respectively. The spectra were recorded in the absorbance mode over the range 400-4000 cm^{-1}. Spectra of AR-SWNTs and AR-MWNTs showed featureless plots distinctive of carbon materials without organic or inorganic impurities grafted on their surface(s). Spectra of F-SWNTs and F-MWNTs exhibited characteristic bands at ~3000 cm^{-1}, ~1730 cm^{-1} and ~1200 cm^{-1}, corresponding to hydroxyl (-OH) and carbonyl (-C=O) stretchings and carbon single bond oxygen (-C-O) bending vibrations, respectively. The observed modifications in the spectra indicate that molecular vibrations associated with carboxylic acid functional groups (-COOH) grafted to either the wall(s) or the ends of the tubes are present after acid treatment.

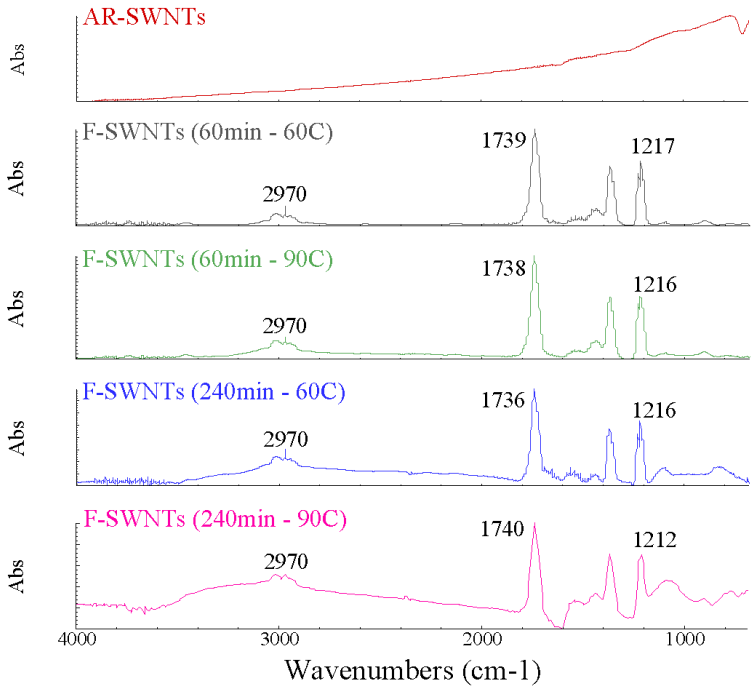

Figure 8. IR spectra of as-received SWNTs (AR-SWNTs) and functionalized SWNTs (F-SWNTs) at different times and temperatures.

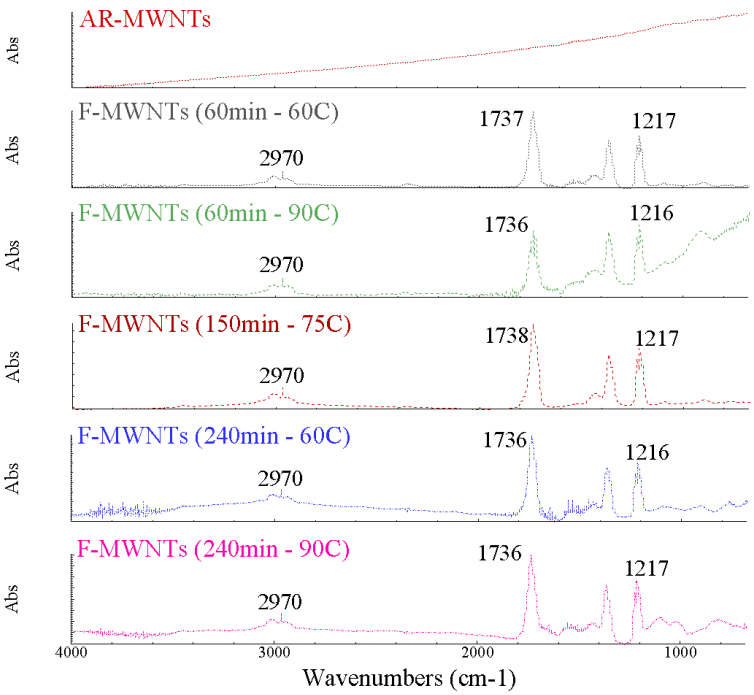

Figure 9. IR spectra of as-received MNWTs (AR-MWNTs) and functionalized MWNTs (F-MWNTs) at different times and temperatures.

4.1.2 TGA of SWNTs and MWNTs

Further confirmation of the presence of impurities on the surface(s) of CNTs could be inferred by TGA. The analyses were performed in a Nitrogen atmosphere at a ramp rate of 10^{o}C/min and a temperature sweep between 40^{o}C and 1000^{o}C. TGA plots of SWNTs and MWNTs are shown in Figure 10 and Figure 11, respectively. Both the AR-SWNTs and the AR-MWNTs showed a negligible weight loss characteristic of unmodified CNTs. On the contrary, F-SWNTs and F-MWNTs showed an initial weight loss of 12% and 8%, respectively, between 50^{o}C and 130^{o}C attributed to moisture absorbed by the CNTs after the functionalization procedure. A weight loss of about 19% for F-SWNTs and 16% for F-MWNTs between 200^{o}C and 400^{o}C suggested that COOH groups were present on the surface(s) of CNTs [80]. Furthermore, an increase in weight loss was observed when more hydrophilic groups were depleted from the surface(s) of CNTs upon heating. Such trend could be accredited to the different functionalization procedures performed. Therefore, the higher temperature and the longer time of functionalization, the higher amount of organic groups grafted on the surface(s) of CNTs.

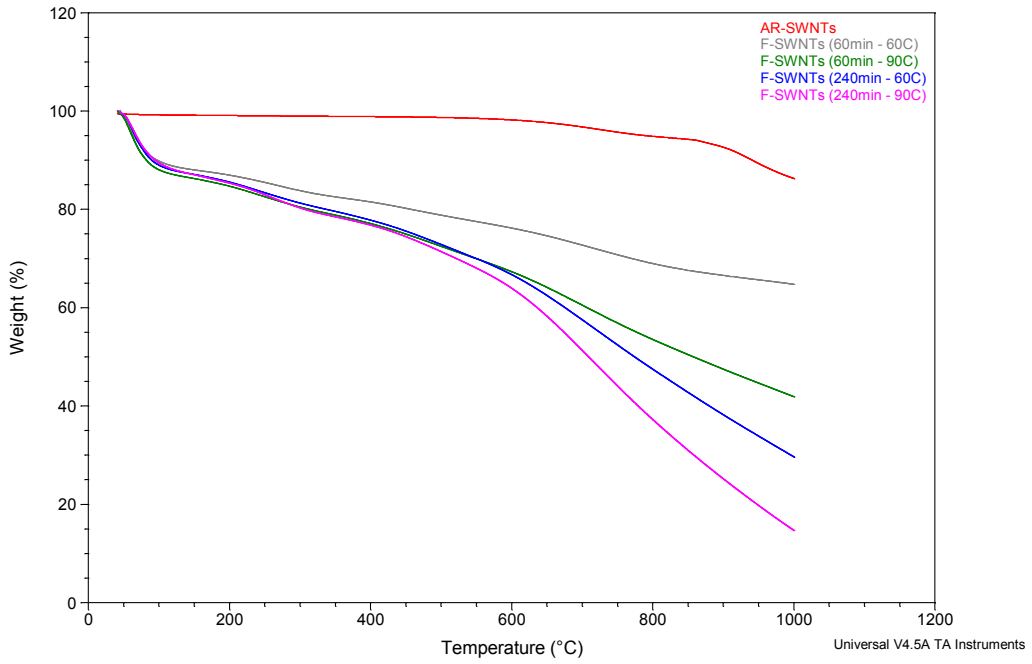

Figure 10. TGA plots of as-received SWNTs (AR-SWNTs) and functionalized SWNTs (F-SWNTs) at different times and temperatures.

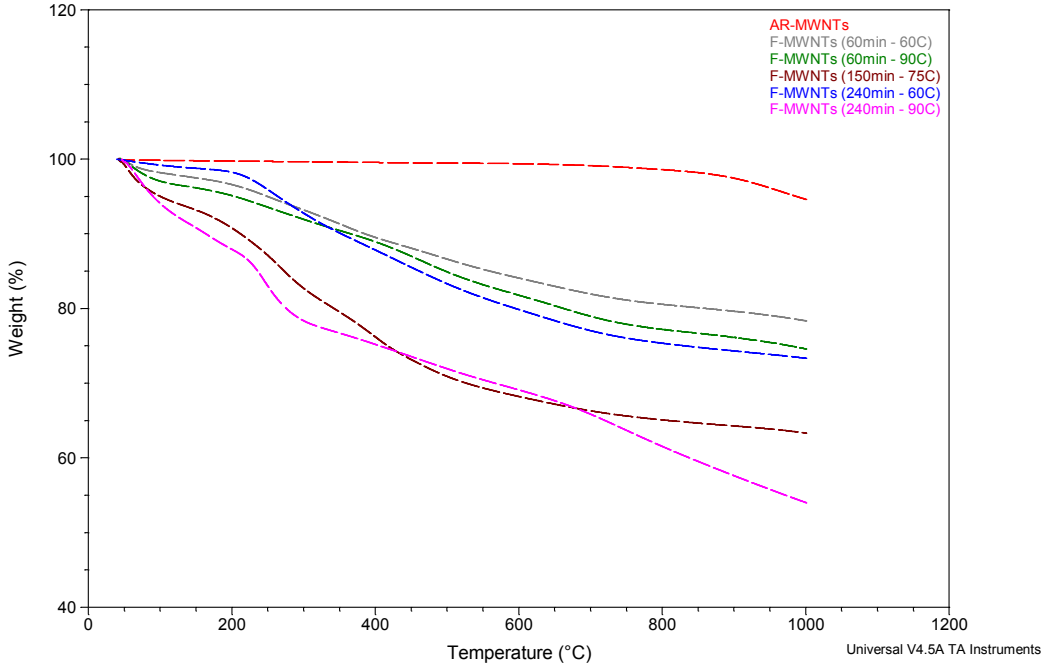

Figure 11. TGA plots of as-received MWNTs (AR-MWNTs) and functionalized MWNTs (F-MWNTs) at different times and temperatures.

4.2 Effect of Microballoon Type and Concentration on the Physical and Mechanical Properties of Potting Compounds

Four different types of glass microballoons were mixed with the base resin to obtain compounds with properties similar to those of EC-3500. Tests were conducted under dry conditions at room temperature (RT) to determine if the desired potting compound properties could be obtained through the use of microballoons alone. The results are shown for all possible combinations of microballoon specimens made following the DOE-I (Figure 12, Figure 13 and Figure 14). The high compressive and lap shear strength (100.9 MPa and 18.75 MPa, respectively) of the potting compounds containing high-density glass microballoons (H50) suggested that a one-part potting compound with strength higher than that of EC-3500 could be manufactured; however, the density (751.85 kg/m^3) was approximately 16% higher than the desired one (between 608.7 and 688.7 kg/m^3).

When 5 wt% of the low-density microballon (S15HS) was mixed with H50, a decrease of 15% in density, 36% in compressive strength and 34% in lap shear strength was observed. These results indicated that the failure of the potting compounds depended on the properties of the weakest microballoons present in the material.

The compounds containing 45 wt% S38HS & 5 wt% S60HS, compound #2, and 45 wt% H50 & 5 wt% S15HS, compound #11, gave results very similar to those of EC-3500 with a density of 652.86 kg/m^3 and a compressive and lap shear strength of 72.3 MPa and 13.89 MPa, respectively. Based on these results, the sample fabricated with 45 wt% S38HS & 5 wt% S60HS microballoons (#2) was chosen as the first standard to be modified with nanotubes. From here on, this microballoon combination would be referred to as compound **A**. This formulation (S38HS & S60HS) has proven to have mechanical properties similar to those of EC-3500

(density of 635.76 kg/m^3, compressive and lap shear strength of 75.02 and 13.32 MPa, respectively) but in the desired form of a one-part potting compound. According to these results, this compound could be used to replace EC-3500, giving the same performance while eliminating the difficulties associated with handling two-part potting compounds.

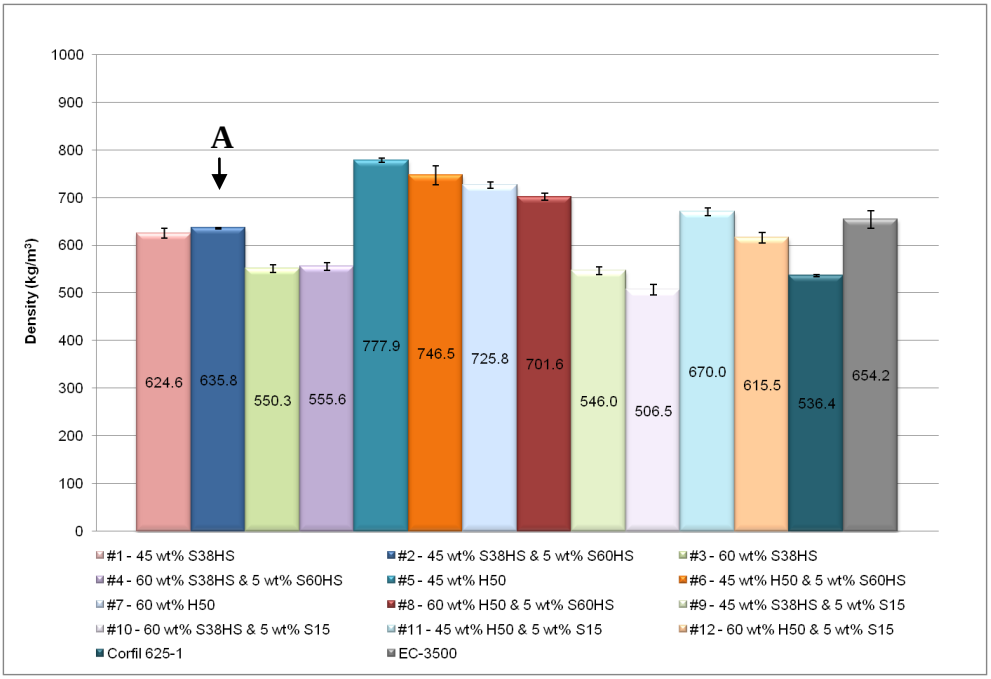

Figure 12. Density results for the glass microballoon specimens tested at RT.

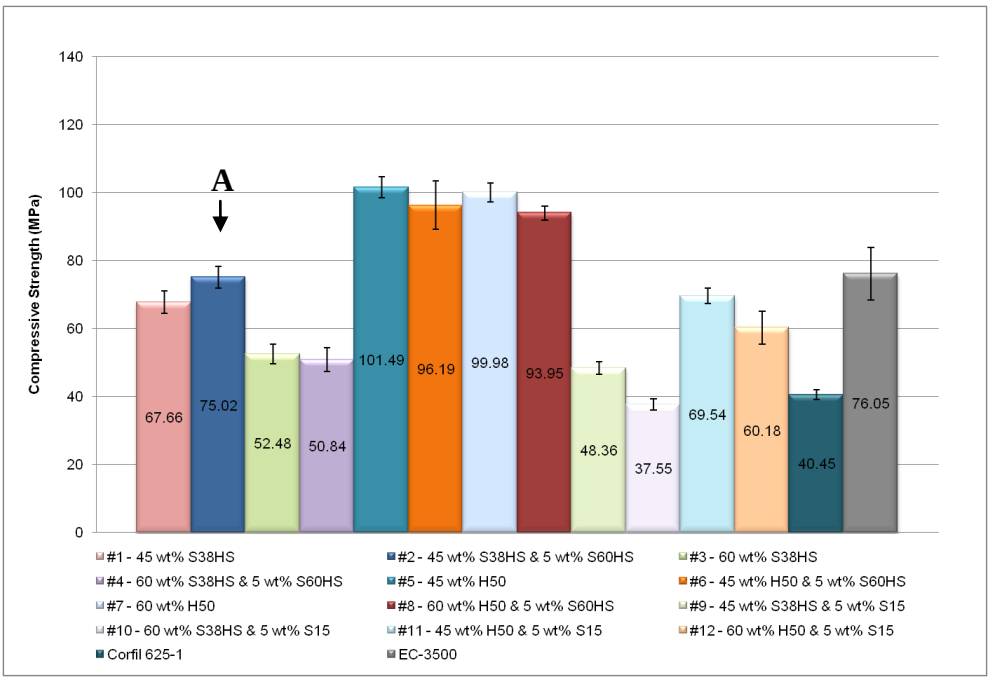

Figure 13. Compressive strength results for the glass microballoon specimens tested at RT.

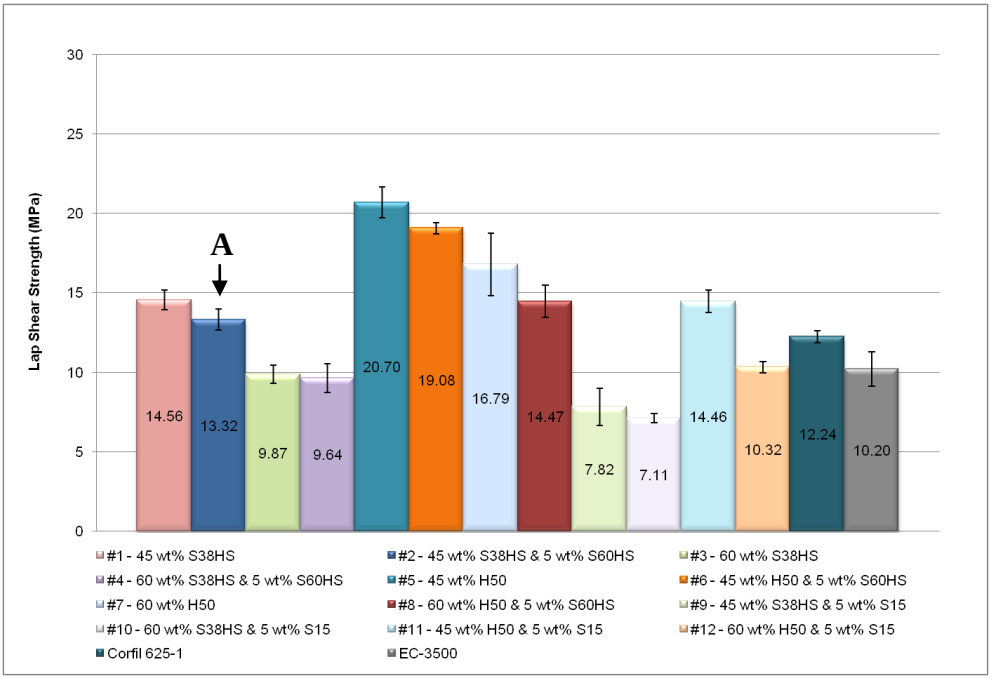

Figure 14. Lap shear strength results for the glass microballoon specimens tested at RT.

4.3 Effect of Microballoon Type and Concentration on the Physical and Mechanical Properties of Potting Compounds Subjected to Hot/Wet Conditions

Results of the hot/wet compression and lap shear testing can be observed in Figure 15 and Figure 16, respectively. A decrease of 64% and 35% in compressive and lap shear strength was observed for all compounds tested with respect to their counterpart at RT, respectively. Based on these results, the second combination of silica glass microballoons (60 wt% H50 & 5 wt% S60HS) was selected. Henceforth, such combination would be referred to as compound **B**. This formulation showed compressive and lap shear strength values relatively close to the ones observed for EC-3500 after conditioning for 30 days. Although the density of this compound (#8) is 7.2% higher than that of EC-3500, as shown in Figure 12, it represents a good alternative to further understand the mechanical properties of potting compounds after being mixed with carbon nanotubes. Under dry conditions at RT, the aforementioned formulation has not only higher compressive and lap shear strength (93.95 MPa and 14.47 MPa, respectively) than EC-3500 but also the lowest density compared to the specimens containing the high-density microballoons (H50). A more representative way to detail the compounds to be used in the next study is shown in Table 6.

TABLE 6

MECHANICAL AND PHYSICAL PROPERTIES OF COMPOUNDS A, B, CORFIL 625-1, AND EC-3500

Compound		**Density (kg/m^3)**	**Compressive strength (MPa)**		**Lap shear strength (MPa)**	
Type	Name		RT	Hot/wet	RT	Hot/wet
45 wt% S38HS & 5 wt% S60HS	**A**	635.8	75.02	27.45	13.32	8.76
60 wt% H50 & 5 wt% S60HS	**B**	701.6	93.95	33.35	14.47	10.71
Corfil 625-1	**625-1**	536.4	40.45	17.62	12.24	10.58
EC-3500	**EC-3500**	654.2	76.05	37.81	10.20	6.12

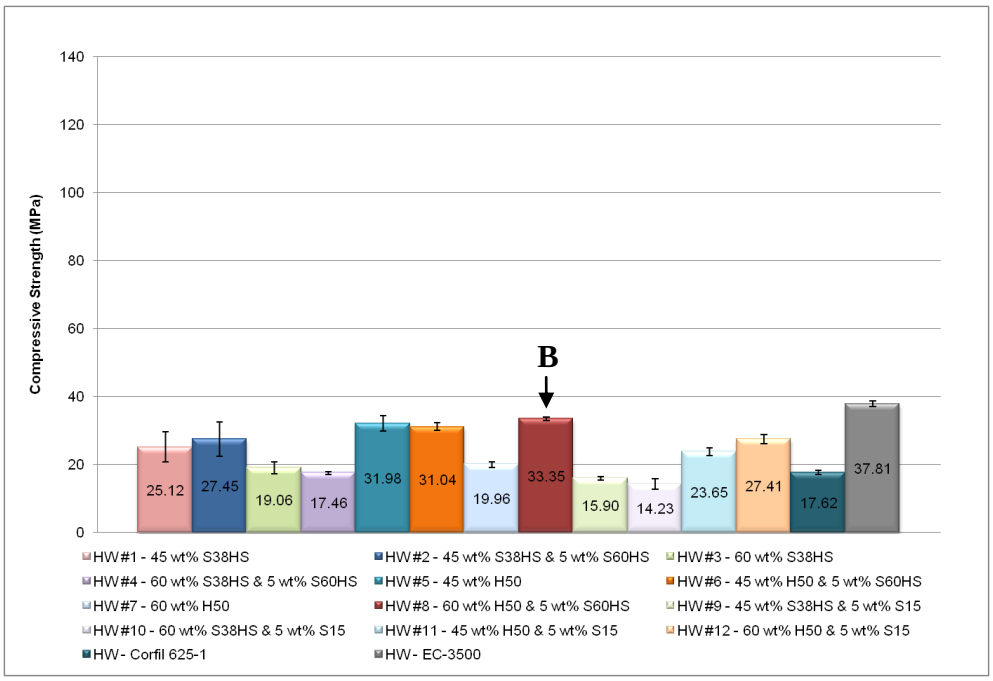

Figure 15. Compressive strength results for the glass microballoon specimens conditioned at 71°C and 85% RH, and tested at 82°C.

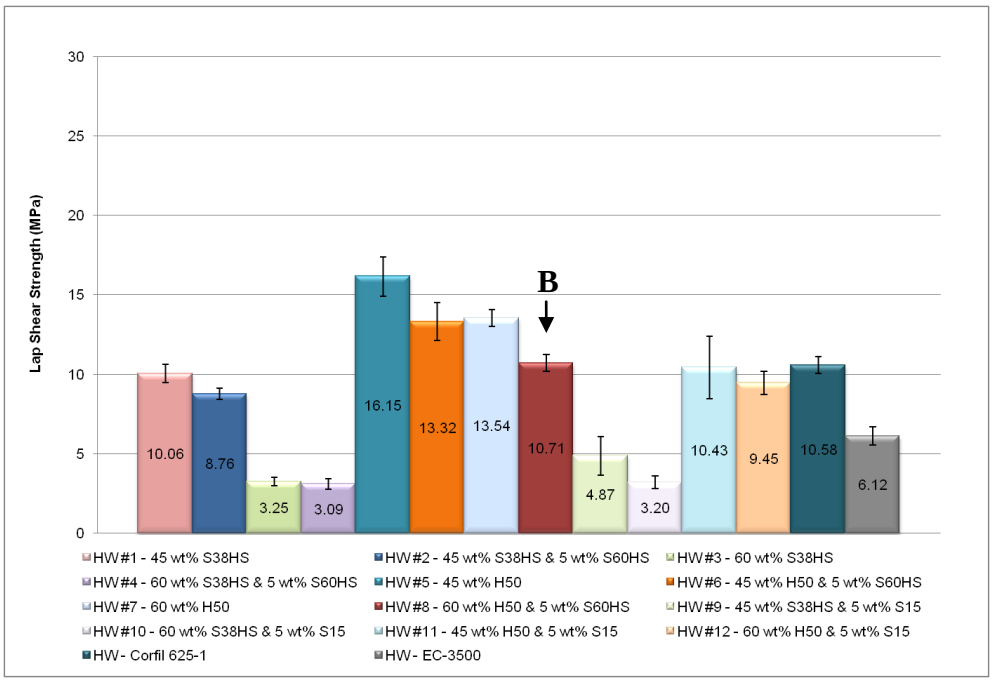

Figure 16. Lap shear strength results for the glass microballoon specimens conditioned at 71°C and 85% RH, and tested at 82°C

4.4 Effect of Carbon Nanotube Addition on the Physical and Mechanical Properties of Potting Compounds

The results shown herein correspond to nano-enhanced potting compounds tested under dry conditions at RT right after cure. The average values of compressive and lap shear strength are discussed in three categories: (1) specimens prepared with vacuum, (2) specimens prepared with no vacuum, and (3) specimens containing either the medium-high density microballoons, compound A (45 wt% S38HS & 5 WT% S60HS), or the high-high density microballoons, compound B (60 wt% H50 & 5 wt% S60HS), mixed either with vacuum or with no vacuum.

4.4.1 Properties of Nano-enhanced Potting Compounds Prepared with Vacuum

In order to determine if excess air was being added during the mixing process, vacuum was applied to sixteen different nano-enhanced specimens. Eight of them contained the medium-high density glass microballoons (compound **A**) while the remaining eight contained the high-high density glass microballoons (compound **B**). After comparing the results obtained for these nanocomposites with the values attained for compounds **A**, **B**, and those in which vacuum had not been applied, it was observed that the suction of air from the nano-enhanced specimens during mixing caused a remarkable contribution on the compressive and lap shear strength with an increase in density of 9% (Figure 18 - Figure 21). Nevertheless, as observed in Figure 17, Figure 22 and Figure 25, vacuum mixing proved to have little effect on the plain potting compounds (compounds with no CNTs). The S38HS & S60HS specimen showed no significant changes in any of its properties (density, compressive and lap shear strength). Although the H50 & S60HS specimen showed an increase of 15% and 25% in compressive and lap shear strength, respectively, its increase is tied to a 9% boost in density, confirming the dependence of the mechanical properties of potting compounds on the type of microballoons used.

As previously mentioned, specimens prepared with F-CNTs showed enhancement in both compressive and lap shear strength relative to their counterparts prepared without F-CNTs. In Figure 23 and Figure 24, it is indicated that the compressive strength of compounds containing the microballoon combination **A** increased by 18.35% with the addition of F-SWNTs and 14.3% with the addition of F-MWNTs. The lap shear strength, on the other hand, showed an increase of 40% for compounds containing F-SWNTs and 45% for those mixed with F-MWNTs (Figure 26 and Figure 27). For compounds containing the high-high density microballoons, combination **B**, the values of compressive strength showed an increase of 27% for specimens mixed with F-SWNTs and 21.5% for those mixed with F-MWNTs. Furthermore, the lap shear strength results showed an increase of 40% for specimens containing F-SWNTs and 46% for specimens containing F-MWNTs.

The nano-enhanced potting compound with a combination of 0.5 wt% F-MWNTs and compound **A** (#9) showed an increase in compressive and lap shear strength of 24% and 68% compared with its baseline, 130% and 83% relative to 625-1, and 22.5% and 119% with respect to EC-3500 with a density of 687.35 kg/m^3, respectively.

Besides comparing the results obtained for these nano-enhanced potting compounds with compound **A** and **B**, an increase in compressive strength of 17% for F-SWNT and 16% for F-MWNT compounds containing the medium-high density microballoons was observed with respect to EC-3500. Likewise, an increase in lap shear strength of 83% and 89% compared with EC-3500 was shown for the same microballoon compounds mixed with F-SWNTs or F-MWNTs, respectively. Finally, the density was observed to increase in average by 5% for both F-SWNT and F-MWNT compounds containing **A**-type microballoons compared with EC-3500.

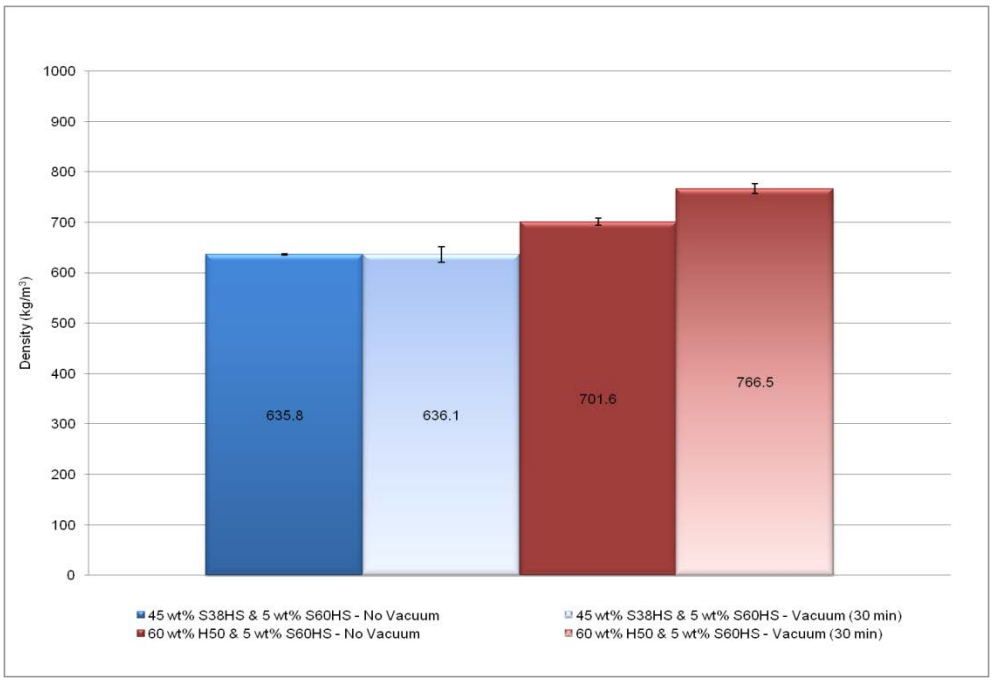

Figure 17. Density results for microballoon specimens (S38HS & S60HS and H50 & S60HS) mixed with vacuum and without vacuum.

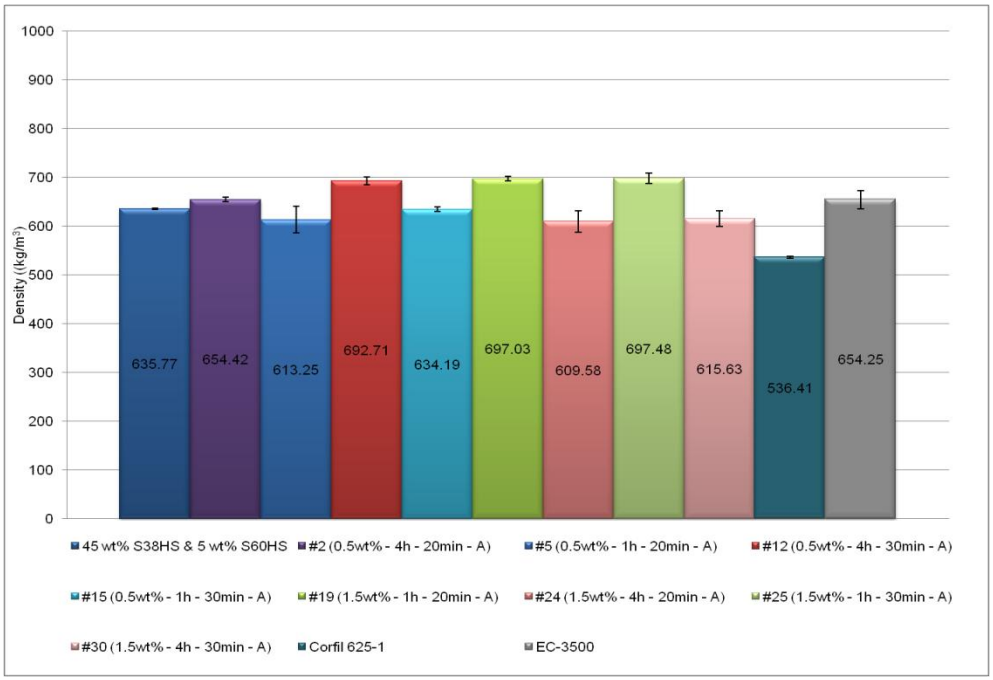

Figure 18. Density results for specimens containing F-SWNTs and S38HS & S60HS glass microballoons.

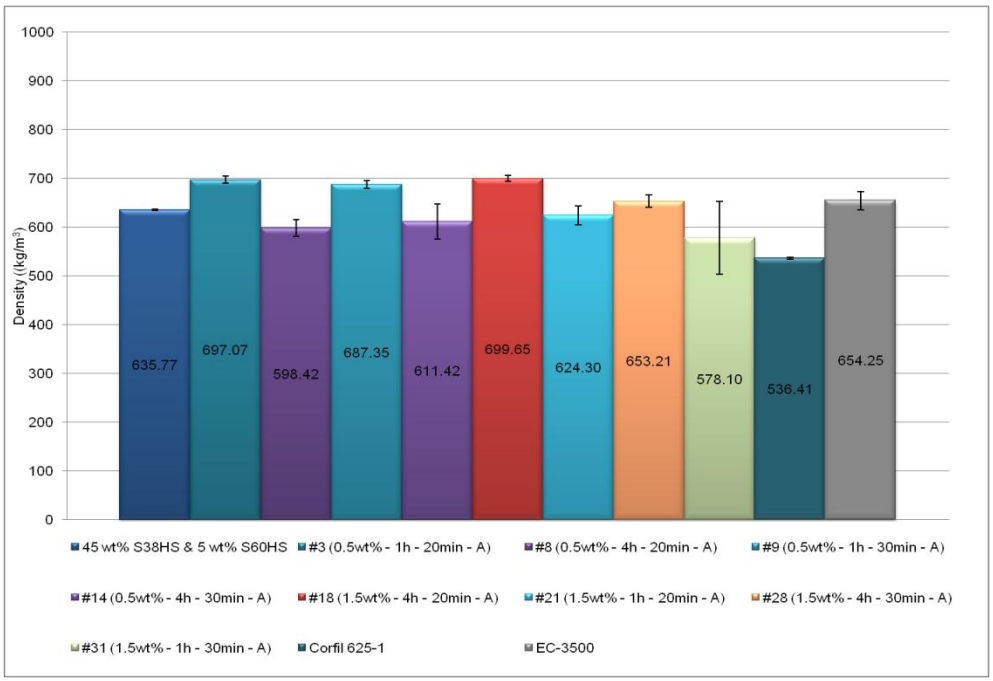

Figure 19. Density results for specimens containing F-MWNTs and S38HS & S60HS glass microballoons.

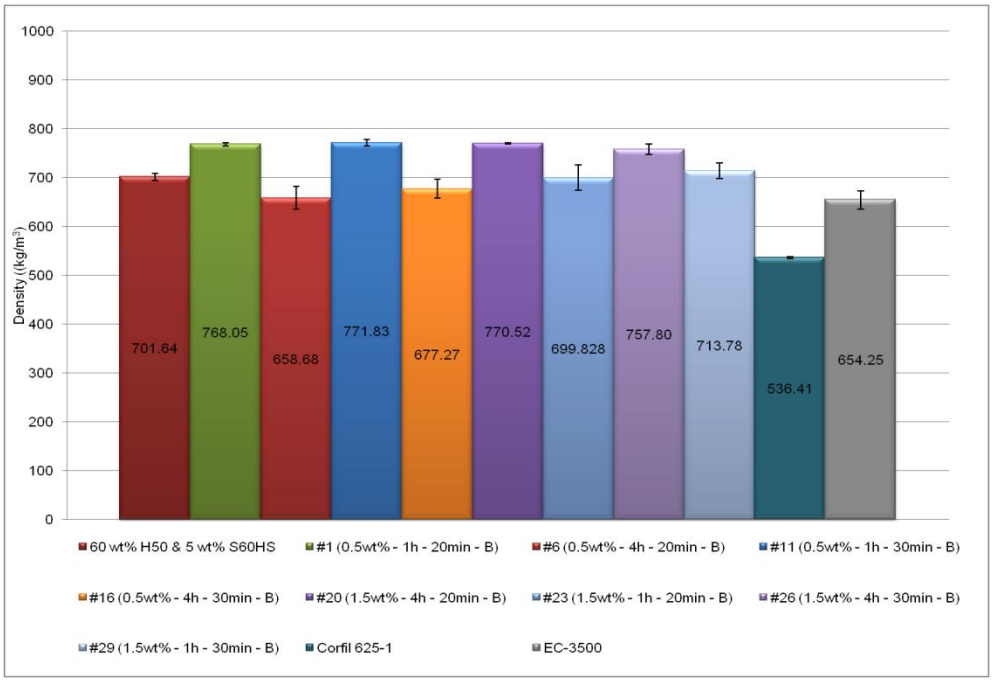

Figure 20. Density results for specimens containing F-SWNTs and H50 & S60HS glass microballoons.

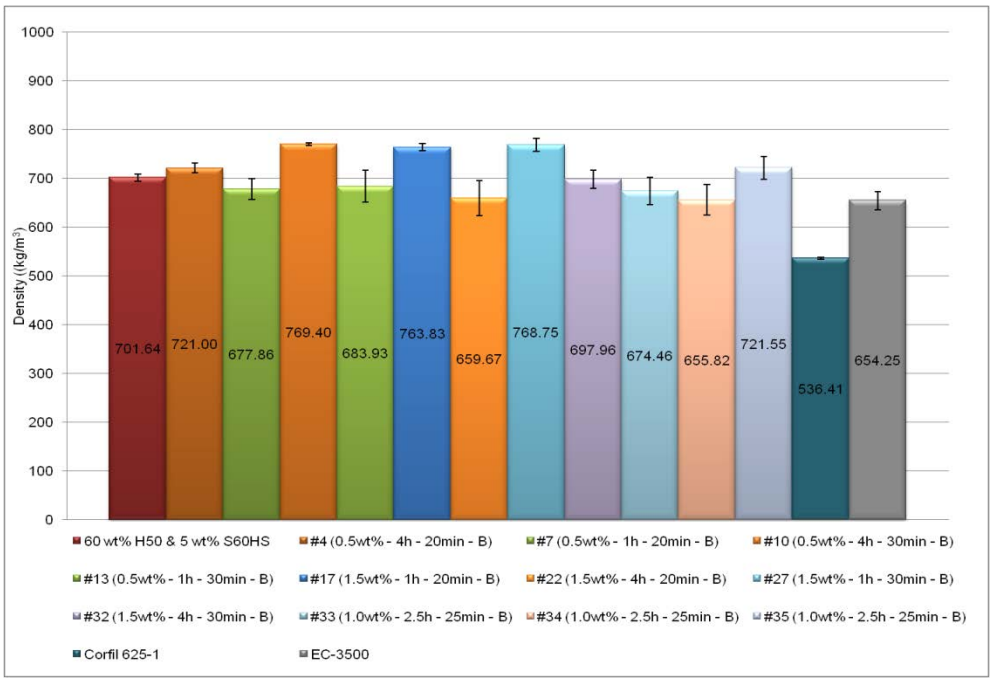

Figure 21. Density results for specimens containing F-MWNTs and H50 & S60HS glass microballoons.

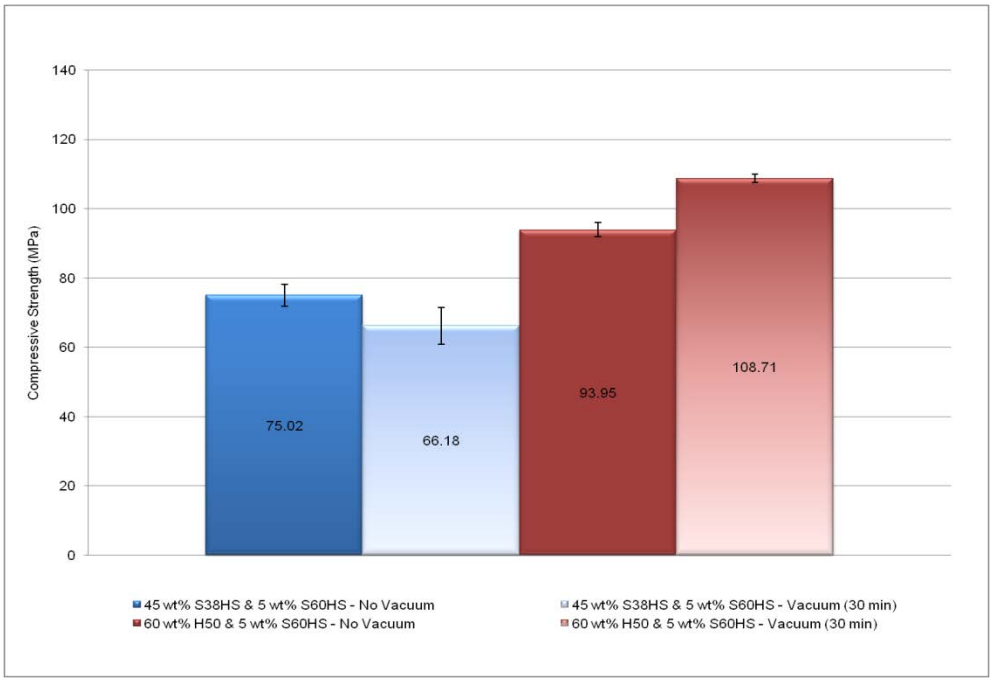

Figure 22. Compressive strength results for microballoon specimens (S38HS & S60HS and H50 & S60HS) mixed with vacuum and without vacuum.

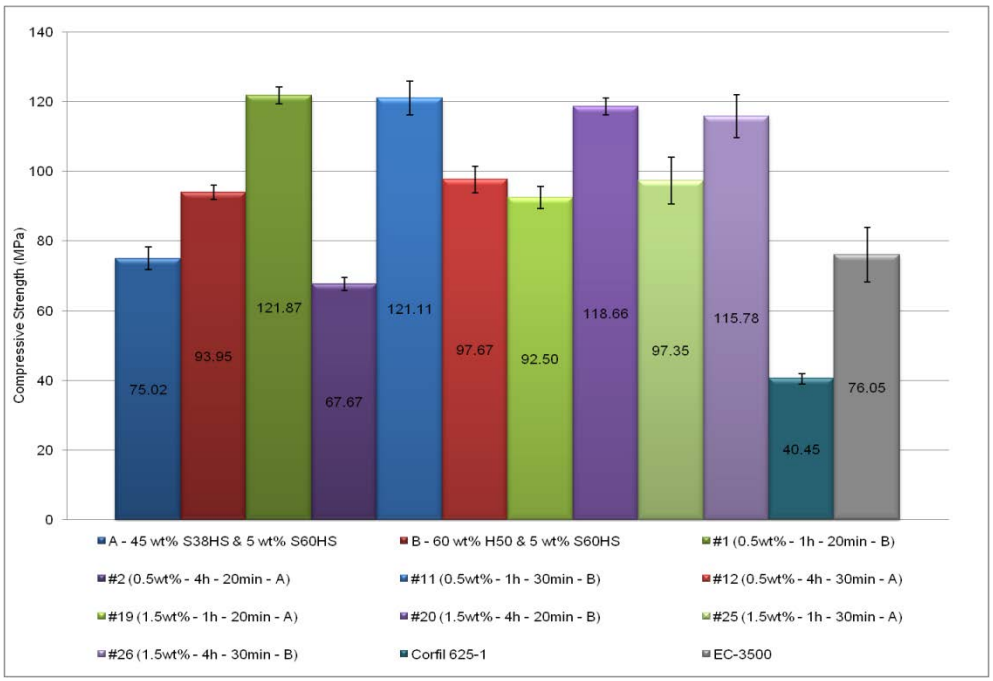

Figure 23. Compressive strength results for specimens containing F-SWNTs and mixed using vacuum.

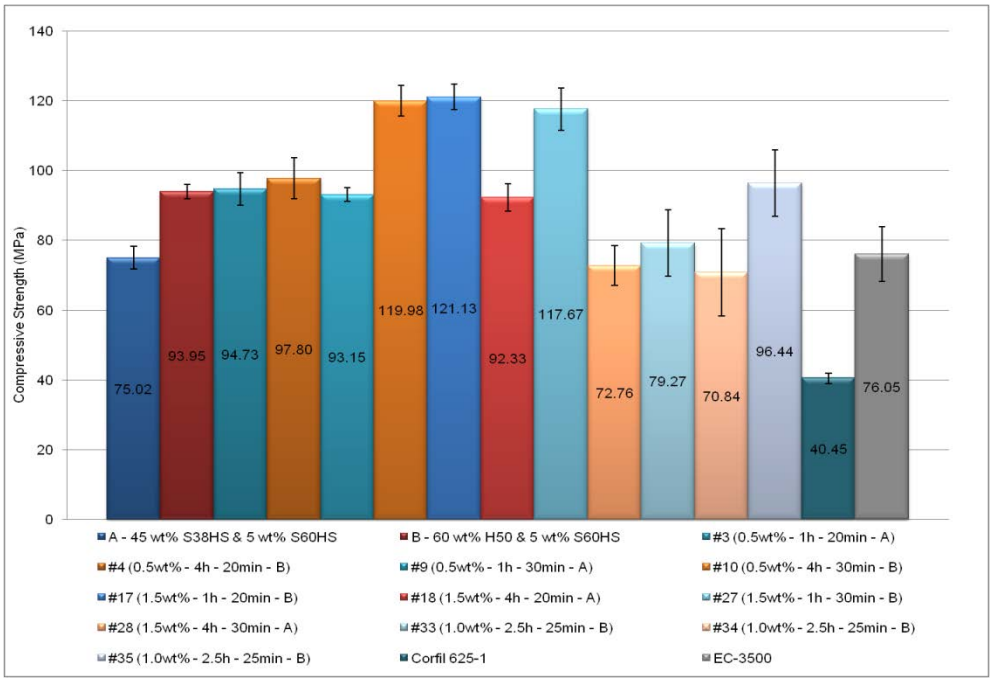

Figure 24. Compressive strength results for specimens containing F-MWNTs and mixed using vacuum.

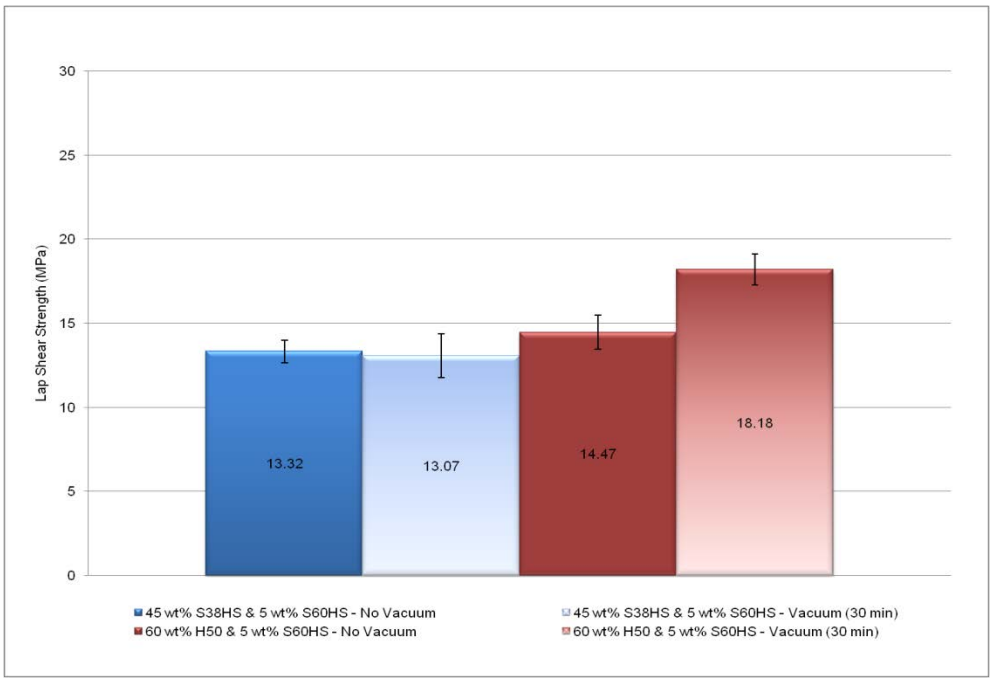

Figure 25. Lap shear strength results for microballoon specimens (S38HS & S60HS and H50 & S60HS) mixed with vacuum and without vacuum.

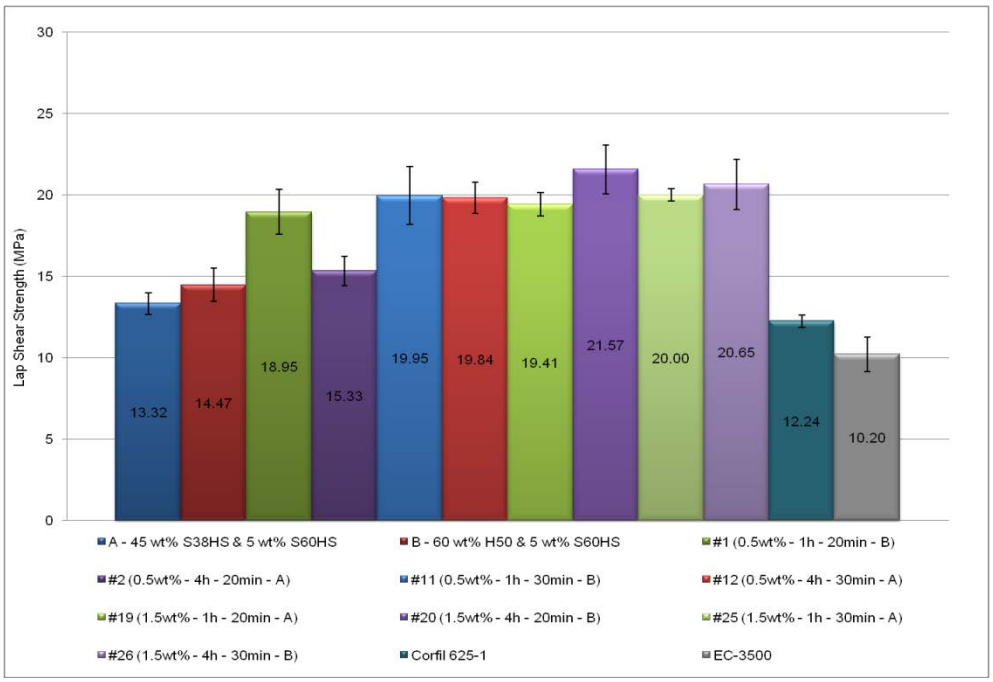

Figure 26. Lap shear strength results for specimens containing F-SWNTs and mixed using vacuum.

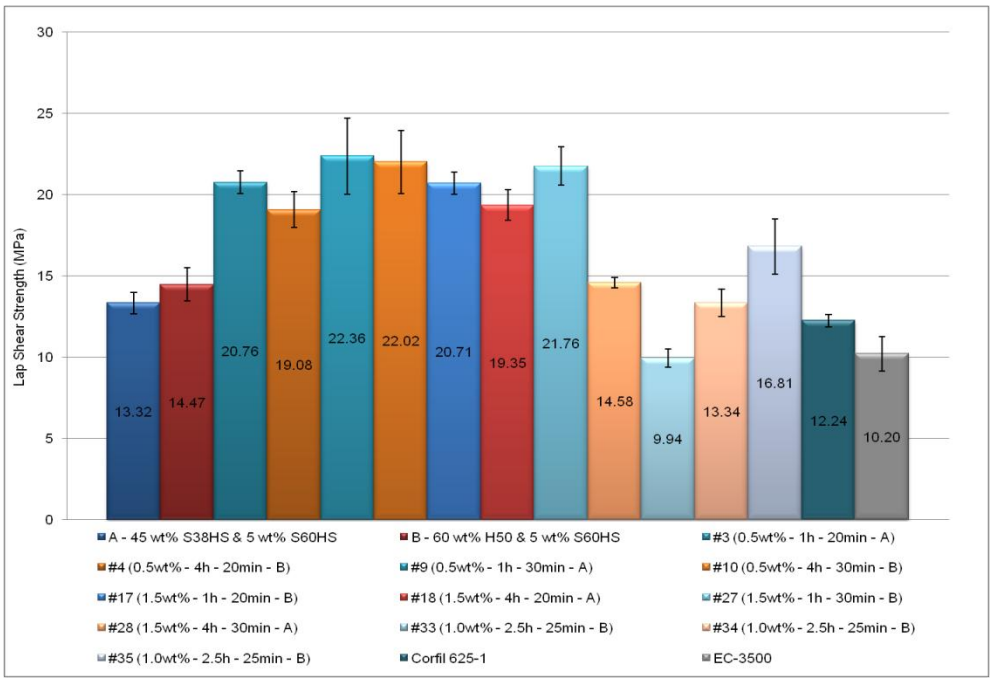

Figure 27. Lap shear strength results for specimens containing F-MWNTs and mixed using vacuum.

4.4.2 Properties of Nano-enhanced Potting Compounds Prepared without Vacuum

Even though three different mixing techniques (ultrasonic, calendering, and centrifugal) were employed to disperse F-CNTs in the polymer resin of compounds **A** and **B**, the mechanical properties of the resulting CNT-resin-glass microballoon composites mixed without applying vacuum did not show major improvements compared with the neat compounds (mixed without F-CNTs) and EC-3500. The initial decrease in compressive and lap shear strength could be attributed to an increase in the frequency distribution of defects associated with the presence of voids, as shown in Figure 28. Furthermore, a poor interfacial interaction due to entrapped air between the nanotubes, the microballoons and the polymer matrix results in premature composite failure, since the reinforcing nanotubes could either act as a void and therefore as a stress concentration or simply pull out of the matrix without contributing to the strength of the material.

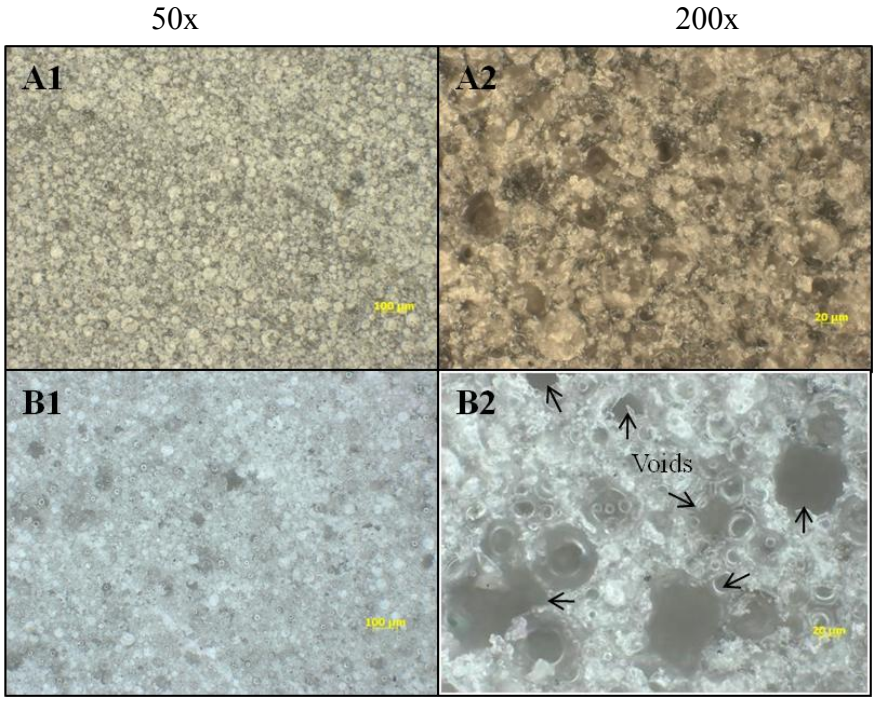

Figure 28. Microscopy images of carbon nanotube potting compounds mixed at (A) full vacuum (specimen #9), and (B) zero vacuum (specimen #14). Magnifications correspond to 50x and 200x for left and right columns, respectively.

With respect to the neat potting compounds (compounds **A** and **B**), the dispersion of F-CNTs without applying vacuum resulted in a decrease in compressive strength of 16% for specimens mixed with F-SWNTs and compound **A**, 24.6% for specimens mixed with F-MWNTs and compound **A**, 14% for specimens mixed with F-SWNTs and compound **B**, and 20% for specimens mixed with F-MWNTs and compound **B**. In addition, the lap shear strength showed a decrease of 22% for specimens mixed with F-SWNTs and compound **A**, 7% for specimens mixed with F-MWNTs and compound **A**, 25% for specimens mixed with F-SWNTs and compound **B**, and 9% for specimens mixed with F-MWNTs and compound **B**.

By comparing the results obtained for these nano-enhanced potting compounds with those of EC-3500, it was shown that the compressive strength decreased by 18% and 26% for specimens containing **A**-type microballoons with F-SWNTs or F-MWNTs, respectively.

Although the compressive strength of the aforementioned compounds decreased with respect to EC-3500, the lap shear strength showed an increase of 3% and 21.6% for the same set of microballoon compounds containing F-SWNTs or F-MWNTs, correspondingly. However, such increase in strength might have been attributed to microballoon reinforcement rather than CNT reinforcement. The results for all the nano-enhanced potting compounds mixed without applying vacuum are shown in Figure 29 - Figure 32.

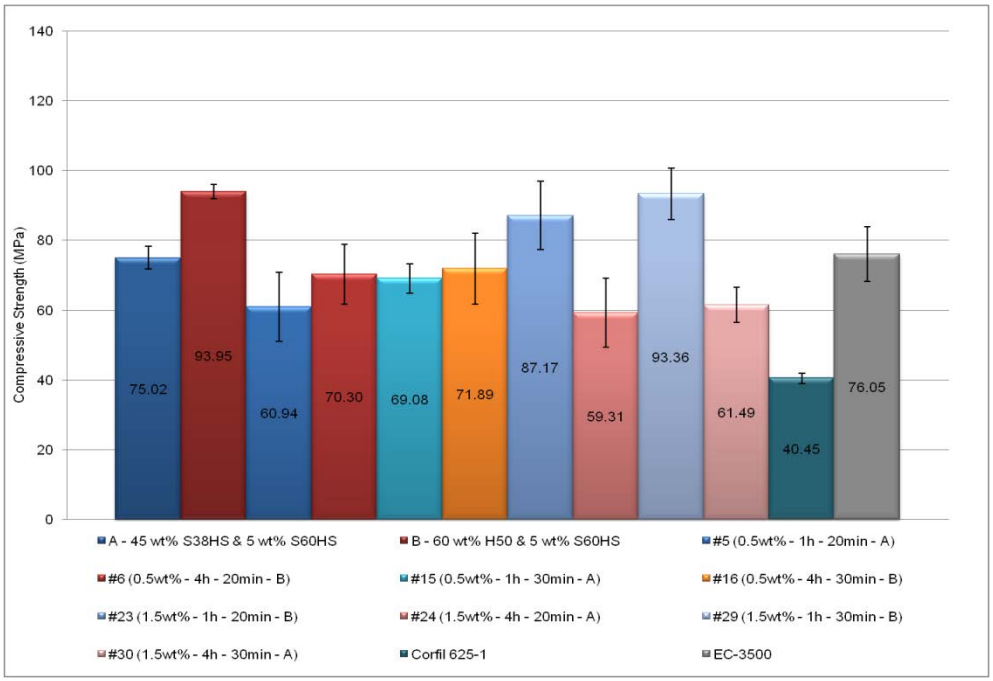

Figure 29. Compressive strength results for specimens containing F-SWNTs and mixed without vacuum.

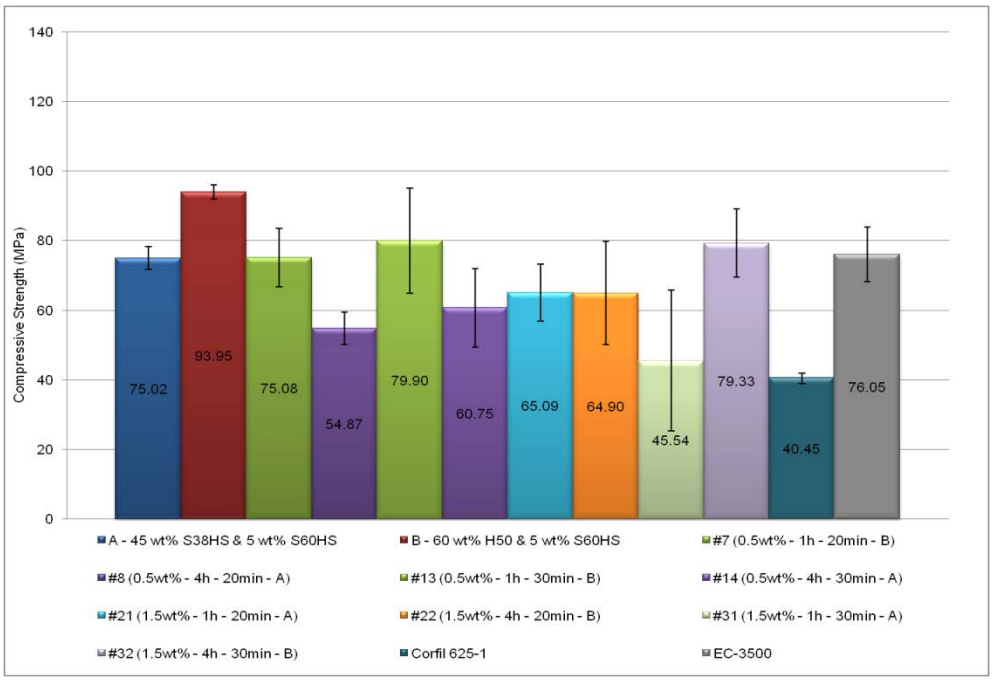

Figure 30. Compressive strength results for specimens containing F-MWNTs and mixed without vacuum.

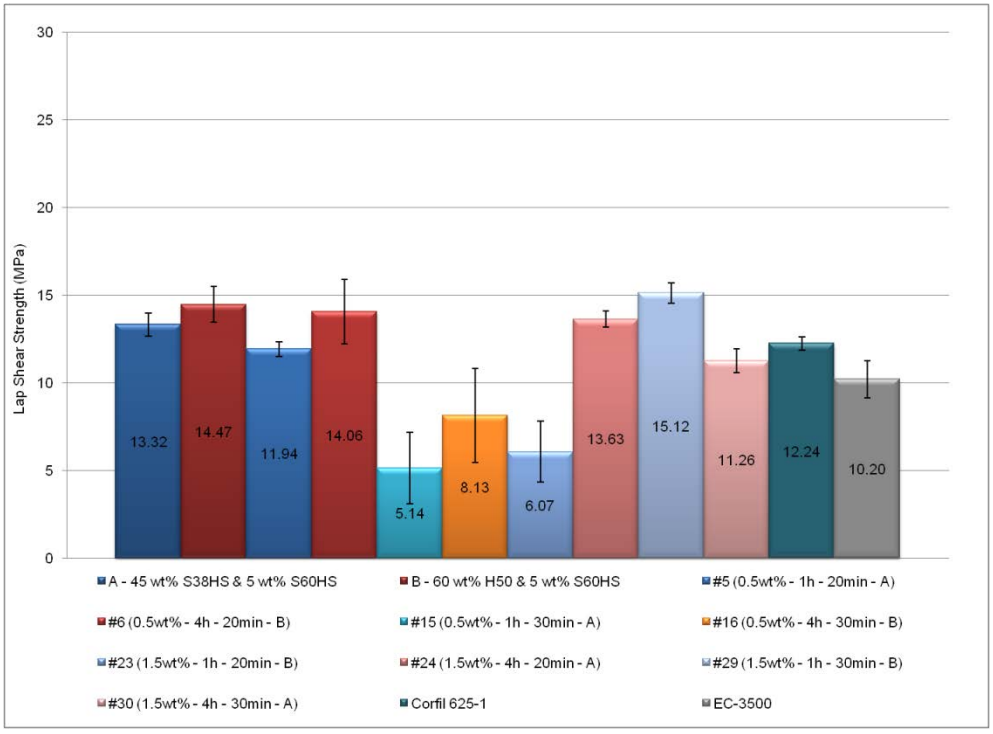

Figure 31. Lap shear strength results for specimens containing F-SWNTs and mixed without vacuum.

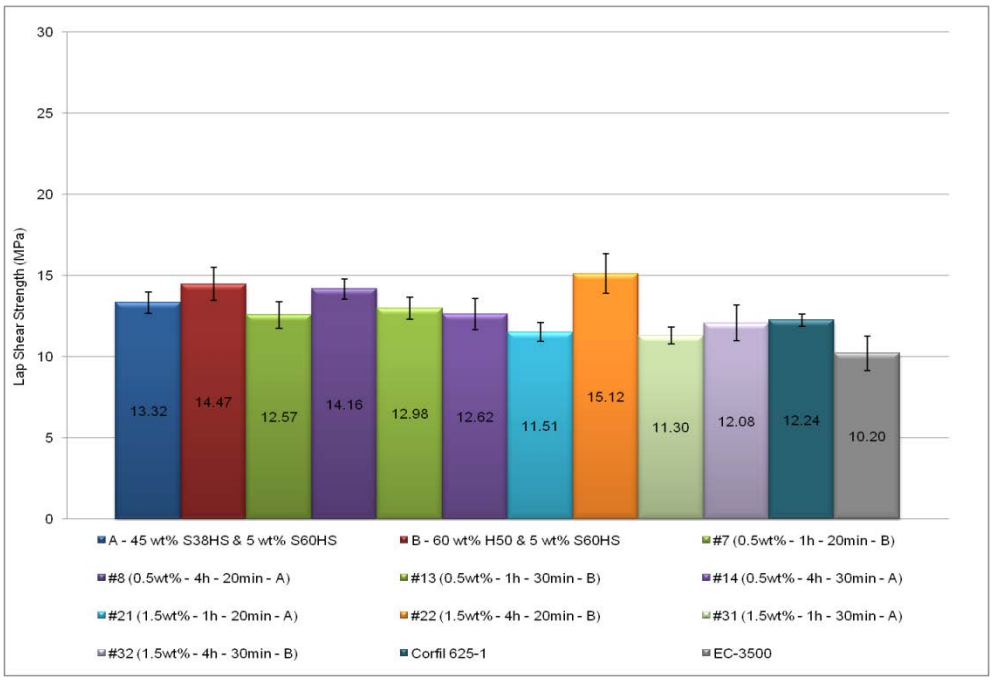

Figure 32. Lap shear strength results for specimens containing F-MWNTs and mixed without vacuum.

4.4.3 Effect of F-SWNTs and F-MWNTs on the Mechanical Properties of Selected Microballoon Compounds

A different way to look at the effect of F-SWNTs and F-MWNTs on the compressive and lap shear strength of potting compounds prepared with **A**-type microballoons is shown in Figure 33, Figure 34, Figure 37 and Figure 38. In these figures, the compressive and lap shear strength results for specimens prepared with and without vacuum are compared. The addition of F-SWNTs and F-MWNTs has shown to be significant as long as the CNT-resin mixture was dispersed with the microballoons under vacuum conditions. This suggested that a decrease in molecular mobility due to a decrease in free volume (by removing air from the mixture) might account for mechanical load transfer from the polymer matrix to the nanotubes. The addition of F-CNTs at a low weight percentage (0.5 or 1.5 wt%) showed an increase of more than 15% in compressive strength and more than 40% in lap shear strength compared with the results

obtained for the neat compound. Furthermore, an increase in compressive and lap shear strength of more than 15% and more than 80% was shown with respect to EC-3500, respectively.

As in the CNT-compound **A** composites, the same trend was observed for the high-high density nano-enhanced compounds (CNT-compound **B**). When either F-SWNTs or F-MWNTs were added to the polymer matrix and mixed with the microballoons at maximum vacuum conditions, an increase of more than 20% and 40% in compressive and lap shear strength was observed with respect to the neat compound, respectively. These results confirmed the sensitivity of nanotube/polymer composites to the parameters of fabrication. Although the average density (768.5 kg/m^3) of all these compounds was approximately 9% higher than that of the base material (701.64 kg/m^3), the results observed in Figure 35, Figure 36, Figure 39 and Figure 40 suggested the existence of interfacial interaction between the resin, the microballoons, and the nanotubes when vacuum was used as part of the mixing method.

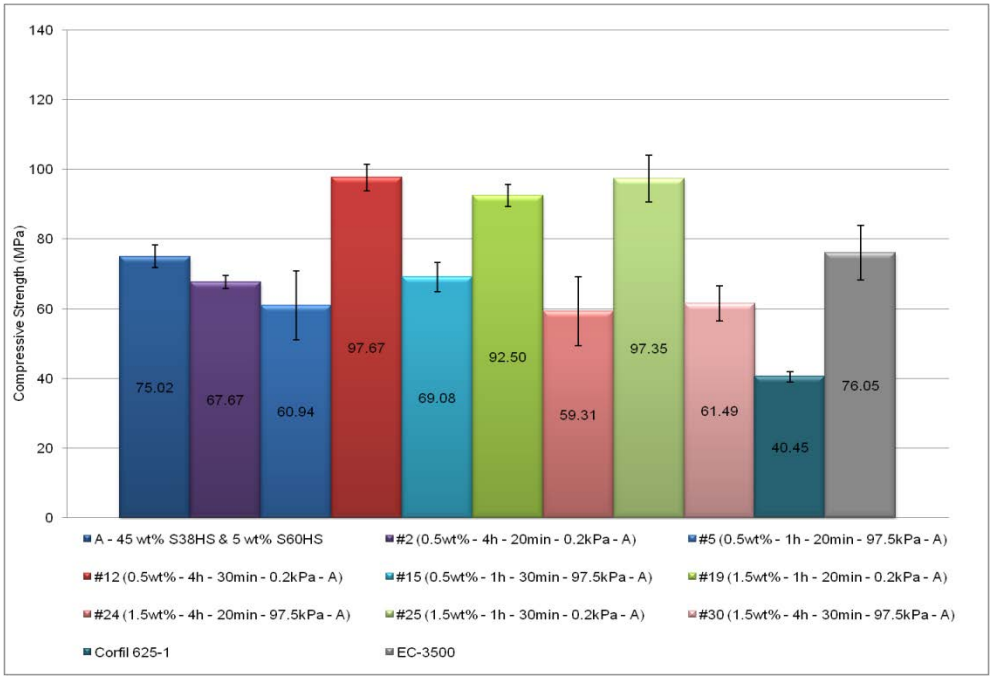

Figure 33. Compressive strength results for specimens prepared with F-SWNTs and S38HS & S60HS glass microballoons.

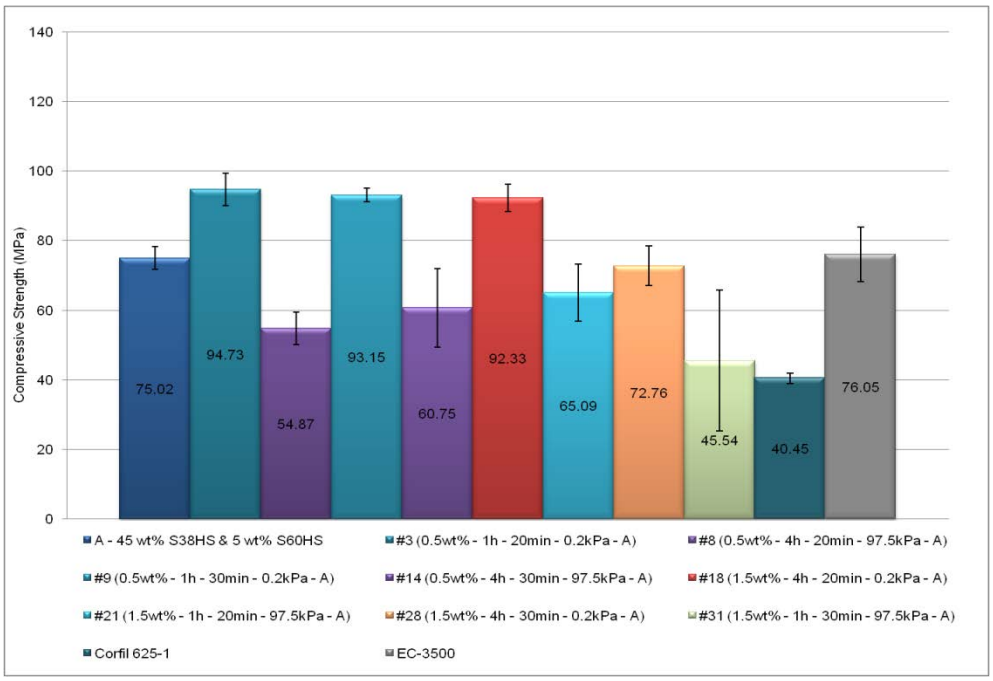

Figure 34. Compressive strength results for specimens prepared with F-MWNTs and S38HS & S60HS glass microballoons.

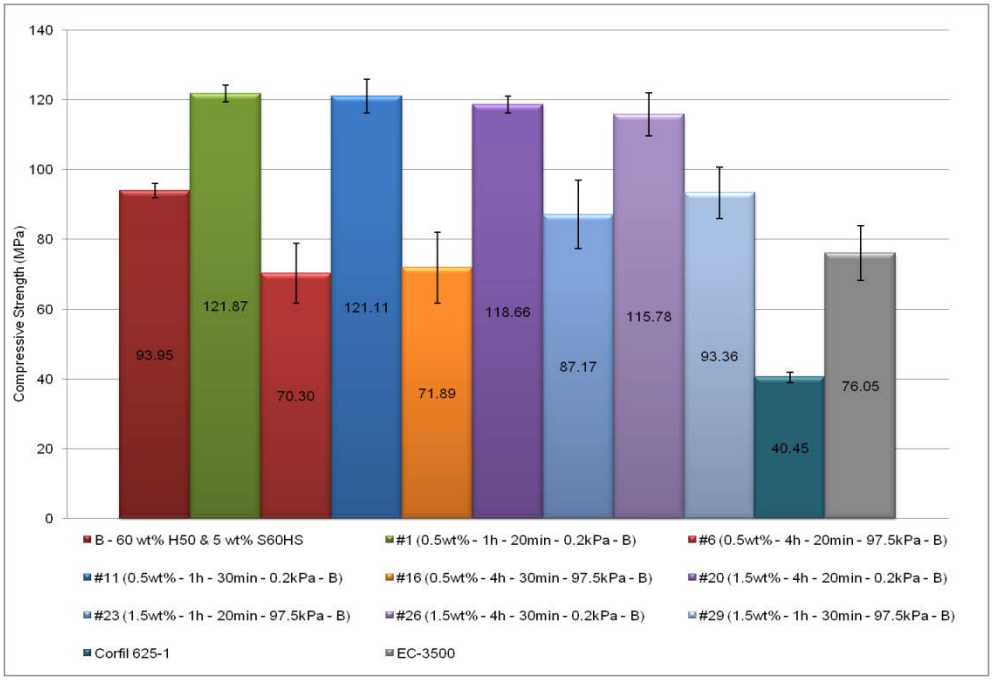

Figure 35. Compressive strength results for specimens prepared with F-SWNTs and H50 & S60HS glass microballoons.

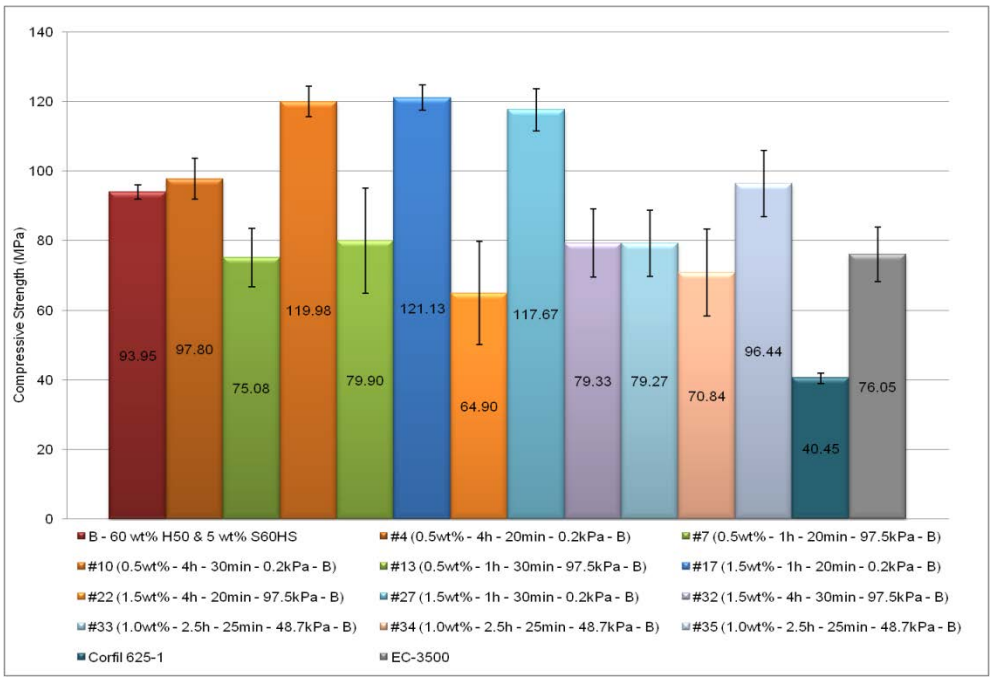

Figure 36. Compressive strength results for specimens prepared with F-MWNTs and H50 & S60HS glass microballoons.

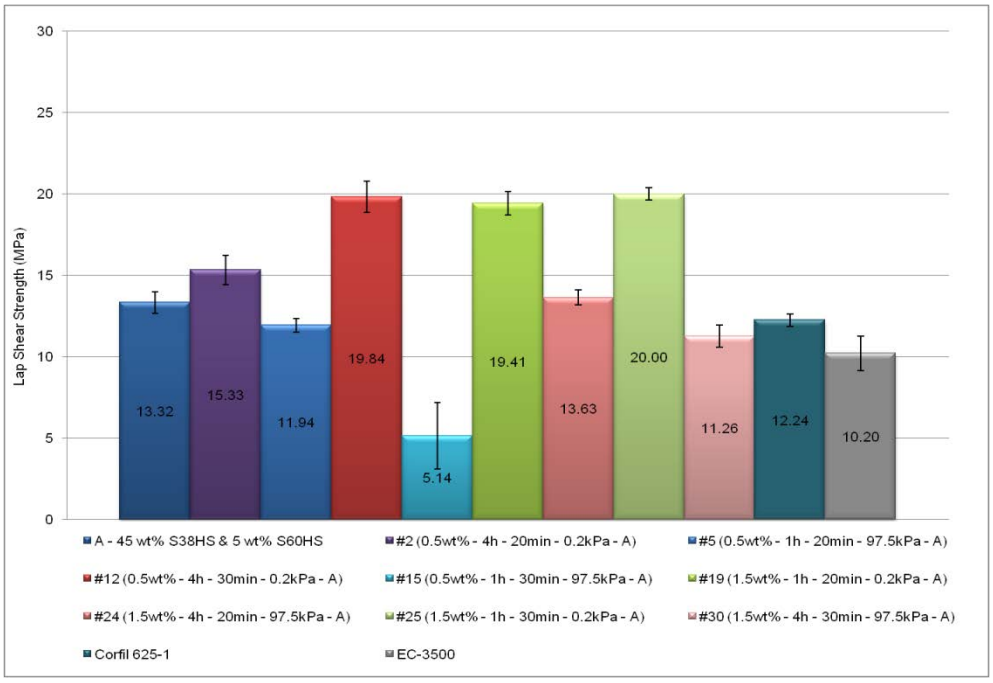

Figure 37. Lap shear strength results for specimens prepared with F-SWNTs and S38HS & S60HS glass microballoons.

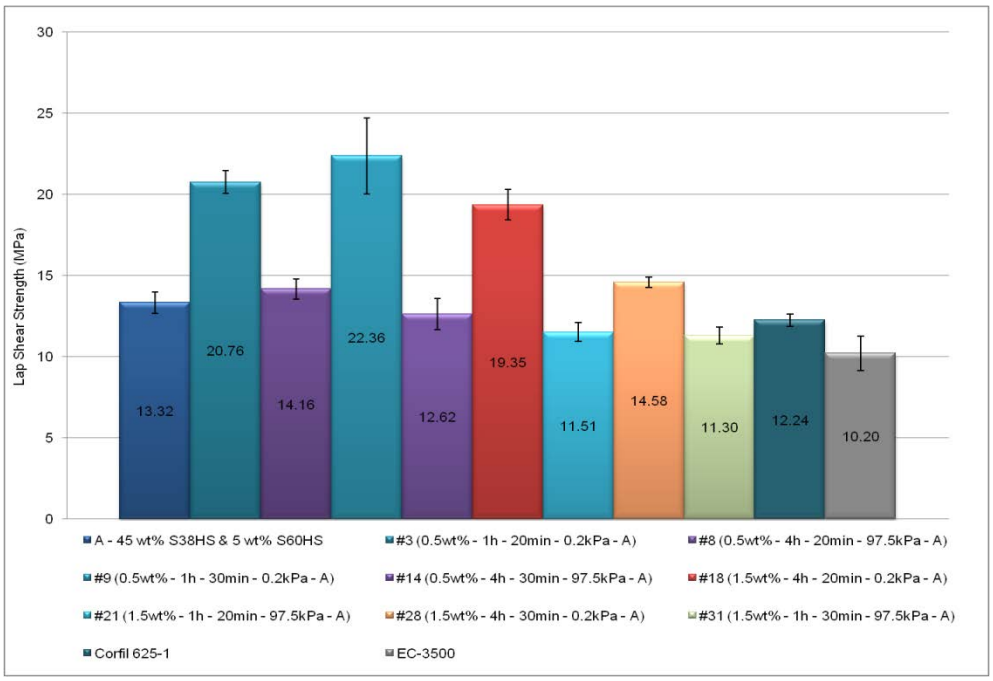

Figure 38. Lap shear strength results for specimens prepared with F-MWNTs and S38HS & S60HS glass microballoons.

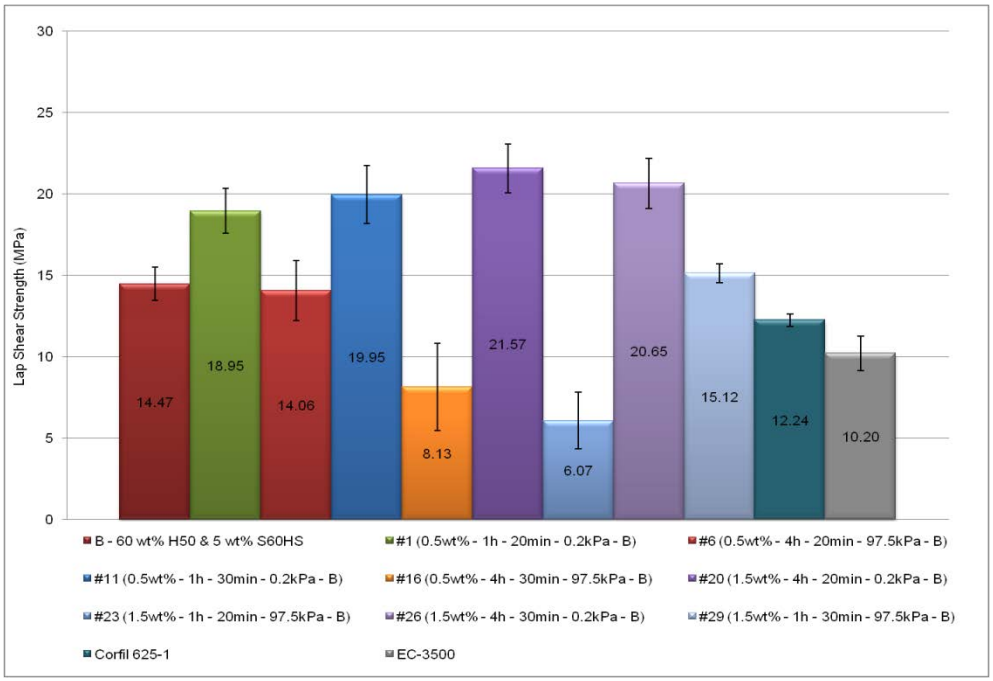

Figure 39. Lap shear strength results for specimens prepared with F-SWNTs and H50 & S60HS glass microballoons.

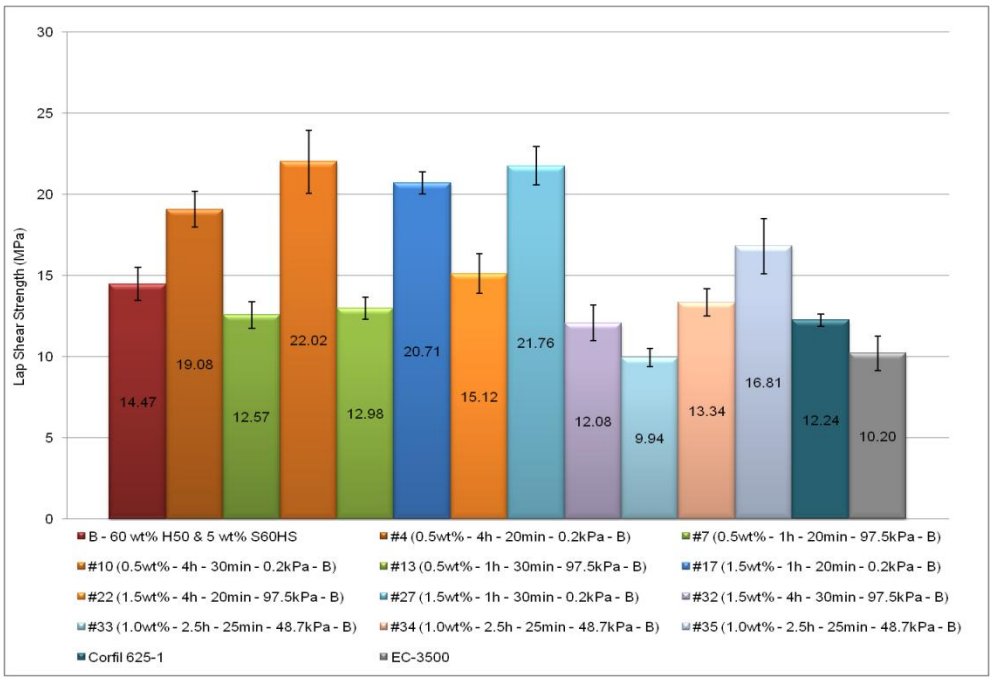

Figure 40. Lap shear strength results for specimens prepared with F-MWNTs and H50 & S60HS glass microballoons.

4.5 Effect of Carbon Nanotube Addition on the Physical and Mechanical Properties of Potting Compounds Subjected to Hot/Wet Conditions

At the end of the conditioning period, the weight gain monitored on a daily basis was less than 1% for compression specimens and less than 0.1% for lap shear specimens prepared with or without vacuum. The compressive and lap shear strength results for specimens subjected to conditioning are shown in the following subsections.

4.5.1 Properties of Nano-enhanced Potting Compounds Prepared with Vacuum and Subjected to Hot/Wet Conditions

After comparing the results obtained in Figure 41, Figure 42, Figure 43 and Figure 44 with those attained for compounds tested under dry conditions at RT (Figure 23, Figure 24, Figure 26 and Figure 27), a decrease of 53% and 57% in compressive strength was observed for compounds containing F-CNTs and **A**-type or **B**-type microballoons, respectively. Similarly, a

decrease of 41.5% and 40% in lap shear strength was showed for compounds containing F-CNTs and **A**-type or **B**-type microballoons, respectively.

Although a high humidity environment imposed a substantial decrease in the compressive and lap shear strength of the nano-enhanced potting compounds, a significant increase in strength with respect to the base materials was observed for both F-SWNT and F-MWNT compounds prepared using vacuum. An increase of about 100% in compressive strength was attained for both F-SWNT and F-MWNT compounds containing **A**-type microballoons compared with the baseline and 625-1. Similarly, an increase of 18.2% and 9% in compressive strength was achieved for F-SWNT and F-MWNT compounds with the same combination of microballoons relative to EC-3500, respectively.

From a different point of view, the lap shear strength was increased by 36% when adding F-SWNTs and 14% when adding F-MWNTs to compounds mixed with **A**-type microballoons compared with the baseline. Moreover, an increase of 88% and 58% with respect to EC-3500 was obtained when adding F-SWNTs and F-MWNTs to compounds mixed with the abovementioned microballoons, respectively.

The mixture 0.5 wt% F-MWNTs and **A**-type microballoons (#9 in Figure 44) showed the highest increase in lap shear strength (61.83%) relative to its baseline with a compressive strength (36.59 MPa) similar to that of EC-3500 (36.75 MPa) and a density of 687.35 kg/m^3. Similarly, an increase of 60.21% and 124.30% in lap shear strength was observed for the same compound with respect to 625-1 and EC-3500, respectively. These results ratified that interfacial interaction between the CNTs and the polymer matrix could exist as a result of a decrease in porosity.

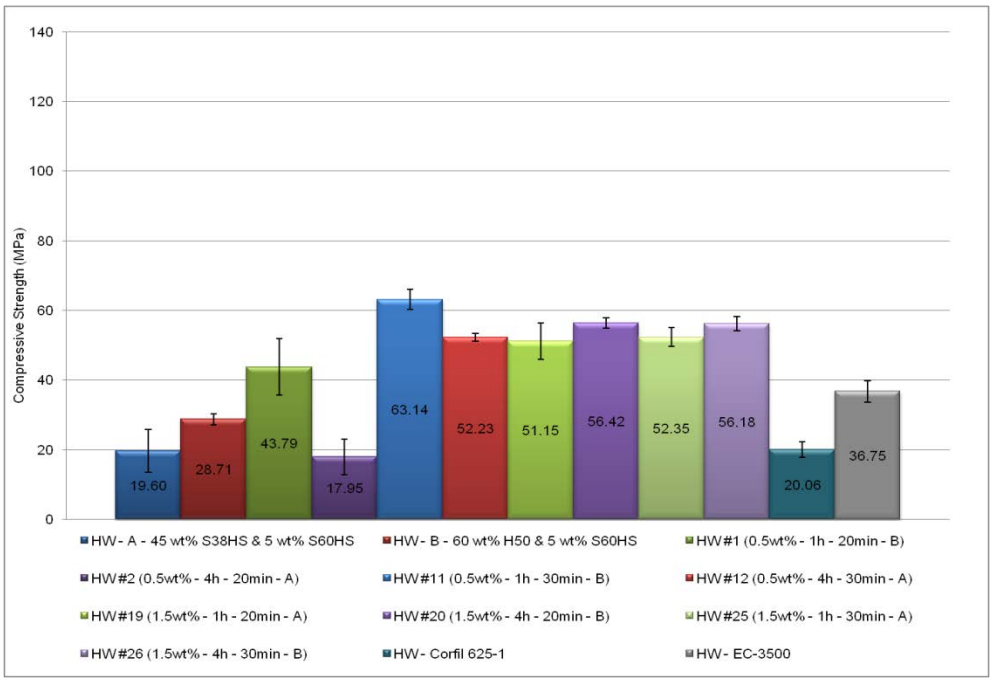

Figure 41. Compressive strength results for F-SWNT-resin-glass microballoon specimens mixed using vacuum and subjected to hot/wet conditioning.

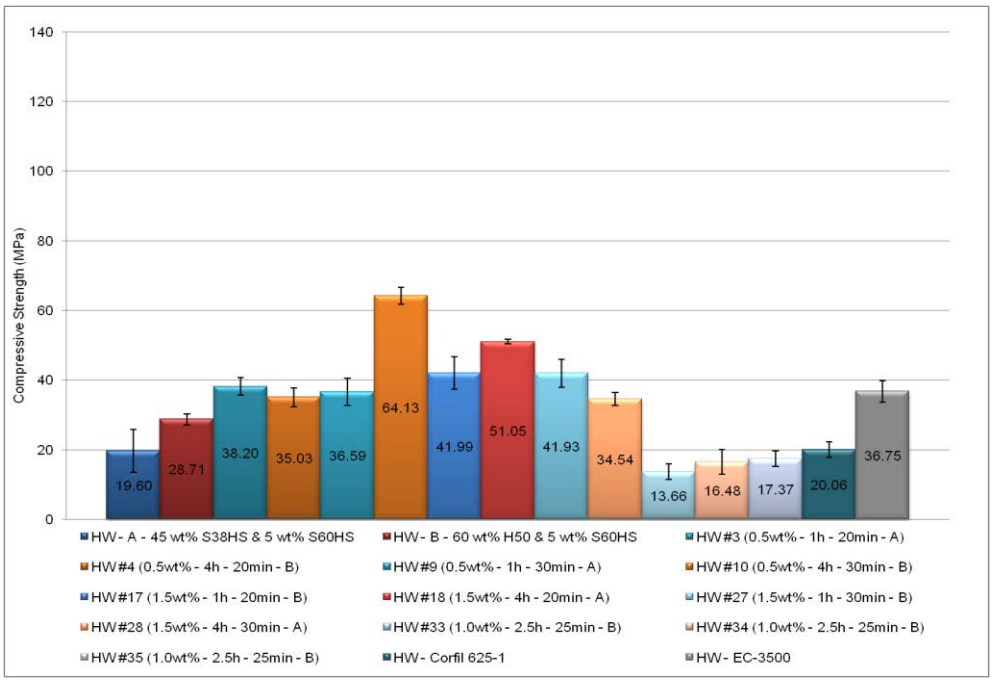

Figure 42. Compressive strength results for F-MWNT-resin-glass microballoon specimens mixed using vacuum and subjected to hot/wet conditioning.

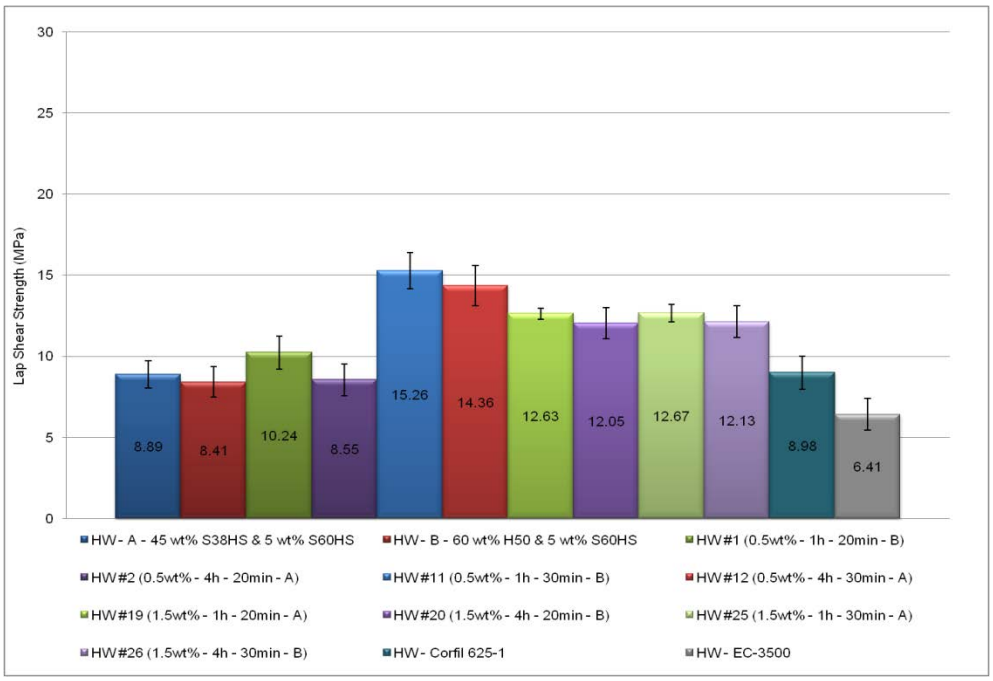

Figure 43. Lap shear strength results for F-SWNT-resin-glass microballoon specimens mixed using vacuum and subjected to hot/wet conditioning.

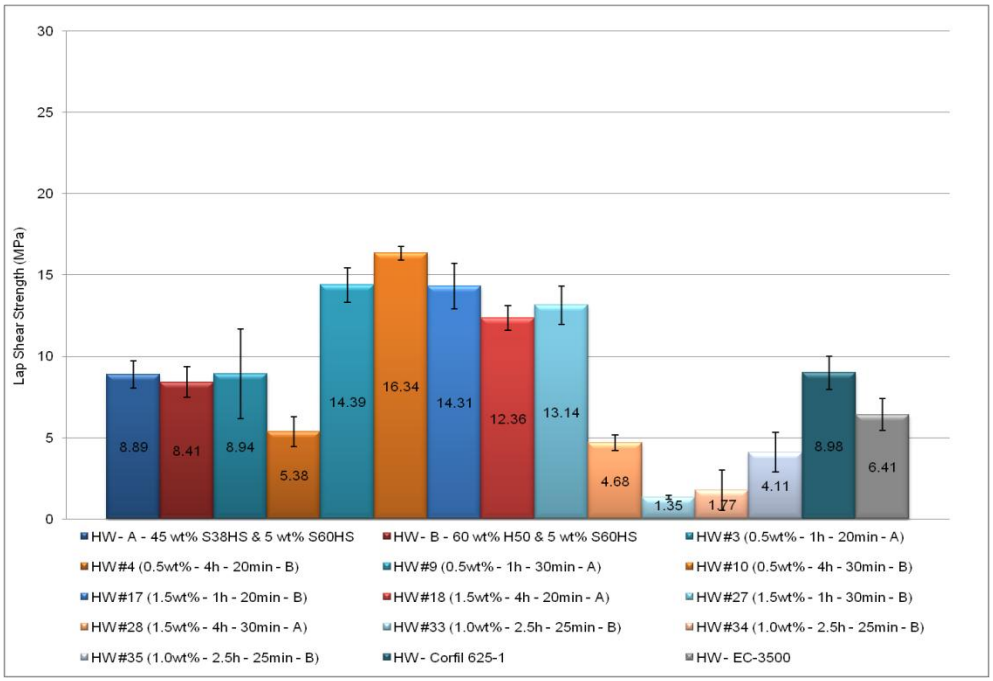

Figure 44. Lap shear strength results for F-MWNT-resin-glass microballoon specimens mixed using vacuum and subjected to hot/wet conditioning.

4.5.2 Properties of Nano-enhanced Potting Compounds Prepared without Vacuum and Subjected to Hot/Wet Conditions

Dispersion of F-CNTs in compounds mixed with no vacuum and subjected to environmental conditioning resulted in a decrease in compressive strength of 83% for specimens containing F-SWNTs and compound **A**, 76.7% for specimens mixed with F-MWNTs and compound **A**, 79.71% for specimens mixed with F-SWNTs and compound **B**, and 80.3% for specimens mixed with F-MWNTs and compound **B** compared with their counterparts tested at RT. Similarly, the lap shear strength showed a decrease of 73.25% for specimens mixed with F-SWNTs and compound **A**, 71.6% for specimens mixed with F-MWNTs and compound **A**, 83.36% for specimens mixed with F-SWNTs and compound **B**, and 79.1% for specimens mixed with F-MWNTs and compound **B** with respect to their counterparts tested at RT. The hot/wet testing results for these compounds are shown in Figure 45, Figure 46, Figure 47 and Figure 48.

A similar drop in mechanical properties was also observed compared with the base potting compounds, 625-1, and EC-3500. Results showed a decrease in compressive and lap shear strength of 40% and 65% with respect to the neat potting compounds, 36% and 65% compared with 625-1 as well as 65% and 60% in comparison to EC-3500, respectively. Such a poor performance in properties could be attributed to two possible effects: The first one might be due to hygrothermal expansion of thin wall microballoons. At high temperature and high relative humidity, some of the thin wall microballoons could fracture creating additional space for water to accumulate. As a result, a sharp decrease in compressive and lap shear properties would be observed relative to the dry nanocomposites. The other effect might be caused by the presence of a high number of voids within the molecular structure (as shown in Figure 28), allowing vapor water to diffuse throughout the CNT-resin-microballoon interface and accumulate more easily in

the pores. Water molecules are attracted and absorbed by the presence of polar groups (-OH, -NH etc.) in the polymer chains and the CNTs. Such attraction and absorption can break the hydrogen bonding present between chains and cause plasticization due to morphologic disruption, leading to premature failure of the specimens. Therefore, by controlling the amount of free volume or reducing the interstitial gap between defects (voids), better mechanical properties under hygrothermal conditions could be attained, as shown in the previous subsection.

The lap shear strength of specimen #23 (1.5 wt% F-SWNTs and 60 wt% H50 & 5 wt% S60HS microballoons) was not quantified because the bond integrity between the nano-enhanced potting compound and the lap shear coupon became very weak, impeding handing and testing of the specimen.

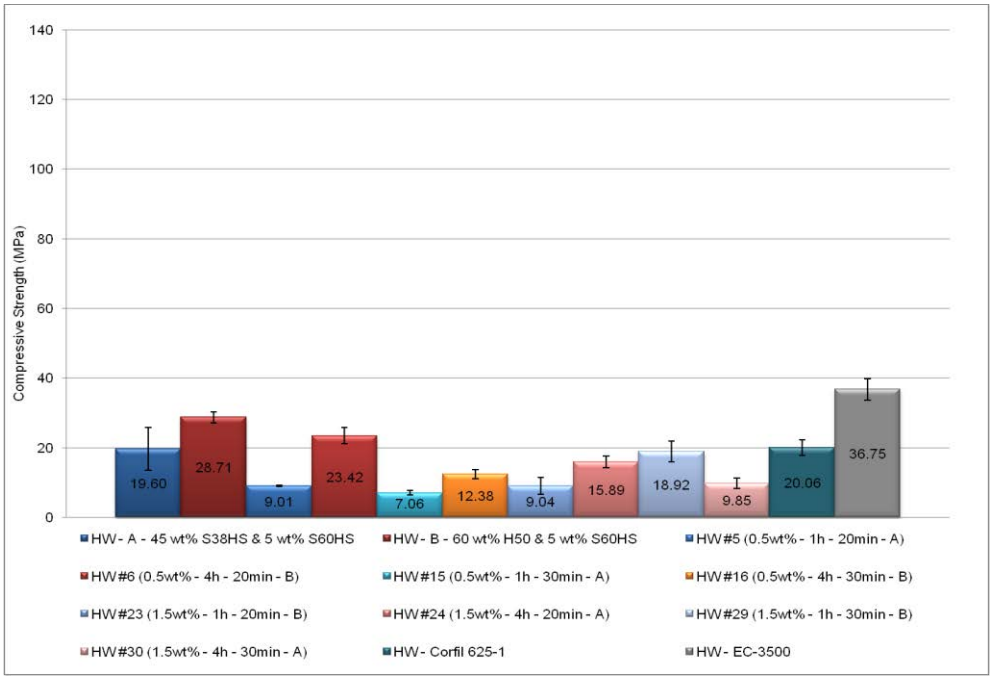

Figure 45. Compressive strength results for F-SWNT-resin-glass microballoon specimens mixed without vacuum and subjected to hot/wet conditioning.

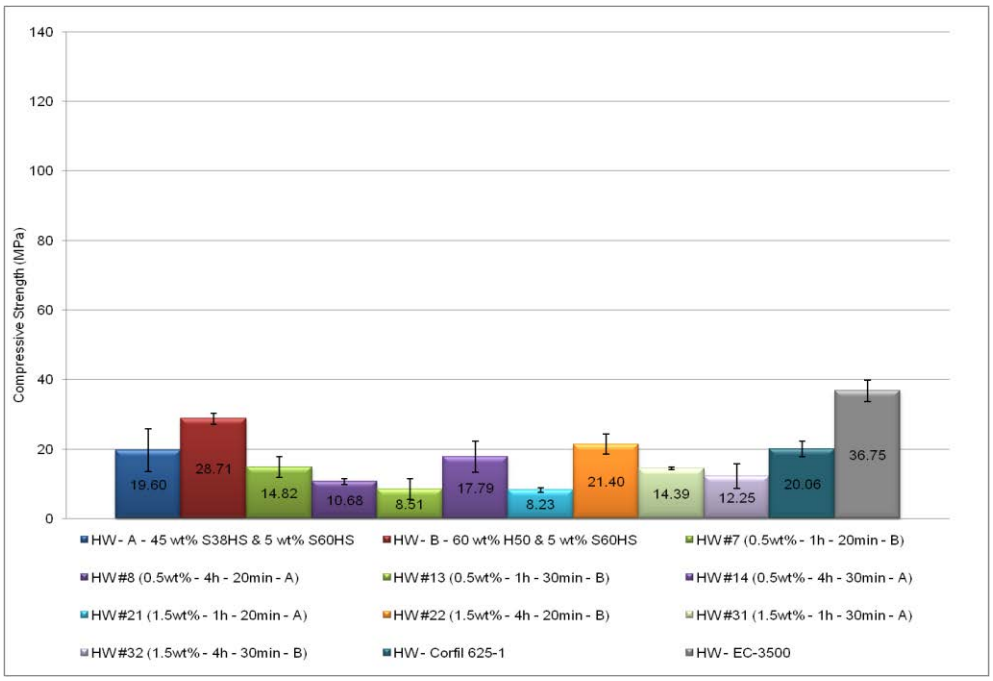

Figure 46. Compressive strength results for F-MWNT-resin-glass microballoon specimens mixed without vacuum and subjected to hot/wet conditioning.

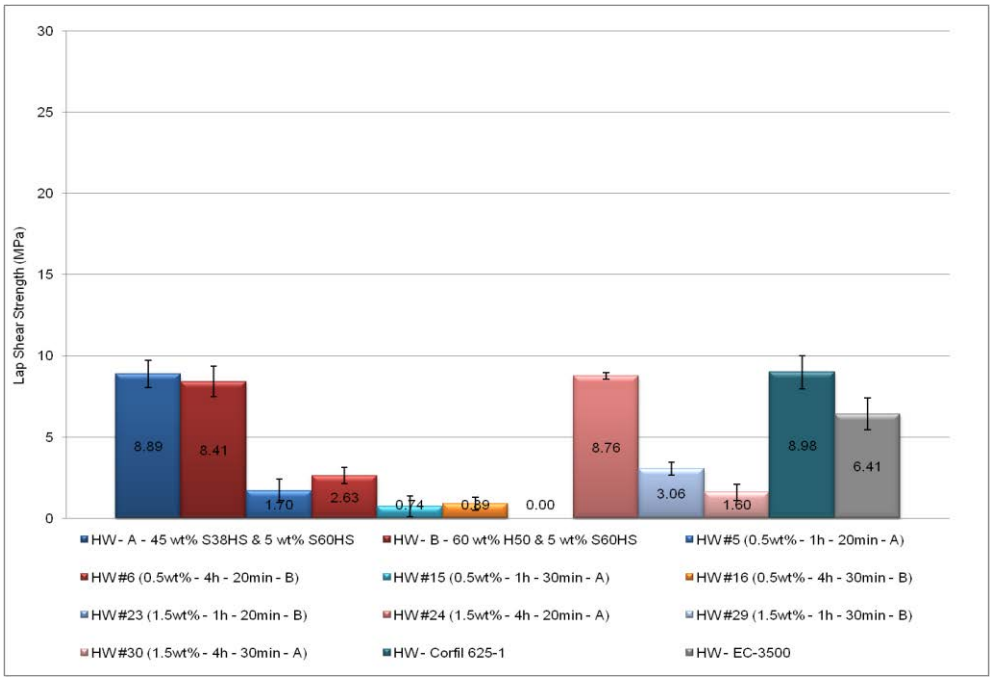

Figure 47. Lap shear strength results for F-SWNT-resin-glass microballoon specimens mixed without vacuum and subjected to hot/wet conditioning.

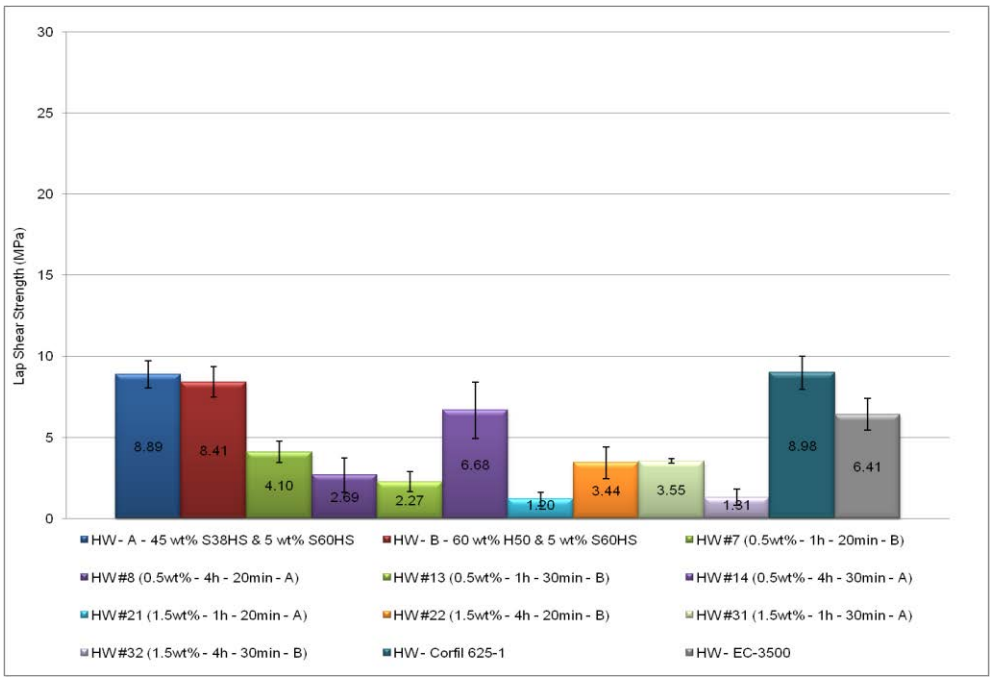

Figure 48. Lap shear strength results for F-MWNT-resin-glass microballoon specimens mixed without vacuum and subjected to hot/wet conditioning.

4.5.3 Effect of F-SWNTs and F-MWNTs on Specimens Prepared with the Selected Microballoons and Subjected to Hot/Wet Conditions

The effect of F-CNTs on the compressive and lap shear strength of potting compounds prepared with **A**-type microballoons and exposed to hot/wet conditions is shown in Figure 49, Figure 50, Figure 53 and Figure 54. In these figures, the strength results for specimens prepared with and without vacuum are compared. As shown in these figures, the addition of F-SWNTs or F-MWNTs became significant only when a good interaction between the reinforcement materials (microballoons and CNTs) and the polymer matrix took place (vacuum mixing). This interaction could account for load transfer even though the nano-enhanced compounds were subjected to hygrothermal conditions. As such, the dispersion of F-CNTs in specimens prepared with vacuum and subjected hot/wet conditions showed more than 100% increase in compressive strength with respect to the base compound and 625-1 as well as more than 10% increase compared with EC-

3500. Furthermore, the lap shear strength increased by more than 15% with respect to the baseline, more than 13% relative to 625-1, and more than 60% compared with EC-3500.

Similarly, the results obtained for the high-high density nano-enhanced compounds prepared with vacuum and exposed to conditioning showed an increase in compressive strength of more than 70% in comparison to its baseline, more than 140% compared with 625-1, and more than 30% with respect to EC-3500. The lap shear strength, on the other hand, increased by more than 40% with respect to its baseline, more than 30% compared with 625-1, and more than 90% in comparison to EC-3500. These results are described in Figure 51, Figure 52, Figure 55 and Figure 56.

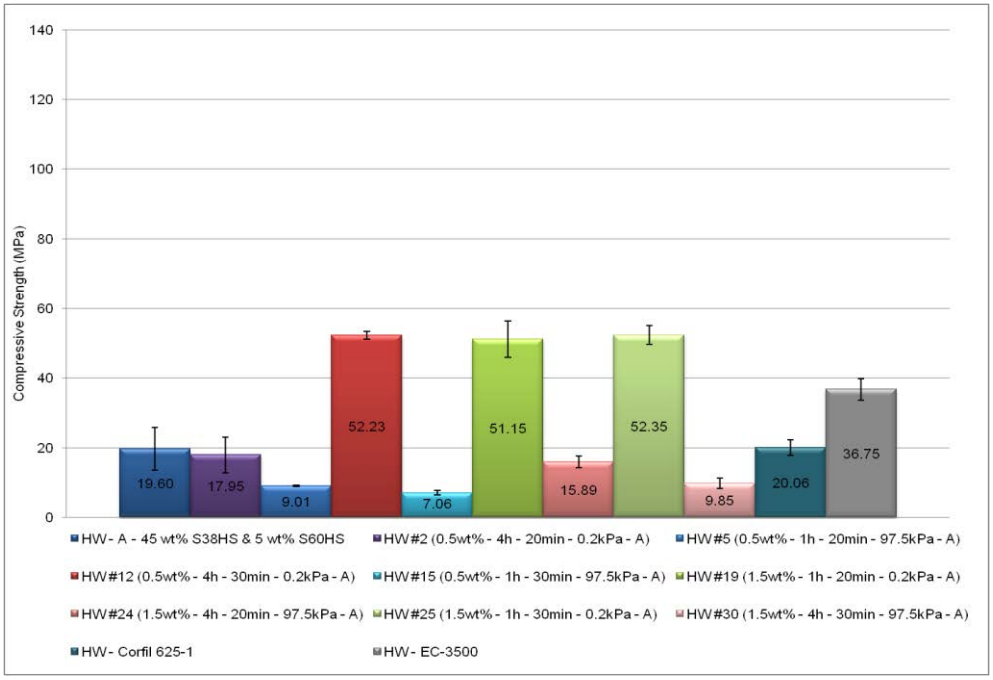

Figure 49. Compressive strength results for specimens prepared with F-SWNTs and S38HS & S60HS glass microballoons and subjected to hot/wet conditioning

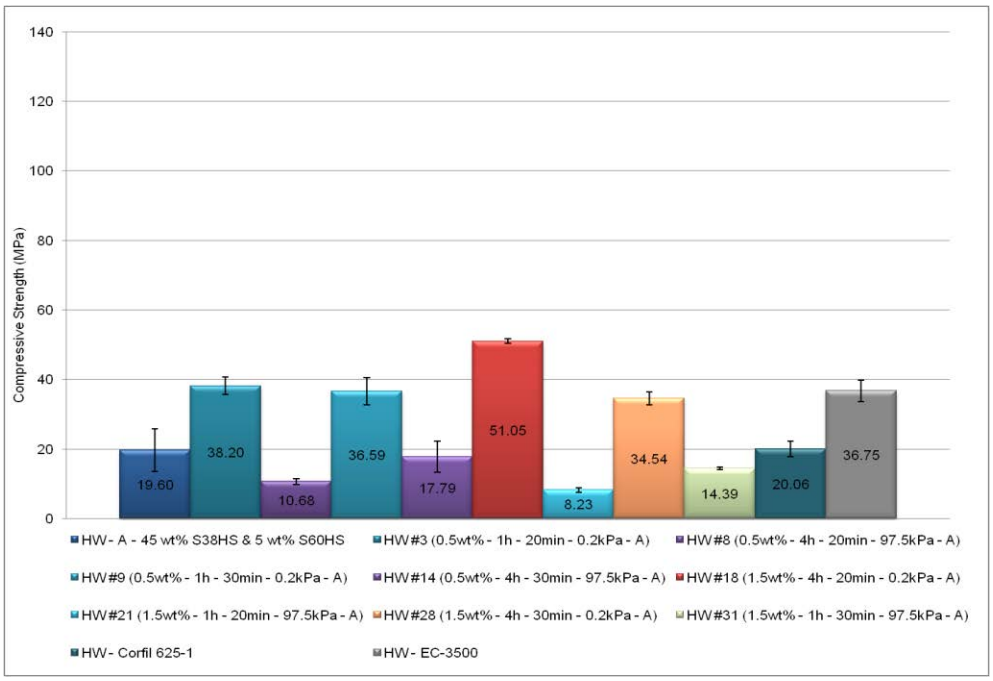

Figure 50. Compressive strength results for specimens prepared with F-MWNTs and S38HS & S60HS glass microballoons and subjected to hot/wet conditioning.

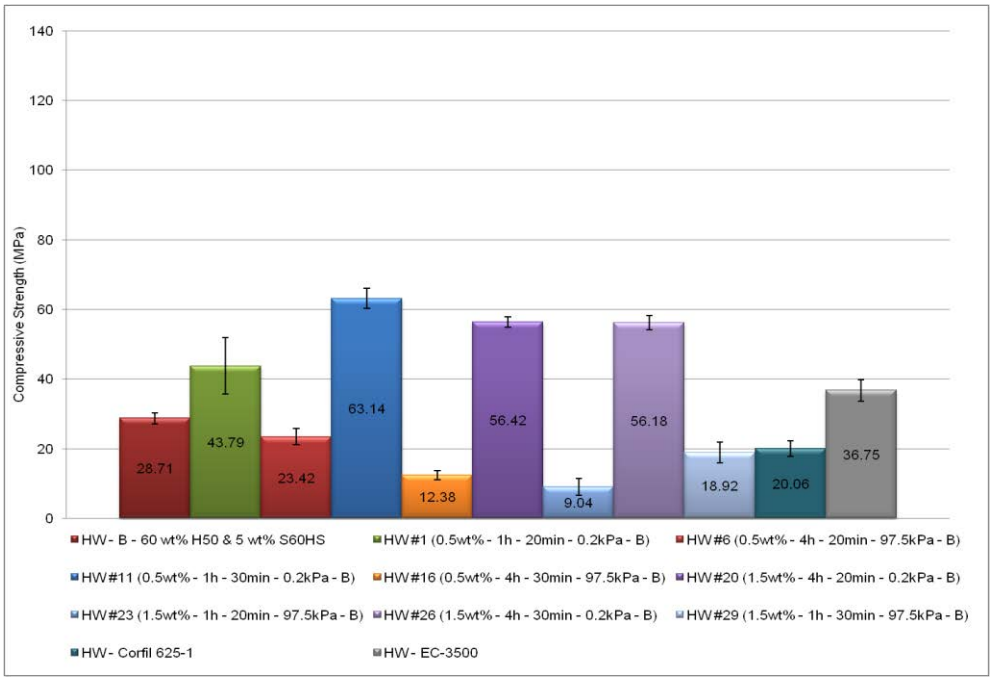

Figure 51. Compressive strength results for specimens prepared with F-SWNTs and H50 & S60HS glass microballoons and subjected to hot/wet conditioning.

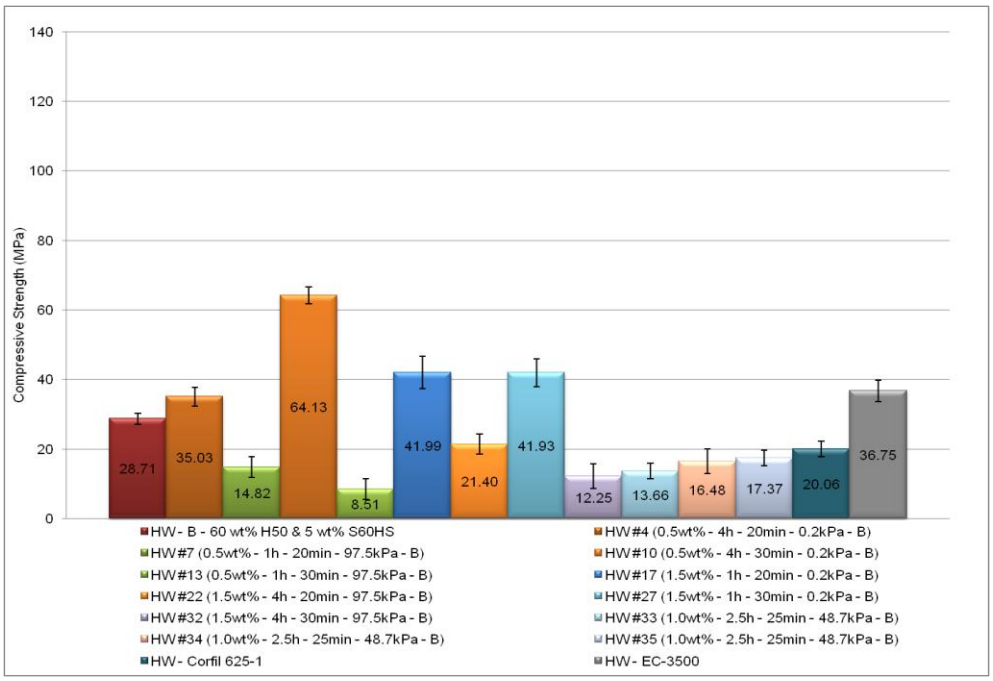

Figure 52. Compressive strength results for specimens prepared with F-MWNTs and H50 & S60HS glass microballoons and subjected to hot/wet conditioning.

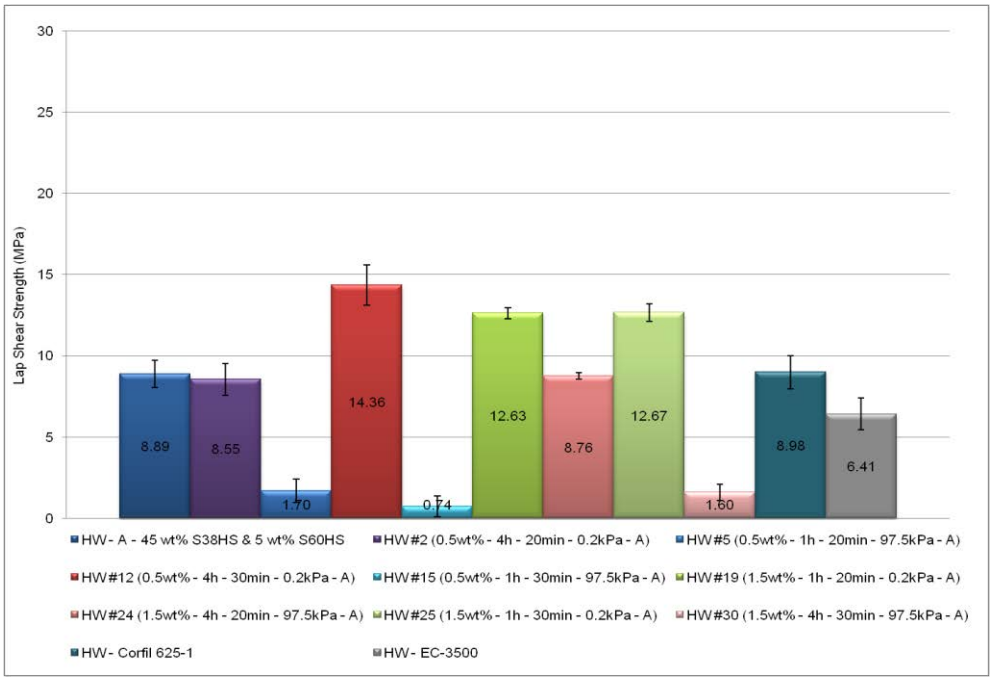

Figure 53. Lap shear strength results for specimens prepared with F-SWNTs and S38HS & S60HS glass microballoons and subjected to hot/wet conditioning.

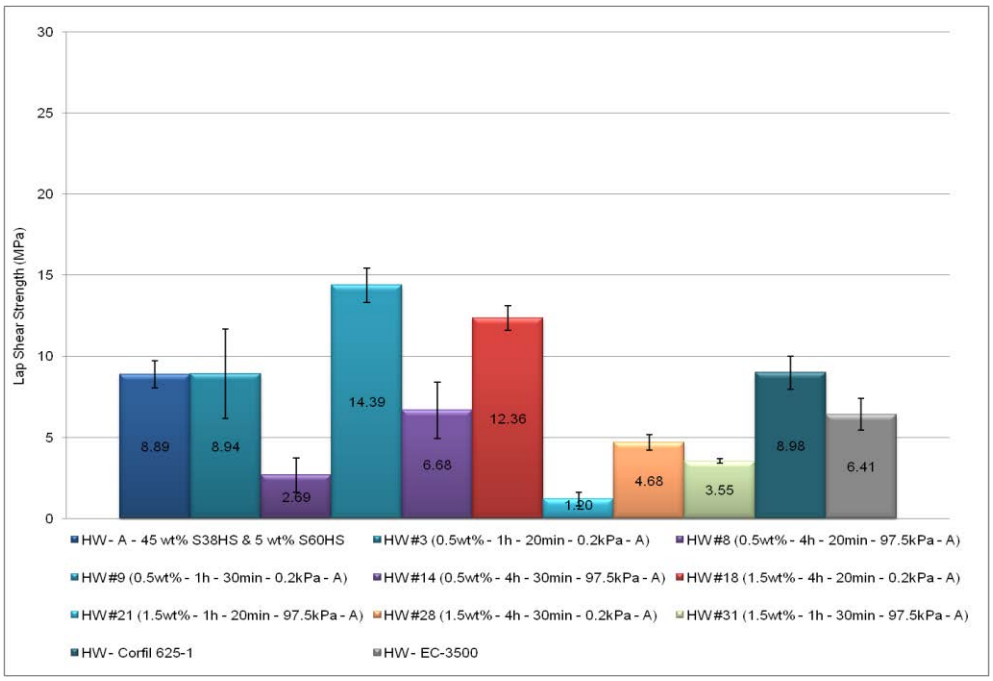

Figure 54. Lap shear strength results for specimens prepared with F-MWNTs and S38HS & S60HS glass microballoons and subjected to hot/wet conditioning.

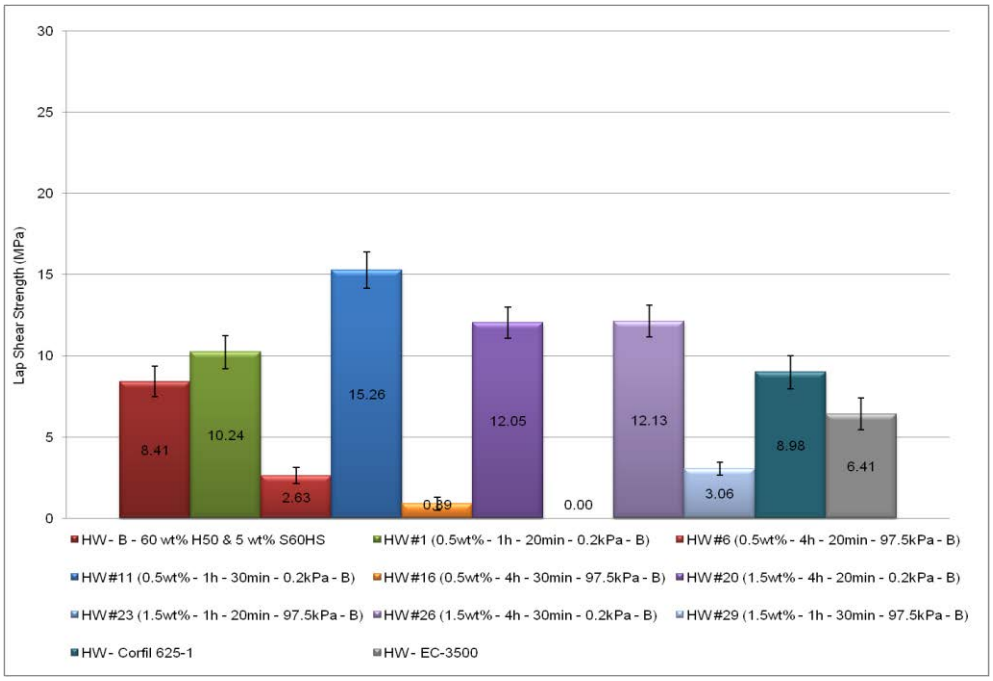

Figure 55. Lap shear strength results for specimens prepared with F-SWNTs and H50 & S60HS glass microballoons and subjected to hot/wet conditioning.

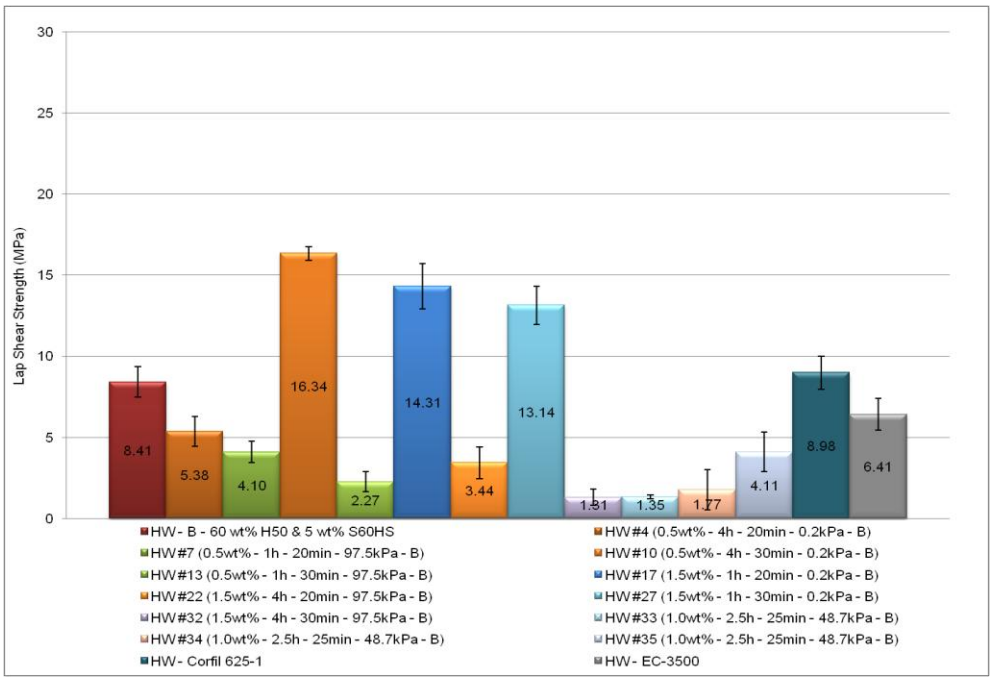

Figure 56. Lap shear strength results for specimens prepared with F-MWNTs and H50 & S60HS glass microballoons and subjected to hot/wet conditioning.

CHAPTER 5

CONCLUSIONS

In order to understand the effect of glass microballoons and carbon nanotubes on the mechanical and physical properties of a potting compound, two studies were carried out. The first study evaluated the effect of the microballoon reinforcement on the density as well as the compressive and lap shear strength of a potting compound. The second study assessed the effect of carbon nanotube (CNT) reinforcement on those properties. In the first study, several specimens were prepared and tested under dry and hot/wet conditions. The density and strength results were compared with the values obtained for EC-3500 under both conditions. From these results, two standard compounds (45 wt% S38HS & 5 wt% S60HS and 60 wt% H50 & 5 wt% S60HS) were selected as base materials for manufacturing of nanocomposite potting compounds in the second study.

To make CNT-based potting compounds with superior mechanical properties, it was essential to develop proper techniques to exfoliate and disperse carbon nanotubes (CNTs) in the base materials. The feasibility of dispersing CNTs in a polymer resin relied on two main factors: functionalization and mixing. Functionalization was performed to graft organic groups (C=O, -OH, COOH) to the surface(s) of the nanotubes, which are more hydrophilic with epoxy resins. This prevented CNT re-agglomeration and enhanced both dispersion and interfacial interaction with the polymer matrix. Mixing, on the other hand, was important to attain CNT reinforcement. Through this research, a novel technique involving solution dispersion, high shear, and centrifugal mixing was developed to uniformly disperse CNT in resin-glass microballoon compounds. It was shown that, by adjusting processing conditions, compounds with different morphologies and different mechanical properties were attained, emphasizing the importance of

CNT processing on the final properties of nano-enhanced potting compounds. In this respect, the new mixing approach proved to be a promising alternative to enhance dispersion and interfacial interaction of nanotubes in the resin of potting compounds.

Vacuum mixing at 0.2 kPa proved to have a significant effect on the compressive and lap shear strength of potting compounds prepared with either functionalized SWNTs (F-SWNTs) or functionalized MWNTs (F-MWNTs). The compressive and lap shear strength of compounds containing F-SWNTs and the medium-high density glass microballoons (45 wt% S38HS & 5 wt% S60HS) increased by 17% and 83% with respect to EC-3500, respectively. Similarly, the compressive and lap shear strength of compound containing F-MWNTs and the same combination of microballoons increased by 16% and 89% compared with EC-3500, respectively. However, the nano-enhanced potting compound with a combination of 0.5 wt% F-MWNTs and 45 wt% S38HS & 5 wt% S60HS (#9) showed an increase in compressive and lap shear strength of 24% and 68% compared with its baseline, 130% and 83% relative to Corfil 625-1, and 22.5% and 119% with respect to EC-3500 with a density of 687.35 kg/m^3, respectively. On the other hand, in spite of having a density out of the specified range (608.7-688.7 kg/m^3), the nano-enhanced potting compounds containing the high-high density glass microballoons (60 wt% H50 & 5 wt% S60HS) showed a trend similar to the nano-enhanced compound containing the medium-high density microballoons.

The nano-enhanced compounds prepared without vacuum during the mixing process showed a substantial decrease in compressive and lap shear strength of 22% and 12% with respect to EC-3500, respectively. This behavior was attributed to the presence of large free volume (voids) in the CNT-resin-microballoon specimens. Moreover, the study showed that temperature, humidity, and time played an important role in the mechanical properties of the

potting compounds. For the nano-enhanced specimens mixed with vacuum and subjected to hygrothemal conditions, a decrease of more than 50% in compressive strength and more than 40% in lap shear strength was observed in comparison to the dry specimens. Even though a hot/wet environment imposed such significant decrease in the mechanical properties, an increase of 18.2% and 9% in compressive strength was obtained for compounds containing S38HS & S60HS microballoons with F-SWNTs or F-MWNTs in comparison to EC-3500, respectively. On the other hand, the lap shear strength was increased by 88% when adding F-SWNTs and by 58% when adding F-MWNTs to compounds mixed with the aforementioned microballoons with respect to EC-3500.

Similar to dry conditions, the nano-enhanced compound #9 showed the highest increase in lap shear strength (61.83%) relative to its baseline with a compressive strength (36.59 MPa) equivalent to that of EC-3500 (36.75 MPa). Likewise, an increase in lap shear strength of 60.21% and 124.30% with respect to Corfil 625-1 and EC-3500 was attained for the same compound, respectively. Hence, based on the processing conditions and materials used, the F-MWNTs were found to be better nanomaterials for this application than the F-SWNTs.

Finally, the effect of humidity was more accentuated for nano-enhanced potting compounds mixed with no vacuum. With respect to the values obtained for the dry specimens, the hot/wet results showed a decrease of 80% and 77% in compressive and lap shear strength, respectively. Such an inferior performance in mechanical properties could be attributed to several factors such as: (1) lack of interfacial interaction between the matrix, the microballoons and the nanotubes, (2) matrix failure due to vapor absorption and stress concentration, (3) thin wall microballoon fracture, and (4) high number of voids within the molecular structure. Therefore, as the temperature and moisture increased above the room temperature, the strength

values decreased. Such an effect is in agreement with the results reported by others for potting compound made with S22 and K46 microballoons [12]. Also, good nanotube dispersion techniques are critical to reinforcing efficiency because nanotubes tend to aggregate when they are dispersed in polymeric materials affecting the mechanical properties of the nanocomposite.

By employing different carbon nanomaterials as well as different microballoons, the physical and mechanical properties of the potting compounds can be tailored to meet particular density and strength requirements. With further investigation into modeling of nano-enhanced potting compounds and knowledge of the interactions between the microballoons, resin, and nanotubes, ideal low-density one-part potting compounds can be developed to maintain the integrity of sandwich laminates in both dry and hygrothermal conditions.

REFERENCES

LIST OF REFERENCES

[1] Liming Honeycomb Composites Co. Ltd. Honeycomb panel structure. [cited 2010 March 14]; Available from: www.hycomb.cn/UserFiles/image/08093642625.jpg.

[2] M. Puterman, M. Narkis, and S. Kenig, Syntactic Foams I. Preparation, Structure and Properties. Journal of Cellular Plastics, 1980. 16(4): p. 223-229.

[3] M. Narkis, M. Puterman, and S. Kenig, Syntactic Foams II. Preparation and Characterization Of Three-Phase Systems. Journal of Cellular Plastics, 1980. 16(6): p. 326-330.

[4] N. Gupta and R. Nagorny, Tensile properties of glass microballoon-epoxy resin syntactic foams. Journal of Applied Polymer Science, 2006. 102(2): p. 1254-1261.

[5] N. Gupta and E. Woldesenbet, Microballoon Wall Thickness Effects on Properties of Syntactic Foams. Journal of Cellular Plastics, 2004. 40(6): p. 461-480.

[6] N. Gupta, E. Woldesenbet, and P. Mensah, Compression properties of syntactic foams: effect of cenosphere radius ratio and specimen aspect ratio. Composites Part A: Applied Science and Manufacturing, 2004. 35(1): p. 103-111.

[7] E. Woldesenbet and S. Peter. Volume fraction effect on high strain rate properties of syntactic foam composites. 2009. Van Godewijckstraat 30, Dordrecht, 3311 GZ, Netherlands: Kluwer Academic Publishers.

[8] G. Tagliavia, M. Porfiri, and N. Gupta, Vinyl Ester--Glass Hollow Particle Composites: Dynamic Mechanical Properties at High Inclusion Volume Fraction. Journal of Composite Materials, 2009. 43(5): p. 561-582.

[9] E. Rizzi, E. Papa, and A. Corigliano, Mechanical behavior of a syntactic foam: experiments and modeling. International Journal of Solids and Structures, 2000. 37(40): p. 5773-5794.

[10] E.C. Hobaica and S.D. Cook, The Characteristics of Syntactic Foams Used for Buoyancy. Journal of Cellular Plastics, 1968. 4(4): p. 143-148.

[11] J.S. Earl and R.A. Shenoi, Determination of the Moisture Uptake Mechanism in Closed Cell Polymeric Structural Foam during Hygrothermal Exposure. Journal of Composite Materials, 2004. 38(15): p. 1345-1365.

[12] N. Gupta and E. Woldesenbet, Hygrothermal studies on syntactic foams and compressive strength determination. Composite Structures, 2003. 61(4): p. 311-320.

[13] K. Okuno and R.T. Woodhams, Mechanical properties and characterization of phenolic resin syntactic foams. Journal of Cellular Plastics, 1974. 10(5): p. 237-244.

[14] N. Gupta, et al., Characterization of Mechanical and Electrical Properties of Epoxy-Glass Microballoon Syntactic Composites. Ferroelectrics, 2006. 345(1): p. 1 - 12.

[15] L. Bardella and F. Genna, On the elastic behavior of syntactic foams. International Journal of Solids and Structures, 2001. 38(40-41): p. 7235-7260.

[16] H.S. Kim and H.H. Oh, Manufacturing and impact behavior of syntactic foam. Journal of Applied Polymer Science, 2000. 76(8): p. 1324-1328.

[17] N. Gupta, et al., Studies on compressive failure features in syntactic foam material. Journal of Materials Science, 2001. 36(18): p. 4485-91.

[18] N. Gupta, E. Woldesenbet, and Kishore, Compressive fracture features of syntactic foams-microscopic examination. Journal of Materials Science, 2002. 37(15): p. 3199-3209.

[19] H.S. Kim and P. Plubrai, Manufacturing and failure mechanisms of syntactic foam under compression[small star, filled]. Composites Part A: Applied Science and Manufacturing, 2004. 35(9): p. 1009-1015.

[20] J.C. Charlier, Defects in Carbon Nanotubes. Accounts of Chemical Research, 2002. 35(12): p. 1063-1069.

[21] E.T. Thostenson, Z. Ren, and T.-W. Chou, Advances in the science and technology of carbon nanotubes and their composites: a review. Composites Science and Technology, 2001. 61(13): p. 1899-1912.

[22] B.I. Yakobson, C.J. Brabec, and J. Bernholc, Nanomechanics of Carbon Tubes: Instabilities beyond Linear Response. Physical Review Letters, 1996. 76(14): p. 2511.

[23] D. Troya, S.L. Mielke, and G.C. Schatz, Carbon nanotube fracture-differences between quantum mechanical mechanisms and those of empirical potentials. Chemical Physics Letters, 2003. 382(1-2): p. 133-41.

[24] X. Hao, H. Qiang, and Y. Xiaohu, Buckling of defective single-walled and double-walled carbon nanotubes under axial compression by molecular dynamics simulation. Composites Science and Technology, 2008. 68(7-8): p. 1809-1814.

[25] Q. Lu and B. Bhattacharya, The role of atomistic simulations in probing the small-scale aspects of fracture--a case study on a single-walled carbon nanotube. Engineering Fracture Mechanics, 2005. 72(13): p. 2037-2071.

[26] Q. Liu, et al., Diameter-Selective Growth of Single-Walled Carbon Nanotubes with High Quality by Floating Catalyst Method. ACS Nano, 2008. 2(8): p. 1722-1728.

[27] B. Peng, et al., Measurements of near-ultimate strength for multiwalled carbon nanotubes and irradiation-induced crosslinking improvements. Nat Nano, 2008. 3(10): p. 626-631.

[28] E.T. Thostenson, C. Li, and T.-W. Chou, Nanocomposites in context. Composites Science and Technology, 2005. 65(3-4): p. 491-516.

[29] X. Zhao, et al., Smallest carbon nanotube is 3 A in diameter. Physical Review Letters, 2004. 92(12): p. 125502-1-125502-3.

[30] G. Eres, et al., In situ control of the catalyst efficiency in chemical vapor deposition of vertically aligned carbon nanotubes on predeposited metal catalyst films. Applied Physics Letters, 2004. 84(10): p. 1759-1761.

[31] C.P. Deck and K. Vecchio, Growth mechanism of vapor phase CVD-grown multi-walled carbon nanotubes. Carbon, 2005. 43(12): p. 2608-2617.

[32] S. Iijima, Helical microtubules of graphitic carbon. Nature, 1991. 354(6348): p. 56-58.

[33] X. Lv, et al., Synthesis of high quality single-walled carbon nanotubes at large scale by electric arc using metal compounds. Carbon, 2005. 43(9): p. 2020-2022.

[34] C. Journet, et al., Large-scale production of single-walled carbon nanotubes by the electric-arc technique. Nature, 1997. 388(6644): p. 756-758.

[35] M.H. Björn Hornbostel, Jirka Cech, Ursula Dettlaff and Siegmar Roth, Arc discharge and laser ablation synthesis of singlewalled carbon nanotubes. 2006.

[36] A.G. Rinzler, et al., Large-scale purification of single-wall carbon nanotubes: process, product, and characterization. Applied Physics A (Materials Science Processing), 1998. 67(1): p. 29-37.

[37] P. Nikolaev, et al., Gas-phase catalytic growth of single-walled carbon nanotubes from carbon monoxide. Chemical Physics Letters, 1999. 313(1-2): p. 91-7.

[38] C.L. Cheung, et al., Diameter-Controlled Synthesis of Carbon Nanotubes. The Journal of Physical Chemistry B, 2002. 106(10): p. 2429-2433.

[39] E. Dervishi, et al., High-aspect ratio and horizontally oriented carbon nanotubes synthesized by RF-cCVD. Diamond and Related Materials. In Press, Corrected Proof.

[40] J. Minjae, et al. Growth of carbon nanotubes by chemical vapor deposition. 2001. Switzerland: Elsevier.

[41] C. Young Chul, et al., Controlling the diameter, growth rate, and density of vertically aligned carbon nanotubes synthesized by microwave plasma-enhanced chemical vapor deposition. Applied Physics Letters, 2000. 76(17): p. 2367-9.

[42] M. Meo and M. Rossi, Prediction of Young's modulus of single wall carbon nanotubes by molecular-mechanics based finite element modelling. Composites Science and Technology, 2006. 66(11-12): p. 1597-1605.

[43] M. Meo and M. Rossi, Tensile failure prediction of single wall carbon nanotube. Engineering Fracture Mechanics, 2006. 73(17): p. 2589-2599.

[44] T. Ragab and C. Basaran, A framework for stress computation in single-walled carbon nanotubes under uniaxial tension. Computational Materials Science, 2009. 46(4): p. 1135-1143.

[45] M. Locascio, et al., Tailoring the load carrying capacity of MWCNTs through Inter-shell atomic bridging. Experimental Mechanics, 2009. 49(2): p. 169-182.

[46] E.T. Thostenson, S. Ziaee, and T.-W. Chou, Processing and electrical properties of carbon nanotube/vinyl ester nanocomposites. Composites Science and Technology, 2009. In Press, Corrected Proof.

[47] K.P. Ryan, et al., Carbon nanotubes for reinforcement of plastics? A case study with poly(vinyl alcohol). Composites Science and Technology, 2007. 67(7-8): p. 1640-1649.

[48] P. Guo, et al., Fabrication and mechanical properties of well-dispersed multiwalled carbon nanotubes/epoxy composites. Composites Science and Technology, 2007. 67(15-16): p. 3331-3337.

[49] B. Fiedler, et al., Fundamental aspects of nano-reinforced composites. Composites Science and Technology, 2006. 66(16): p. 3115-3125.

[50] W. Chen, H. Lu, and S.R. Nutt, The influence of functionalized MWCNT reinforcement on the thermomechanical properties and morphology of epoxy nanocomposites. Composites Science and Technology, 2008. 68(12): p. 2535-2542.

[51] F.H. Gojny, et al., Influence of different carbon nanotubes on the mechanical properties of epoxy matrix composites - A comparative study. Composites Science and Technology, 2005. 65(15-16): p. 2300-2313.

[52] M. Nadler, et al., Effect of CNT surface functionalisation on the mechanical properties of multi-walled carbon nanotube/epoxy-composites. Composites Part A: Applied Science and Manufacturing, 2009. 40(6-7): p. 932-937.

[53] Y. Liu, et al., Dispersion of multi-walled carbon nanotubes by ionic liquid-type Gemini imidazolium surfactants in aqueous solution. Colloids and Surfaces A: Physicochemical and Engineering Aspects. In Press, Accepted Manuscript.

[54] J.R. Simpson, et al., The effect of dispersant on defects in length-separated single-wall carbon nanotubes measured by Raman spectroscopy. Carbon, 2009. 47(14): p. 3238-3241.

[55] L. Ji, et al., Preparation and properties of multi-walled carbon nanotube/carbon/polystyrene composites. Carbon, 2009. 47(11): p. 2733-2741.

[56] X. Chen, et al., Functionalized Multi-Walled Carbon Nanotubes Prepared by In Situ Polycondensation of Polyurethane. Macromolecular Chemistry and Physics, 2007. 208(9): p. 964-972.

[57] A. Battisti, A.A. Skordos, and I.K. Partridge, Monitoring dispersion of carbon nanotubes in a thermosetting polyester resin. Composites Science and Technology, 2009. 69(10): p. 1516-1520.

[58] M. Nadler, et al., Preparation of colloidal carbon nanotube dispersions and their characterisation using a disc centrifuge. Carbon, 2008. 46(11): p. 1384-1392.

[59] E.T. Thostenson and T.-W. Chou, Processing-structure-multi-functional property relationship in carbon nanotube/epoxy composites. Carbon, 2006. 44(14): p. 3022-3029.

[60] F.H. Gojny, et al., Carbon nanotube-reinforced epoxy-composites: enhanced stiffness and fracture toughness at low nanotube content. Composites Science and Technology, 2004. 64(15): p. 2363-2371.

[61] E.A. Zaragoza-Contreras, et al., Evidence of multi-walled carbon nanotube fragmentation induced by sonication during nanotube encapsulation via bulk-suspension polymerization. Micron. 40(5-6): p. 621-627.

[62] L. Ci and J. Bai, The reinforcement role of carbon nanotubes in epoxy composites with different matrix stiffness. Composites Science and Technology, 2006. 66(3-4): p. 599-603.

[63] W.S. Chow and P.L. Tan, Epoxy/Multiwall Carbon Nanotube Nanocomposites Prepared by Sonication and Planetary Mixing Technique. Journal of Reinforced Plastics and Composites, 2009: p. 0731684409348346.

[64] E.T. Thostenson and C. Tsu-Wei, Aligned multi-walled carbon nanotube-reinforced composites: processing and mechanical characterization. Journal of Physics D (Applied Physics), 2002. 35(16): p. 77-80.

[65] P.S.A. J.H. Park, S.Y. Jeon, J.B. Yoo, Carbon nanotube composite: Dispersion routes and field emission parameters. Composites Science and Technology, 2007. 68(3-4): p. 753-759.

[66] K. Yang, et al., Effects of carbon nanotube functionalization on the mechanical and thermal properties of epoxy composites. Carbon, 2009. 47(7): p. 1723-1737.

[67] S.J.V. Frankland, et al., Molecular simulation of the influence of chemical cross-links on the shear strength of carbon nanotube-polymer interfaces. Journal of Physical Chemistry B, 2002. 106(12): p. 3046-8.

[68] S. Wang, et al., Load-transfer in functionalized carbon nanotubes/polymer composites. Chemical Physics Letters, 2008. 457(4-6): p. 371-375.

[69] T.G.D. Río, et al., Influence of single walled carbon nanotubes on the effective elastic constants of poly(ethylen terephthalate). Composites Science and Technology. In Press, Accepted Manuscript.

[70] E. Woldensenbet and N. Sankella, Flexural Properties of Nanoclay Syntactic Foam Sandwich Structures. Journal of Sandwich Structures and Materials, 2009. 11(5): p. 425-444.

[71] J. Baalman, et al., Potting Compound Strength Enhancement using Carbon Nanomaterials in Sampe 2008: Memphis

[72] J. Baalman, et al., Experimental investigation of potting compound strength enhancement using carbon nanofibers and glass/ceramic microspheres in Sampe 2009: Baltimore

[73] G. Li and M. John, A self-healing smart syntactic foam under multiple impacts. Composites Science and Technology, 2008. 68(15-16): p. 3337-3343.

[74] M. Dimchev, R. Caeti, and N. Gupta, Effect of carbon nanofibers on tensile and compressive characteristics of hollow particle filled composites. Materials & Design. 31(3): p. 1332-1337.

[75] N. Gupta and R. Maharsia, Enhancement of energy absorption in syntactic foams by nanoclay incorporation for sandwich core applications. Applied Composite Materials, 2005. 12(3-4): p. 247-61.

[76] Exakt. Exakt three roll mills [cited 2010 March 14]; Available from: www.exakt.de/EXAKT-Three-Roll-Mil.38+M5208757... <http://www.exakt.de/EXAKT-Three-Roll-Mil.38+M52087573ab0.0.html>.

[77] Thinky. THINKY Mixer. [cited 2008 March 14]; Available from: http://www.thinky.co.jp/en/products/vacuum_mixer/arv-310.html.

[78] A. International, ASTM D695-02a Standard Test Method for Compressive Properties of Rigid Plastics, in D695 - 02a. 2002.

[79] A. International, Standard Test Method for Apparent Shear Strength of Single-Lap-Joint Adhesively Bonded Metal Specimens by Tension Loading (Metal-to-Metal), in D 1002-05. 2005.

[80] J.L. Figueiredo, et al., Modification of the surface chemistry of activated carbons. Carbon, 1999. 37(9): p. 1379-1389.

APPENDICES

APPENDIX A

DESIGN OF EXPERIMENT I - GLASS MICROBALLOONS

Factor	A	B	C
	Microballon Type	Microballoons WT%	Additional Microballoons
1	0	0	0
2	0	0	1
3	0	1	0
4	0	1	1
5	1	0	0
6	1	0	1
7	1	1	0
8	1	1	1
9	0	0	-1
10	0	1	-1
11	1	0	-1
12	1	1	-1

Microballon Type		
0	S38HS	
1	H50	
Microballoons WT%		
0	45%	
1	60%	
Additional Microballoons		
0	0%	
1	5%	S60HS
-1	5%	S15HS

1	S38HS	45%	0%
2	S38HS	45%	5% S60HS
3	S38HS	60%	0%
4	S38HS	60%	5% S60HS
5	H50	45%	0%
6	H50	45%	5% S60HS
7	H50	60%	0%
8	H50	60%	5% S60HS
9	S38HS	45%	5% S15HS
10	S38HS	60%	5% S15HS
11	H50	45%	5% S15HS
12	H50	60%	5% S15HS

APPENDIX B

DESIGN OF EXPERIMENTS II - CARBON NANOTUBES

Factor	A	B	C	D	E	F	G	H
	Nanotubes (wt%)	Mixing Time (min)	Vacuum (KPa)	Sonication Power (W)	Functionalization Time (min)	Functionalization Temp (°C)	Nanotube type	Bead Type
1	-1	-1	-1	-1	-1	-1	-1	1
2	-1	-1	-1	-1	1	-1	-1	-1
3	-1	-1	-1	1	-1	-1	1	-1
4	-1	-1	-1	1	1	-1	1	1
5	-1	-1	1	-1	-1	1	-1	-1
6	-1	-1	1	-1	1	1	-1	1
7	-1	-1	1	1	-1	1	1	1
8	-1	-1	1	1	1	1	1	-1
9	-1	1	-1	-1	-1	1	1	-1
10	-1	1	-1	-1	1	1	1	1
11	-1	1	-1	1	-1	1	-1	1
12	-1	1	-1	1	1	1	-1	-1
13	-1	1	1	-1	-1	-1	1	1
14	-1	1	1	-1	1	-1	1	-1
15	-1	1	1	1	-1	-1	-1	-1
16	-1	1	1	1	1	-1	-1	1
17	1	-1	-1	-1	-1	1	1	1
18	1	-1	-1	-1	1	1	1	-1
19	1	-1	-1	1	-1	1	-1	-1
20	1	-1	-1	1	1	1	-1	1
21	1	-1	1	-1	-1	-1	1	-1
22	1	-1	1	-1	1	-1	1	1
23	1	-1	1	1	-1	-1	-1	1
24	1	-1	1	1	1	-1	-1	-1
25	1	1	-1	-1	-1	-1	-1	-1
26	1	1	-1	-1	1	-1	-1	1
27	1	1	-1	1	-1	-1	1	1
28	1	1	-1	1	1	-1	1	-1
29	1	1	1	-1	-1	1	-1	1
30	1	1	1	-1	1	1	-1	-1
31	1	1	1	1	-1	1	1	-1
32	1	1	1	1	1	1	1	1
33	0	0	0	0	0	0	0	0
34	0	0	0	0	0	0	0	0
35	0	0	0	0	0	0	0	0

APPENDIX B (Continued)

COMBINATION OF SPECIMENS

Factor	A	B	C	D	E	F	G	H
	Nanotubes (wt%)	Mixing Time (min)	Vacuum (KPa)	Sonication Power (W)	Functionalization Time (min)	Functionalization Temp (°C)	Nanotube type	Bead Type
1	0.005	20	0.2	5	1	60	SW	B
2	0.005	20	0.2	5	4	60	SW	A
3	0.005	20	0.2	10	1	60	MW	A
4	0.005	20	0.2	10	4	60	MW	B
5	0.005	20	97.5	5	1	90	SW	A
6	0.005	20	97.5	5	4	90	SW	B
7	0.005	20	97.5	10	1	90	MW	B
8	0.005	20	97.5	10	4	90	MW	A
9	0.005	30	0.2	5	1	90	MW	A
10	0.005	30	0.2	5	4	90	MW	B
11	0.005	30	0.2	10	1	90	SW	B
12	0.005	30	0.2	10	4	90	SW	A
13	0.005	30	97.5	5	1	60	MW	B
14	0.005	30	97.5	5	4	60	MW	A
15	0.005	30	97.5	10	1	60	SW	A
16	0.005	30	97.5	10	4	60	SW	B
17	0.015	20	0.2	5	1	90	MW	B
18	0.015	20	0.2	5	4	90	MW	A
19	0.015	20	0.2	10	1	90	SW	A
20	0.015	20	0.2	10	4	90	SW	B
21	0.015	20	97.5	5	1	60	MW	A
22	0.015	20	97.5	5	4	60	MW	B
23	0.015	20	97.5	10	1	60	SW	B
24	0.015	20	97.5	10	4	60	SW	A
25	0.015	30	0.2	5	1	60	SW	A
26	0.015	30	0.2	5	4	60	SW	B
27	0.015	30	0.2	10	1	60	MW	B
28	0.015	30	0.2	10	4	60	MW	A
29	0.015	30	97.5	5	1	90	SW	B
30	0.015	30	97.5	5	4	90	SW	A
31	0.015	30	97.5	10	1	90	MW	A
32	0.015	30	97.5	10	4	90	MW	B
33	0.01	25	48.75	8	2.5	75	MW	B
34	0.01	25	48.75	8	2.5	75	MW	B
35	0.01	25	48.75	8	2.5	75	MW	B

APPENDIX B (Continued)

VARIABLES

	Variables	**-1**	**1**	**0**
A	Nanotubes (wt%)	0.5	1.5	1.0
B	Mixing Time (min)	20	30	25
C	Vacuum (kPa)	0.2	97.5	48.8
D	Sonication Power (W)	5	10	8
E	Acid Time (min)	60	240	120
F	Acid Temp (^{o}C)	60	90	75
G	Nanotube Type	SWNTs	MWNTs	MWNTs
H	Bead type	45 % wt S38HS & 5 wt% S60HS	60 wt% H50 & 5 wt% S60HS	60 wt% H50 & 5 wt% S60HS